Flavor Bounds on The ALP–Fermion Couplings Under The "Invisible Axion" Assumption

ALFREDO WALTER MARIO GUERRERA

Dipartamento di Fisica e Astronomia "G. Galilei", Università degli Studi di Padova e
Istituto Nazionale Fisica Nucleare, Sezione di Padova, I-35131 Padova, Italy

Supervisor: S.Rigolin

Contents

Introduction

In recent years particle physics has encountered an unexpected slow down compared to the glorious days of the second half of the 20th century. The Standard Model (SM) of elementary particles alongside the Einstein's theory of General Relativity for gravity provides the study of Nature with a remarkably simple framework, that at present, explains almost all the physical processes observed in the Universe. Only physics beyond the Planck scale, where a full theory of Quantum Gravity is required, and experimental evidence such as dark matter and neutrino masses seem to escape from this general framework. It seems that new physics can only appear at scales well below the reach of terrestrial colliders. These extreme scales are so high that no new feasible experiments could ever test them.

After the discovery of the Higgs boson at the Large Hadron Collider (LHC) at CERN [1], open questions are still standing and await clues or answers, either from the LHC or from other experiments. Some of these are: Is there a path to the unification of all the fundamental forces? Why is there more matter than anti–matter? Are there "hidden" space dimensions? What are dark matter and dark energy? Alongside these open questions probably the most pressing ones are concerns in the theoretical exploration and understanding of the SM itself. There are indeed many good reasons to be at least concerned with the currents state of the theory and in particular with the origin of many of its parameters. Typically these values are obtained experimentally and rarely have a dynamical reason to have the value they have today. The mechanisms driving their evolutions are typically not clear and some of the values are deemed not "natural". To recover a satisfying picture fit to tackle the more delicate questions risen by the SM itself there

is a need to postulate some type of physics beyond the Standard Model.

The LHC project was conceived to elucidate the mechanism by which the W and Z bosons acquire mass while the photon does not. The postulate of a field frozen below a critical energy and interacting with some of the d.o.f., due to symmetry arguments, explains the different possible masses in the model. The purposes of the experiments there were to search for the Higgs boson and to look for some clues of physics beyond the theoretical knowledge. As of today none has been found, but the machine did characterize a scalar resonance, the first scalar particle deemed as fundamental.

Nonetheless even with this result naturalness issues with the parameters of the model are still standing. The mass of the Higgs boson is among these parameters. Another important naturalness issue emerges in the reign of QCD. Experimentally strong interactions appear to conserve CP symmetry to a very high degree of precision, nonetheless in the years between the 1970's and the 80's the theory of QCD, due to its non–trivial vacuum structure, brought to light the issue of Strong CP Violation via an extra term in the Lagrangian proportional to the CP–violating topological gluon density $G\tilde{G}$ that was ignored before, the θ term. An economical solution to the issue and to a number of other SM problems is the introduction of a light pseudo–scalar degree of freedom a the axion. The only mandatory coupling is the one to the $G\tilde{G}$ term. Once the axion field relaxes to a vacuum expectation value, its potential will force the infamous θ phase responsible for the unobserved neutron Electron Dipole Moment to disappear.

Of course the introduction of new degrees of freedom will have an impact essentially on every branch of high energy physics. The newly introduced resonance can play a role in Cosmology and the thermal history of the Universe as well as Colliders. Having the axions very weakly coupled with the SM degrees of freedom, at the phase transition occurring in the early Universe, where $T \sim f_a$, can parametrically induce different thermal distributions useful to probe possibile dark matter and dark energy models. For light enough particles one can also deduce limits on their coupling from Astrophysical observations, such as supernova bounds, helioseismology and measurement based on the Hertzsprung–Russell diagram.

The simple solution of an extra spin 0^- particle, coming from a $U(1)$ in

the UV is very easily realised theoretically. This is of course one of the reasons for the popularity of axions. String theory and GUT among others naturally produce many light scalar fields that can be assembled into axions or Axion-Like Particles (ALPs). Indeed all the properties discussed up until now are independent to a large extent on the particular UV completion of the model. Tuning the high energy origin and behaviour of the axion can dynamically solve low–energy issues of the SM. Notable examples are: Relaxion models [2] where the presence of an axion dynamically relaxes the value of the Higgs mass with respect to its naturally large value, Flaxion models [3] where the particular flavor structure of the axion coupling to the SM degrees of freedom explains the hierarchical structure of low–energy fermion phenomenology in the quark and the lepton sector.

In this manuscript the axion solution to the Strong CP Problem is explored. The first step is to understand the problem and its solutions. Many of the techniques and results discussed in Chapter 1 carry strong conceptual importance and are central topics and milestones in understanding QFTs. Namely Sec.1.1–1.3 contain a discussion on fundamental QFT knowledge of Strong Interactions and QCD. The rest of the chapter tackles the introduction of the axions and ALPs in general with a brief tour of the Chiral Lagrangian of QCD. A number of model independent aspect of the theory of these light–pseudo scalar bosons are discussed and the most notable UV complete models are derived. In the final part of the chapter a discussion on the difficulties, and the introduction of ALPs is studied.

In Chapter 2 the ALP Effective Field Theory expansion truncated at order $1/f_a$ is presented and some of its Renormalization Group flow properties are discussed. Meaningful relations between the parameters and the operators of the model derived from the symmetries of the theory are studied. The redundancies of the description are addressed and a set of well defined physical operators and couplings is indicated in order to project limits onto them. A set of CP–Violating dimension–5 operators along with the consequences that they entail are discussed in Sec.2.6, some of the models able to generate them are introduced.

A brief review of the present experimental bounds and searches is discussed in Chapter 3. Most of the attention is dedicated to Terrestrial Facili-

ties and Fixed Target Experiments while some attention is dedicated to the indirect measurement of ALPs and axions parameters via cosmological and astrophysical probes. Some future prospects are discussed.

In Chapter 4 a general discussion on hadronization techniques can be found. Particular attention is devoted to the possible criticalities one might encounter when applying these methods. Indeed the opening arguments are aimed at understanding the approximations in the Brodsky–Lepage approach to factorisation. Once the correct technology is introduced a number of hadronized amplitude are obtained, using both Brodsky–Lepage methods and Lattice QCD results. A set of new meson-to-meson ALP form factors is computed and presented for the first time enabling the phenomenological study of the following chapter. A discussion on the possible issue emerging from the asymptotic regions of momenta distributions is presented.

Finally in Chapter 5 the whole machinery developed is applied to a number of phenomenological studies, up to three particles final states. Some restrictions on the ALPs theory space are recovered utilizing terrestrial results in the hypothesis that the ALP would escape detection, the so called "invisible ALP." The limits obtained are always projected onto flavor conserving ALP–fermion couplings, as the flavor violating ones are taken to be dominated by loop induced contributions. The searches are divided based on the different possible final states allowed by these hypothesis and by the energies reached by flavor experiments.

Chapter 1

Axions and Axion–Like Particles

In theoretical particle physics the study of matter fields, their symmetries and their associated conservations laws intertwines in what is known as a gauge theory or a Quantum Field Theory (QFT). It turns out that classical symmetries of a theory are not always "respected" in QFTs, and in a sense quantization can spoil them. This should not come as too much of a surprise given the very different nature of a classical field theory and a quantum one. These kind of symmetry violations associated to quantum effects are called "anomalies" and the symmetry that gets broken at the quantum level is labelled as **anomalous.** Strange or unpredicted effects appearing at the quantum level are nothing new and are rarely worrying, instead anomalies must be treated carefully and are a major feature of QFT with the power to modify the spectrum of the theory in unexpected ways and to even invalidate the whole theoretical structure.

Two main types of symmetries are present in QFTs, global symmetries, sometimes called accidental, and local (or gauge) symmetries. The former are associated to charges and conserved currents while the latter represent redundancies in the representation of the physical degrees of freedom described by the theory. Gauge symmetries are introduced by hand in order to build the theory using the simplest possible representation of the Poincaire group that contains the desired degrees of freedom. If a global symmetry

is anomalous the theory is perfectly fine and only the phenomenology will have important modifications. If, instead, a gauge symmetry is anomalous the theory breaks down and the internal consistency is ruined. In some cases is possible to avoid the anomaly, but doing so imposes strict constraints on the physical content, e.g. QED with a single Weyl fermion is inconsistent because it would have an anomalous local $U(1)$. Anomalies have a profound impact on a theory, they can dictate the field content of a model and influence the phenomenology of it. In QCD one has a beautiful realisation of a global anomaly that helped understand deep facts about Yang–Mills theories and the theory of strong interactions them self. In what follows a discussion of the QCD anomaly, its phenomenological impact and the inconsistencies encountered with experiments is presented. The introduction of a new spin 0^- degree of freedom, an axion or an ALP, is chosen as a possible solution.

1.1   The $U(1)$ axial anomaly

For massless quarks $m_u = m_d = m_s = 0$, the QCD lagrangian contains a global invariance under an extended symmetry group. The $U(1)$ axial trasformation is given by

$$\psi = \begin{pmatrix} u \\ d \\ s \end{pmatrix} \rightarrow \psi' = e^{-i\theta\gamma_5}\psi. \tag{1.1}$$

In this limit, which we shall adopt until further notice, Noether's theorem can be applied to identify the classically conserved axial current.

$$J_{5\mu}^{(0)} = \bar{u}\gamma_\mu\gamma_5 u + \bar{d}\gamma_\mu\gamma_5 d + \bar{s}\gamma_\mu\gamma_5 s, \qquad\qquad \partial^\mu J_{5\mu}^{(0)} = 0 \tag{1.2}$$

where the superscript on $J_{5\mu}^{(0)}$ denotes an $SU(3)$ **singlet** current. In the full quantum theory the approximate symmetry is lost because the current divergence has an anomaly. One can see this in a number of ways, the most hands on is due to Adler Bell and Jackiw [4, 5], while for a deeper understanding Fujikawa's path integral method is reffered in [6] and discussed in Sec. 1.1.1.

An anomaly is said to occur when a symmetry of the classical action is not a true symmetry of the full quantum theory. The Noether current is no longer divergenceless, but receives a contribution arising from quantum corrections. This contribution is typically reffered to as the anomalous part.

It is important to review the work of Adler, Bell and Jackiw in the case of the coupling of an axial $U(1)$ current to two gluons. Define the quantity

$$T^{ab}_{\mu\alpha\beta}(k,q) = i \int d^4x d^4y e^{ik\cdot x} e^{iq\cdot y} \left\langle 0 \left| \mathrm{T}\left(J^{(0)}_{5\mu}(x) J^a_\alpha(y) J^b_\beta(0) \right) \right| 0 \right\rangle \tag{1.3}$$

where J^a_α is a flavor-singlet vector current coupled to gluons

$$J^a_\alpha = \sum_{q=u,d,s} \bar{q}\gamma_\alpha \frac{\lambda^a}{2} q. \tag{1.4}$$

Here the $SU(3)$ matrices relative to the latin indices, a and b pertain the color degree of freedom and not the flavor space [7,8]. There are two Ward identities [9], representing the conservation of axial and vector currents. The vector Ward identity, corresponds to $\partial^\alpha J^a_\alpha = 0$, is

$$q^\alpha T^{ab}_{\mu\alpha\beta}(k,q) = 0, \tag{1.5}$$

while for the case of the axial ward identity is derived via in a similar fashion $\partial^\mu J^{(0)}_{5\mu} = 0$, to obtain

$$k^\mu T^{ab}_{\mu\alpha\beta}(k,q) = 0. \tag{1.6}$$

In order to reveal the anomalous behaviour of this coupling, one can calculate the vertex in lowest-order in perturbation theory and compute the contribution from the two possible momentum route [10]

$$T^{ab}_{\mu\alpha\beta} = -3 \int \frac{d^4p}{(2\pi)^4} \left[\mathrm{Tr}\left(\gamma_\mu\gamma_5 \frac{1}{\not{p}+\not{k}} \gamma_\beta \frac{\lambda_b}{2} \frac{1}{\not{p}-\not{q}} \gamma_\alpha \frac{\lambda_a}{2} \frac{1}{\not{p}} \right) \right.$$
$$\left. + \mathrm{Tr}\left(\gamma_\mu\gamma_5 \frac{1}{\not{p}+\not{k}} \gamma_\alpha \frac{\lambda_a}{2} \frac{1}{\not{p}+\not{q}+\not{k}} \gamma_\beta \frac{\lambda_b}{2} \frac{1}{\not{p}} \right) \right], \tag{1.7}$$

the prefactor 3 comes from the three massless quarks contributing equally to

the amplitude.

It is easy to see that the integrals in the definition of $T^{ab}_{\mu\alpha\beta}$ are linearly divergent, and as such they might be not well defined, this is alredy a hint that the computation is troublesome. To quantify the effect of a shift in the integration variable is instructive to consider

$$I_\gamma = \int d^4p \Big[\frac{p_\gamma}{p^4} - \frac{(p-l)_\gamma}{(p-l)^4} \Big]. \tag{1.8}$$

A linearly divergent integral is of the form $\int d^4p F(p)$ where $p^3 F(p) \neq 0$ but $p^3 F'(p) = p^3 F''(p) = ... = 0$ for $p \to \infty$. In Euclidean coordinates one can Taylor expand and use Gauss' theorem to compute the effect of shifting the integration variable

$$\int d^4p_E \Big[F(p) - F(p-l) \Big] = \int d^4p_E [l^\mu \partial_\mu F(p) - \frac{1}{2} l^\mu l^\nu \partial_\mu \partial_\nu F(p) + ...] =$$
$$= l^\mu \int dS_\mu [F(p) - \frac{1}{2} l^\nu \partial_\nu F(p)]_{p\to\infty} = l^\mu \int dS_\mu F(p)_{p\to\infty}, \tag{1.9}$$

where in the last equality we used the fact that $p^3 F'(p)\big|_{p\to\infty} = 0$. So Eq.(1.9) means that a shift in the integration value will change the result by an amount proportional to said shift, times the integral of the function over the boundary of the physical space. In case of I_γ one finds that

$$I_\gamma = i \int d^4p_E \Big(\frac{p_\gamma}{p^4} - \frac{(p-l)_\gamma}{(p-l)^4} \Big) = i l^\mu \int d^3 S_\mu \frac{p_\gamma}{p^4} = i l^\mu \int d^3 S \frac{p_\mu}{p} \frac{p_\gamma}{p^4}. \tag{1.10}$$

It's easy to see how the integral will not depend on the specific value of p since the dependence will be exactly cancelled. This leaves $I_\gamma = i\frac{\pi^2 l_\gamma}{2}$. To apply this to the case at hand one needs to compute the shift to $T^{ab}_{\mu\alpha\beta}$. Namely one substitutes $p \to p + b_1 q + b_2(-k - q)$ in the first term. To preserve Bose symmetry one needs to change in the second term $p \to p + b_2 q + b_1(-k - q)$.

The change is computed using Eq.(1.7–1.10)

$$\Delta T^{ab}_{\mu\alpha\beta} = -\frac{\delta^{ab}}{16\pi^2}(b_1 - b_2)\epsilon_{\mu\alpha\beta\gamma}(2q + k)^\gamma \tag{1.11}$$

and is induced by the shift in the original integration variable p_μ. Still there is no indication of violation of any global symmetry, just an indication in handling these contributions. One can compute the Ward Identites directly with the same technique by using the shift $p \to q - (q - p)$. The results are trivial once we know of Eq.(1.11), the interesting observation is that the original integration shift shows that one can never satisfy both equation simultaneously

$$
\begin{aligned}
q^\alpha T^{ab}_{\mu\alpha\beta}(k, q) &= -\frac{3\delta^{ab}}{16\pi^2}(1 + b_1 - b_2)\epsilon_{\mu\beta\rho\sigma}q^\sigma k^\rho \\
k^\mu T^{ab}_{\mu\alpha\beta}(k, q) &= \frac{3\delta^{ab}}{8\pi^2}(1 - b_1 + b_2)\epsilon_{\alpha\beta\rho\sigma}q^\sigma k^\rho.
\end{aligned}
\tag{1.12}
$$

The important physical result is that despite the claim of Noether's theorem that there are two sets of conserved currents, namely $SU(3)_c$ vector and $U(1)_A$, one loop calculations indicate that only one of the two can be conserved. Of course one can not violate Gauge symmetry otherwise the theory loses every possible meaning and so the axial current must not be divergenceless. The **anomaly** is that Noether's theorem was wrong, or wrongly applied rather. The violation of the current is not dynamical but purely a loop effect, and it can be show that this is equivalent to the addition of an operator to the QCD lagrangian

$$
\partial^\mu J^{(0)}_{5\mu} = \frac{3\alpha_s}{4\pi}G^a_{\mu\nu}\tilde{G}^{a\mu\nu}, \qquad (\tilde{G}^{a\mu\nu} = \frac{1}{2}\epsilon^{\mu\nu\alpha\beta}G^a_{\alpha\beta}).
\tag{1.13}
$$

1.1.1 Fujikawa's Method

It is instructive to look at the path integral treatment of the issue discussed above, as done in [6]. One defines the theory via the generating functional

$$
Z[a_\mu, A^c_\lambda] = \int [D\psi][D\bar{\psi}] \exp \int \left(\mathcal{L}_{\text{QCD}}(\psi, \bar{\psi}, A^c_\lambda) - a_\mu J^{(0)\mu}_5 \right),
\tag{1.14}
$$

the logarithmic change along the axial current source is given by the functional expansion truncated at first order

$$\ln Z[a_\mu - \partial_\mu\beta, A_\lambda^c] - \ln Z[a_\mu, A_\lambda^c] =$$
$$\int d^4x \partial_\mu \beta(x) \frac{\delta}{\delta a_\mu} \ln(Z[a_\nu, A_\lambda^c])\,|_{a_\nu=0} = -i \int d^4x \beta(x) \partial_\mu \bar{J}_5^{\mu(0)}(x), \tag{1.15}$$

where $-i\bar{J}_5^{\mu(0)}(x)$ is the functional derivative that appears in Eq.(1.15).

The two gluon matrix described above is given by

$$T_{\mu\alpha\beta}^{ab}(x, y, z) = (i)^2 \left[\frac{\delta^2}{\delta A_a^\alpha(y) \delta A_b^\beta(z)} \bar{J}_5^{\mu(0)}(x) \right]_{A_\lambda^c=a_\nu=0}. \tag{1.16}$$

Solving for $\bar{J}_5^{\mu(0)}(x)$ is done by parametrizing the β transformation inside the fermionic part of the lagrangian, meaning that

$$\mathcal{L}_{\text{QCD}}(\psi, \bar{\psi}, A_\mu^c) + \partial^\mu \beta \bar{J}_5^{\mu(0)}(x) = \mathcal{L}_{\text{QCD}}(\psi', \bar{\psi}', A_\mu^c) \tag{1.17}$$

where

$$\psi' = e^{-i\beta\gamma_5}\psi$$
$$\bar{\psi}' = \bar{\psi}e^{-i\beta\gamma_5}. \tag{1.18}$$

Furthermore, one needs to change the path integration from $\psi \to \psi'$. As such, one should keep track of an eventual Jacobian $\mathcal{J}$ associated with this operation

$$\int [D\psi][D\bar{\psi}] = \int [D\psi'][D\bar{\psi}']\mathcal{J},$$

if the jacobian does not depend on the fermion fields one finds that

$$Z[a_\mu - \partial_\beta, A_\lambda^c] = \mathcal{J}Z[a_\mu, A_\lambda^c], \tag{1.19}$$

meaning that

$$\ln \mathcal{J} = -i \int d^4x \beta(x) \partial_\mu \bar{J}_5^{(0)\mu}(x). \tag{1.20}$$

The lesson here is that the quantum current $\bar{J}_5^{(0)\mu}(x)$ will have zero divergence if and only if the Lagrangian **and** the measure of the path integral are invariant (i.e. $\mathcal{J} = 1$) under the $U(1)_A$ transformation. If both the conditions are realised the symmetry is preserved at the quantum mechanical level. It is easy to understand that all the classical symmetries will satisfy the condition relative to the Lagrangian, so that the jacobian of a transformation will be the condition to determine if a symmetry will translate consistently to the quantum theory. In the case at hand the jacobian, if properly renormalised, has the form

$$\mathcal{J} = \exp(-2i \operatorname{tr} \beta\gamma_5) = \exp\left[-i \int d^4x \beta(x) \frac{3\alpha_s}{4\pi} G_{\mu\nu}^a \tilde{G}^{a\mu\nu}\right], \tag{1.21}$$

from here one reads off the current divergence

$$\partial^\mu \bar{J}_{5\mu}^{(0)}(x) = \frac{3\alpha_s}{4\pi} G_{\mu\nu}^a \tilde{G}^{a\mu\nu}. \tag{1.22}$$

The final task is to compute the regularised jacobian, as it will be a divergent quantity. From the Eq.(1.18) one recovers the formal expression

$$\mathcal{J} = \left[\det\left(e^{i\beta\gamma_5}\right)\right]^{-1} \left[\det\left(e^{i\beta\gamma_5}\right)\right]^{-1}. \tag{1.23}$$

The determinant runs over all the indices of the object, namely the 4×4 Dirac indices, the three flavor, color and the spacetime index (i.e. the position x^μ). For finite objects this can be made less formal by using $\det \mathbf{C} = \exp(\operatorname{tr} \ln \mathbf{C})$. This identity allows for the expression

$$\mathcal{J} = \exp(-2i \operatorname{tr} \beta\gamma_5). \tag{1.24}$$

The trace symbol indicates a sum over flavor space, Dirac index, colour and spacetime index,

$$\mathcal{J} = \exp\left(-2i\operatorname{Tr}' \int d^4x \, \langle x| \, \beta\gamma^5 \, |x\rangle\right), \tag{1.25}$$

where Tr' is now the sum over the discrete flavor, colour and Dirac indices.

To regulate the calculation a high energy eigenmode removal via a gauge invariant cutoff is introduced. So the final formal expression is

$$\mathcal{J} = \lim_{M \to \infty} \exp\left(-2i\mathrm{Tr}' \int d^4x \, \langle x| \, \beta\gamma^5 e^{-(\slashed{D}/M)^2} \, |x\rangle\right), \qquad (1.26)$$

where $\slashed{D}$ is the QCD covariant derivative. Using the heat kernel expansion one gets that

$$
\begin{aligned}
\mathcal{J} &= \exp\left(\frac{1}{16\pi^2} \int d^4x \beta(x) \mathrm{Tr}'\left(\gamma^5 \frac{g_s^3 \lambda^a \lambda^b}{16} \sigma^{\mu\nu} G^a_{\mu\nu} \sigma^{\alpha\beta} G^b_{\alpha\beta}\right)\right), \\
&= \exp\left(-\frac{1}{16\pi^2} \int d^4x \beta(x) 3 \cdot 2\delta^{ab} \cdot 4i\epsilon^{\mu\nu\alpha\beta} \frac{g_s^2}{16} G^a_{\mu\nu} G^b_{\alpha\beta}\right) \qquad (1.27) \\
&= \exp\left(-i \int d^4x \, \beta(x) \, \frac{3\alpha_s}{4\pi} \, G^a_{\mu\nu} \tilde{G}^{a\mu\nu}\right).
\end{aligned}
$$

The fact that this is not the identity means that the symmetry is not conserved at the quantum level. If one includes quark masses the anomaly equation is

$$\partial_\mu \bar{J}_5^{(0)\mu}(x) = 2i(m_u \bar{u}\gamma^5 u + m_d \bar{d}\gamma^5 d + m_s \bar{s}\gamma^5 s) + \frac{3\alpha_s}{4\pi} \, G^a_{\mu\nu} \tilde{G}^{a\mu\nu}, \qquad (1.28)$$

meaning that the IR and the UV contribution to the anomaly do not talk to each other. To generalize the result one can define

$$V_\mu^{(b)} = \bar{\psi}\gamma_\mu T_V^{(b)}\psi, \qquad\qquad A_\mu^{(b)} = \bar{\psi}\gamma_\mu\gamma^5 T_A^{(b)}\psi, \qquad (1.29)$$

where $T_V^{(b)}$ and $T_A^{(b)}$ are matrices in the quark flavor space. The anomalous couplings for the currents are

$$
\begin{aligned}
\partial^\mu A_\mu^{(b)} &= \frac{D^{bcd}}{16\pi^2}\epsilon^{\mu\nu\alpha\beta} G^c_{\mu\nu} G^d_{\alpha\beta} + \text{masses} \\
D^{bcd} &= \frac{N_c}{2} \mathrm{Tr}\left(T_A^{(b)}\{T_V^{(c)}, T_V^{(d)}\}\right),
\end{aligned}
\qquad (1.30)
$$

where N_c is the number of colors.

This shows how symmetries of a classical Lagrangian are not always sym-

metries of the full quantum theory. Anomalies spoil the classical symmetry, appearing in perturbation theory within divergent Feynman diagrams. The anomalous breaking is not a dynamical breaking of the symmetry associated with a phase transition, and one should not expect a Goldstone boson. From the path-integral point of view a more rigorous picture is extracted, the symmetry never existed in the first place as the generating functional was never invariant under the transformation law. As such Noether's theorem needs to be supplemented with the jacobian to test the symmetries of a Quantum Theory.

1.2   The θ vacuum

Gauge theories with particularly simple gauge groups, QED and theories with local $U(1)$'s, are completely described by their Lie Algebra, or their differentiable structure. More complicated ones are affected also by global properties of the symmetry space, in particular topological properties play a fundamental role. One is generally concerned with gauge transformations that are connected to the group's identity via infinitesimal steps. What happens if one considers the disconnected parts of the group? Will these topological properties have any effect on the phenomenology? To answer these questions one has to look at "large" gauge transformations which, in the $SU(3)_c$ case at hand, change the color gauge fields in a more drastic, disconnected–to–the–identity fashion [11, 12]. For example the gauge transformation generated by

$$\Lambda_1(\mathbf{x}) = \frac{\mathbf{x}^2 - d^2}{\mathbf{x}^2 + d^2} + 2id\frac{\boldsymbol{\tau} \cdot \mathbf{x}}{\mathbf{x}^2 + d^2}, \tag{1.31}$$

where d is an arbitrary parameter and $\boldsymbol{\tau}$ is an $SU(2)$ Pauli matrix in any $SU(2)$ subgroup of $SU(3)$. Such a transformation is given only by the non–

homogeneous part and changes the null potential into

$$
\begin{aligned}
\mathbf{A}_j^{(1)}(\mathbf{x}) &= -\frac{i}{g_s}(\boldsymbol{\nabla}_j\Lambda_1(\mathbf{x}))\Lambda_1(\mathbf{x})^{-1} \\
&= -\frac{2d}{g_s(\mathbf{x}^2+d^2)^2}[\boldsymbol{\tau}_j(d^2-\mathbf{x}^2)+2\mathbf{x}_j(\boldsymbol{\tau}\cdot\mathbf{x})-2d(\boldsymbol{\tau}\cdot\mathbf{x})_j],
\end{aligned}
\tag{1.32}
$$

where

$$
\mathbf{A}_\mu = A_\mu^a\frac{\boldsymbol{\lambda}^a}{2}.
\tag{1.33}
$$

This pure gauge potential lies in an $SU(2)$ subgroup of the full color $SU(3)$ group, and is "large" in the sense that it cannot be brought continuously into the identity. The $\boldsymbol{\tau}\cdot\mathbf{x}$ factor couples the internal colour indices to the spatial position such that a path in coordinate space implies a corresponding path in the $SU(2)$ color subspace. Associated with every gauge potential $\mathbf{A}_\mu$ is a conserved topological charge called the *winding number*,

$$
n = \frac{ig_s^3}{24\pi^2}\int d^3x\,\mathrm{Tr}\left[\mathbf{A}_i(x)\mathbf{A}_j(x)\mathbf{A}_k(x)\right]\epsilon^{ijk}.
\tag{1.34}
$$

It can be demonstrated by direct substitution that the gauge field of Eq.(1.32) corresponds to the value $n=1$. Fields with any integer value of the winding number n can be obtained by repeated applications of $\Lambda_1(x)$, i.e.

$$
\Lambda_n(\mathbf{x}) = [\Lambda_1(\mathbf{x})]^n.
\tag{1.35}
$$

All gauge potentials can be classified into disjoint sectors labeled by their winding number. The existence of these distinct classes has interesting consequences. Namely consider a gluon field that a $t\to-\infty$ as the zero potential $\mathbf{A}(\mathbf{x})=0$, has some interpolating $\mathbf{A}(\mathbf{x},t)$ for intermediate times, and ends up at $t\to+\infty$ lying in the gauge-equivalent configuration $\mathbf{A}(x)=\mathbf{A}^{(1)}(x)$, these configurations are known to exist [13]. Then the following integral can be shown to be nonvanishing:

$$
\frac{g_s^2}{32\pi^2}\int d^4x\,G_{\mu\nu}^a\tilde{G}^{a\mu\nu}.
$$

This is surprising since the integral is a total divergence as $G\tilde{G}$ can be written as

$$G_{\mu\nu}^a \tilde{G}^{a\mu\nu} = \partial_\mu K^\mu, \qquad K^\mu = \epsilon^{\mu\nu\lambda\sigma} \left[A_\nu^a G_{\lambda\sigma}^a + \frac{1}{3} g_s f_{abc} A_\nu^a A_\lambda^b A_\sigma^c \right], \qquad (1.36)$$

as thus the integral can be written as a surface integral at $t = \pm\infty$:

$$
\begin{aligned}
\frac{g_s^2}{32\pi^2} \int d^4x \; G_{\mu\nu}^a \tilde{G}^{a\mu\nu} &= \frac{g_s^2}{32\pi^2} \int d^4x \; \partial_\mu K^\mu \\
&= \frac{g_s^2}{32\pi^2} \int d^3x \; K^0 \Big|_{t=-\infty}^{t=\infty} \\
&= i \frac{g_s^3}{24\pi^2} \int d^3x \; \epsilon^{ijk} \, \text{Tr} \left(\mathbf{A}_i^{(1)}(x) \mathbf{A}_j^{(1)}(x) \mathbf{A}_k^{(1)}(x) \right) \\
&= 1.
\end{aligned}
$$

$$(1.37)$$

More generally, the integral of $G\tilde{G}$ gives the change in the winding number

$$\frac{g_s^2}{32\pi^2} \int d^4x \; G_{\mu\nu}^a \tilde{G}^{a\mu\nu} = \frac{g_s^2}{32\pi^2} \int d^3x \; K^0 \Big|_{t=-\infty}^{t=\infty} = n_+ - n_- \qquad (1.38)$$

between asymptotic gauge-field configurations.

Thus the vacuum state vector will be characterized by configurations of gluon fields, which fall into classes labelled by winding number. Moreover one can associate unitary operators $\{U_n\}$, acting on state vectors, to gauge transformations $\{\Lambda_n\}$ so that in general

$$U_1 \ket{n} = \ket{n+1}. \qquad (1.39)$$

This implies that a gauge-invariant vacuum state requires contributions from all the classes in a coherent manner

$$\ket{\theta} = \sum_n e^{-in\theta} \ket{n} \qquad (1.40)$$

so that the theta state is invariant under gauge transformation up to a global

phase parametrized by the arbitrary θ parameter. This means that a gauge invariant vacuum must contain coherent contributions from all the separated topological classes. The nontrivial vacuum structure requires an extra input in defining the theory of QCD: the QCD Lagrangian, the scale Λ_{QCD} and finally the vacuum label θ. In a path–integral representation the $\theta = 0$ vacuum would imply transition elements of the form

$$\langle \theta = 0 | \, X \, | \theta = 0 \rangle = \int [D\psi][D\bar{\psi}][DA_\mu] X e^{iS_{QCD}} = \sum_{m,n} \langle m | \, X \, | n \rangle . \quad (1.41)$$

A different value of θ corresponds to a phase in the decomposition

$$\langle \theta | \, X \, | \theta \rangle = \sum_{m,n} e^{i(m-n)\theta} \langle m | \, X \, | n \rangle . \quad (1.42)$$

However, this phase can be accounted for in the path integral by the addition of a new term to S_{QCD}. In particular one can actually write

$$\langle \theta | \, X \, | \theta \rangle = \int [D\psi][D\bar{\psi}][DA_\mu] X e^{iS_{QCD} + i \frac{g_s^2}{32\pi^2} \theta \int d^4 x G_{\mu\nu}^a \tilde{G}^{a\mu\nu}} , \quad (1.43)$$

where X is a generic operator. It has been shown that to implement correctly the computation with the θ dependence one can simply follow the standard path–integral approach with a modified action depending on the vacuum parameter

$$\mathcal{L}_{QCD} = \mathcal{L}_{QCD}^{\theta=0} + \theta \frac{g_s^2}{32\pi^2} G_{\mu\nu}^a \tilde{G}^{a\mu\nu} . \quad (1.44)$$

The θ parameter is considered a coupling constant, and as such there is an important distinction between the vacua of QCD and the different possible vacuum states of a theory with spontaneous symmetry breaking. In the latter case the possible vacuum expectation values allowed from the potential simply distinguish between different equivalent states of a same theory. In QCD instead each value of θ produces different amplitudes values similarly to how a change in Λ_{QCD} would produce different amplitudes. This way different values of θ represent different possible theories that Nature might choose.

1.2.1 Chiral rotations and θ vacua

There is a connection between the axial anomaly and the presence of a θ vacuum. In a massless theory with N_f fermions the $U(1)$ axial current

$$J_{5\mu}^{(0)} = \sum_k \bar{\psi}_k \gamma_\mu \gamma^5 \psi_k \tag{1.45}$$

is not conserved due to the anomaly

$$\partial^\mu J_{5\mu}^{(0)} = \frac{N_f \alpha_s}{4\pi} G_{a\mu\nu} \tilde{G}^{a\mu\nu}. \tag{1.46}$$

However one can define a new conserved current using Eq.(1.36) as

$$\tilde{J}_{5\mu}^{(0)} = J_{5\mu}^{(0)} - \frac{N_f \alpha_s}{4\pi} K_\mu. \tag{1.47}$$

The associated charge

$$\tilde{Q}_5 = \int d^3x \, \tilde{J}_{5,0}(x) \tag{1.48}$$

and the current itself are conserved but are not gauge–invariant. Under a Λ_1 transformation, defined in Eq.(1.39), the operator $\tilde{Q}_5$ is modified

$$U_1 \tilde{Q}_5 U_1^{-1} = \tilde{Q}_5 - 2N_f. \tag{1.49}$$

As such the different θ vacua of the theory are related by chiral transformations

$$U_1 e^{i\alpha\tilde{Q}_5} |\theta\rangle = U_1 e^{i\alpha\tilde{Q}_5} U_1^{-1} U_1 |\theta\rangle = e^{i\theta - 2N_f\alpha} e^{i\alpha\tilde{Q}_5} |\theta\rangle \tag{1.50}$$

or rather, using the fact that

$$U_1 |\theta\rangle = e^{i\theta} |\theta\rangle \tag{1.51}$$

one obtains

$$e^{i\alpha\tilde{Q}_5} |\theta\rangle = |\theta - 2N_f\alpha\rangle. \tag{1.52}$$

The lesson is that in Yang–Mills theories there are inequivalent pure gauge field configurations that have to be classified in different topological classes.

This in turn means that finding a gauge invariant vacuum state is not a trivial task. The anomaly between $SU(3)_c$ and $U(1)_A$ leads to non trivial transformations laws of the gauge invariant vacuum under both symmetries. The special case of massless quarks is free from these difficulties as one can rotate away any effect due to θ, but massive theories will unavoidably have a term that is CP–violating. In summary the non–trivial vacuum of Yang–Mills theories requires that the path integral is extended to include gauge field configurations with non zero quantum charges, and in turn requires the inclusion in the effective action of the CP violating term $G\tilde{G}$.

1.3 The $U(1)$ puzzle

An argument supporting the picture discussed in the previous sections is the fact that there is no light state corresponding to the Nambu–Goldstone boson of a spontaneously broken $U(1)_A$ flavor symmetry in the hadronic spectrum. This effect was dubbed the $U(1)$ puzzle, or the $U(1)$ problem by Weinberg [14]. The solution is easily seen since $U(1)_A$ was never a symmetry of the theory due to the topologically non–trivial structure of QCD. The global anomaly of QCD changes the prediction of the theory and in particular the spectrum of the Low–Energy Chiral Lagrangian. Once more consider the massless QCD Lagrangian with the 3 lightest flavor

$$\mathcal{L}_{\text{QCD}} = -\frac{1}{4}(F^a_{\mu\nu})^2 + i\bar{q}^j_L \slashed{D} q^i_L + i\bar{q}^j_R \slashed{D} q^i_R, \tag{1.53}$$

where the chiral fermions are the fundamental degree of freedom. The symmetry of the classical theory is $U(3)_L \times U(3)_R$, and the QCD vacuum is $\langle \bar{q}_L q_R \rangle \approx V^3 \approx \Lambda^3_{QCD}$, spontaneously breaking the flavor group into it's diagonal part, $U(3)_{\text{diagonal}}$. Thus there should be nine massless Goldstone boson, written as a matrix as $\pi^a T^a$. In particular the diagonal part of the matrix is associated with the neutral ones, of which there are three. Since quarks do have masses, the global symmetry being broken is only approximate, and as such the Goldstone bosons will have masses according to the Gell-Mann-Oakes-Renner relation $m^2_\pi F^2_\pi \approx V^3 m_q$. The experimental spectrum is however in strong disagreement with this prediction, at least for the

heaviest neutral particle, the η'. In theory its mass should be bounded by $\sqrt{3}m_{\pi^0}$ to around 200 MeV, but experiments measure it closer to 1 GeV. The heaviness of the η'. is sometimes called the $U(1)$ puzzle, since one of the Goldstone boson associated with a $U(1)$ factor of $U(3)_{\text{diagonal}}$ is missing. The solution is rather simple, The true symmetry of the theory is not the one we assumed because the axial $U(1)$ is anomalous, as such the mass of the particle associated to it will also get contributions from the triangle diagram $SU(3)_c^2 U(1)_A$. The physics of topologically non trivial gauge configurations has a very direct impact on the spectrum of QCD, shifting the value of the η' mass. One can study the effects using non-perturbative techniques and obtains a satisfactory prediction [15].

1.3.1   QCD vacuum dependence on θ

It should be noted that the dependence of the QCD vacuum energy density on the θ parameter, $E(\theta)$, is extremely important in discussing the axion. Indeed the axion VEV will play the role of an effective θ, so that the same result established for the QCD angle will easily translate to the axion. In the large volume limit, the energy density is related to the Euclidean functional generator, $Z(\theta)$, via (see [13])

$$Z(\theta) = \lim_{V_4 \to \infty} e^{-E(\theta)V_4}. \tag{1.54}$$

The same quantity can be taken in the Euclidean path–integral representation for pure gauge field configurations

$$Z(\theta) = \int \mathcal{D}A \exp\left(-\frac{1}{4} \int d^4 x\, GG + i\theta \frac{g_s^2}{32\pi^2} \int d^4 x\, G\tilde{G} \right)$$
$$\simeq \exp\left(-\frac{8\pi^2}{g_s^2} \right) e^{i\theta}, \tag{1.55}$$

where in the last step one considers the semi–classical approximation, taking only the contribution of a $\nu = 1$ instanton. Finally one should use the dilute–instanton gas approximation, asking the instantons centers to be well

separated. One gets

$$E(\theta) = -2K e^{\frac{-8\pi^2}{g_s^2}} \cos\left(\theta\right),\tag{1.56}$$

where K is a positive constant encoding Jacobian factors due to the instanton zero modes. It turns out that the vacuum energy of QCD is periodic in θ, and has a global minimum for $\theta = 0$. These results will still be true in the case of an axion, even with the theory completed with fermions.

1.4 The strong CP problem

General $\theta \neq 0$ will induce CP violation, or equivalently T violation. The strength of these violations is known to be miniscule, even by the standards of weak interaction. A measurable consequence of a non–zero θ is found in nuclear physics where the CP Violating phase induces directly a permanent electric dipole moment to the neutron. In the Standard Model nothing is forcing θ to be zero, as other sources of CP violation are present in the theory, and as such it seems unnatural for it to be so small by chance without any dynamical reason. Given that θ could be anywhere in $[0, 2\pi]$ having $\theta \approx 0$ is a naturalness problem, the strong CP problem is thus a fine tuning problem. One might assume that QCD does not violate CP, thus imposing $\theta = 0$ a priori. This solution is however not stable under higher order electroweak radiative corrections. The problem gets worse in the full SM theory, as the quark mass matrix itself will shift the value of θ by a finite amount. This process is a consequence of the diagonalization of the quarks mass matrices after the electroweak symmetry breaking. Indeed when the Higgs field condenses the Yukawa's between the doublets and the fermions will generate mass matrices that are neither diagonal nor CP–invariant. To shift the CP violating part in the weak mixing matrix and to diagonalize the matrices one has to perform independent left and right–handed transformations. One encounters an axial rotation in the diagonalization process and as discussed before this induces a shift in the value of θ. To recover the contribution to

the $G\tilde{G}$ operator from the fermionic sector consider the following:

$$\psi_L = S_L^\dagger \psi_L', \qquad \psi_R = S_R^\dagger \psi_R' \qquad \mathbf{m} = S_L^\dagger \mathbf{m}' S_R, \tag{1.57}$$

where primed quantities are the one in the flavour basis, i.e. non diagonal, $\mathbf{m}$ is thus diagonal and is defined to combine all the mass matrices spanning the whole flavor group. The $U(N)$ transformations for L and R quarks have different $U(1)$ factors associated with them that amount to an axial rotation $U(1)_A = e^{i(\phi_R - \phi_L)}$, leading to a change in the θ parameter

$$\theta \to \bar\theta = \theta + 2N_f(\phi_L - \phi_R). \tag{1.58}$$

More generally the shift is proportional to the phase present in the mass matrix that one wants to rotate away, as such the role of $2N_f(\phi_L - \phi_R)$ is generally played by $\arg(\det(\mathbf{m}'))$. So the effective parameter regulating CP violation in the QCD sector is actually $\bar\theta$ composed of two unrelated phases that have to cancel almost exactly without a dynamical reason.

As discussed previously nuclear physics is almost indifferent to $\bar\theta$ but a non–zero value implies a permanent electric dipole moment for the neutron. In fact the CP–violating low energy operator

$$H = -d_n \vec{E} \cdot \vec{S} \tag{1.59}$$

that in relativistic form is

$$\mathcal{L} = -\frac{i}{2} d_n \bar{n} \sigma_{\mu\nu} \gamma_5 n F^{\mu\nu}, \tag{1.60}$$

can be experimentally bound to be $|d_n| < 3 \cdot 10^{-26} e$ cm [16], while the theoretical prediction is $|d_n| = 2.4 \cdot 10^{-16} \bar\theta e$ cm. The bound derived from this simple scenario is

$$\bar\theta < 10^{-10}, \tag{1.61}$$

which is of course not a natural value. There are three candidates solutions to the problem.

1. $\mathbf{m_u} = \mathbf{0}$. If one of the quarks is massless than the flavor group can be broken down in two pieces, $U(N) = U(1) + U(N-1)$. The extra $U(1)$

factor associated with the massless quark could be used to rotate away $\bar{\theta}$. Of course there are no massless quarks so this solution is excluded.

2. **Spontaneously Broken CP** One can assume that CP is a symmetry of the microscopic fundamental theory, but is spontaneously broken. In these scenarios θ can be calculable, and sometimes even small [17–19]. In some string theories, CP is an exact gauge symmetry spontaneously broken in some points of the moduli spaces [20, 21]. This solution is typically excluded since the density of CP preserving states generated by flux vacuua in moduli fixed critical string theory is 10^{-250}. This renders the solution even more unnatural than when we started.

3. **Axions**: An approximate, global symmetry (Peccei-Quinn (PQ)) with a QCD anomaly, gets spontaneously broken. The pseudo–Nambu Goldstone boson which arises from symmetry breaking (the axion) dynamically drives $\bar{\theta} = 0$ in a potential minimum.

Of these solutions the most compelling one seems to be the third one. An introduction of a light scalar particle will prove useful in Cosmology and in Astro–Particle, moreover there is no shortage of light scalar particles predicted by String Theory.

1.4.1   The Axion Solution

The Peccei–Quinn solution to the Strong CP problem [22–25] is to include a new 0^- field $a(x)$, denoted as the *axion field*, with an effective Lagrangian

$$\mathcal{L}^a = \frac{1}{2}(\partial_\mu a)^2 + \frac{g_s^2}{32\pi^2}\frac{a}{f_a}G\tilde{G} + \mathcal{L}(\partial_\mu a, \psi) \qquad (1.62)$$

that is quasi–invariant under the shift $a \to a + cf_a$. Here and in what follows f_a denotes an energy scale, much like the pion decay constant f_π, that will be called the axion decay constant. The shift described above will leave the action invariant up to a term

$$\delta S = c\frac{g_s^2}{32\pi^2}\int d^4x G\tilde{G}. \qquad (1.63)$$

With this set–up it is easy to see how the connection with pure gauge $SU(3)_c$ could relax the Strong CP problem . Indeed one has:

$$\mathcal{L}^a + \mathcal{L}_{QCD} = \mathcal{L}_{QCD}^{\bar{\theta}=0} + \mathcal{L}(\partial_\mu a, \psi) + \left(\frac{a}{f_a} + \bar{\theta}\right)\frac{g_s^2}{32\pi^2}G\tilde{G}, \qquad (1.64)$$

and after a shift the part proportional to $G\tilde{G}$ would be $(\frac{a}{f_a} + \bar{\theta} + c)\frac{g_s^2}{32\pi^2}G\tilde{G}$. Choosing $c = -\bar{\theta}$ would solve the Strong CP problem, provided that $\langle a \rangle = 0$, otherwise CP invariance is again ruined. To prove that $\langle a \rangle = 0$ one can use the Vafa–Witten theorem [26]

$$Z(a) = \int Da \left(\int D\phi e^{-S|_{a=0}+iaG\tilde{G}}\right) = \int Da \left|\int D\phi e^{-S|_{a=0}+iaG\tilde{G}}\right| \leq$$
$$\leq \int Da \int |D\phi e^{-S|_{a=0}+iaG\tilde{G}}| = \int DaD\phi e^{-S_{a=0}} \Rightarrow E(0) \leq E(a),$$
$$(1.65)$$

meaning that the axion potential naturally drives the classical value of the field to zero. In the derivation one has to assume the positiveness of the measure valid only for vector theories, like QCD. The hypothesis is violated in the presence of chiral fermions such as the ones in the Standard Model. Another important way to recover $\langle a \rangle = 0$ is by computing the axion potential using Chiral Lagrangian methods. In doing so a number of model independent insights on axion physics are disclosed. Before exploring the chiral realisation of the theory is somewhat important to know the form of the Lagrangian in Eq.(1.64), and to clarify what types of couplings are expected once a spontaneously broken $U(1)_{PQ}$ is assumed. Consider the associated current J_{PQ}^μ conserved up to anomalous terms

$$\partial_\mu J_{PQ}^\mu = \frac{g_s^2 N}{16\pi^2}G\tilde{G} + \frac{e^2 E}{16\pi^2}F\tilde{F}, \qquad (1.66)$$

where N and E are the QCD and EM anomaly coefficients. From the Goldstone theorem $\langle 0| J_{PQ}^\mu |a\rangle = iv_a p_\mu$, where v_a is the PQ order parameter. It

follows that the effective axion Lagrangian has to contain a piece

$$\mathcal{L}^a \supset \frac{a}{v_a}\frac{g_s^2 N}{16\pi^2}G\tilde{G} + \frac{a}{v_a}\frac{e^2 E}{16\pi^2}F\tilde{F} + \frac{\partial_\mu a}{v_a}J^\mu_{\text{PQ}}, \tag{1.67}$$

due to Eq.(1.66). The specific form of the Peccei–Quinn current will depend on the charges of the PQ symmetric fields. E.g. take a chiral Standard Model field ψ_L. The anomalous current will be

$$J^\mu_{\text{PQ}}\Big|_{\psi_L} = -\bar{\psi}_L\chi_L\gamma_\mu\psi_L, \tag{1.68}$$

where χ_L denotes the PQ charge. It is customary to consider the standard normalization

$$f_a = \frac{v_a}{2N}$$

so that Eq.(1.67) is

$$\begin{aligned}
\mathcal{L}^a &\supset \frac{a}{f_a}\frac{g_s^2}{32\pi^2}G\tilde{G} + \frac{a}{f_a}\frac{e^2 E}{32N\pi^2}F\tilde{F} - \frac{\partial_\mu a}{2Nf_a}(\bar{\psi}_L\chi_L\gamma_\mu\psi_L + \bar{\psi}_R\chi_R\gamma_\mu\psi_R), \\
&= \frac{a}{f_a}\frac{g_s^2}{32\pi^2}G\tilde{G} + \frac{a}{f_a}\frac{c_{0\gamma}}{4}F\tilde{F} + \frac{\partial_\mu a}{2f_a}\bar{\psi}c^0_\psi\gamma_\mu\gamma^5\psi,
\end{aligned} \tag{1.69}$$

where the axion–photon coupling is defined as[1]

$$c^0_\gamma = \frac{\alpha E}{2\pi N}, \tag{1.70}$$

and the axion–fermion one is

$$c^0_\psi = \frac{\chi_L - \chi_R}{2N}. \tag{1.71}$$

1.4.2 Axion potential

For the sake of simplicity let us consider QCD with only the two lightest flavors, where $q = (u, d)^T$ and M_q is the mass matrix diagonal in mass basis.

---

[1]It is customary to indicate the dimensional parameters with c_i's, while the dimensionless ones are typically referred to as $g_i = c_i/f_a$.

The axion effective Lagrangian is

$$\mathcal{L}^a = \frac{1}{2}(\partial_\mu a)^2 + \frac{a}{f_a}\frac{g_s^2}{32\pi^2}G\tilde{G} + \frac{1}{4}g_\gamma^0 aF\tilde{F} + \frac{\partial_\mu a}{2f_a}\bar{q}c_\psi^0\gamma_\mu\gamma^5 q - \bar{q}_L M_q q_R + \text{h.c..} \quad (1.72)$$

One can shift away the $aG\tilde{G}$ term via an axial redefinition of the quark fields:

$$q \to e^{i\gamma^5 a/(2f_a)Q_a}q. \quad (1.73)$$

This transformation generates a term

$$\delta\mathcal{L} = -\frac{g_s^2\,\text{Tr}(Q_a)}{32\pi^2}\frac{a}{f_a}G\tilde{G}, \quad (1.74)$$

that exactly cancels the $G\tilde{G}$ dependence in Eq.(1.72), once $\text{Tr}\{Q_a\} = 1$. Since this transformation is also QED anomalous it will affect the $F\tilde{F}$ term, and generate different interactions with the quarks. In particular

$$\mathcal{L}^a = \frac{1}{2}(\partial_\mu a)^2 + \frac{1}{4}g_\gamma aF\tilde{F} + \frac{\partial_\mu a}{2f_a}\bar{q}c_\psi\gamma_\mu\gamma^5 q - \bar{q}_L M_a q_R + \text{h.c.}, \quad (1.75)$$

where all the parameters are now modified, or axion–dressed. In particular one has

$$g_\gamma = g_\gamma^0 - (2N_c)\frac{\alpha}{2\pi f_a}\,\text{Tr}(Q_a Q^2), \quad \text{where} \quad Q = \text{diag}(2/3, -1/3)$$
$$c_q = c_q^0 - Q_a, \quad (1.76)$$
$$M_a = e^{i\gamma^5 a/(2f_a)Q_a}M_q e^{i\gamma^5 a/(2f_a)Q_a},$$

where N_c indicates the number of colours. The axial quark current is decomposed in an iso–singlet and an iso–triplet component

$$\bar{q}c_q\gamma_\mu\gamma^5 q = \frac{1}{2}\,\text{Tr}(c_q)\bar{q}\gamma_\mu\gamma^5 q + \frac{1}{2}\,\text{Tr}(\sigma^a c_q)\bar{q}\gamma_\mu\gamma^5\sigma^a q. \quad (1.77)$$

One substitutes Eq.(1.77) in Eq.(1.75) and maps it onto the Chiral Lagrangian [27, 28]

$$\mathcal{L}^a_{\chi\text{PT}} = \frac{f_\pi^2}{4}\left(\text{Tr}\left((D^\mu U)^\dagger D_\mu U\right) + 2B_0\,\text{Tr}\left(UM_a^\dagger + M_a U^\dagger\right)\right) + \frac{\partial_\mu a}{2f_a}\frac{1}{2}\,\text{Tr}[c_q\sigma^a]J_a^\mu,$$

(1.78)

where B_0 is a constant related to the condensate and the singlet has been excluded since it refers to the heavy η'. In Eq.(1.78) one identifies the current coupled to the axion via its transformation properties, in particular it has to transform under flavor $SU(2)_L \otimes SU(2)_R$ as the quark iso–triplet would transform. One can show that the pionic iso–triplet current is

$$J_\mu^a = i\frac{f_\pi^2}{2}\,\text{Tr}\left[\sigma^a(UD_\mu U^\dagger - U^\dagger D_\mu U)\right].$$

(1.79)

The parametrization for the pion field is

$$U = \exp\left(i\pi^a\sigma^a/f_a\right) = \mathbb{1}\cos\frac{\pi}{f_\pi} + i\frac{\sigma^a\pi^a}{\pi}\sin\frac{\pi}{f_\pi},$$

(1.80)

with $\pi = \sqrt{(\pi^0)^2 + 2\pi^+\pi^-}$, $f_\pi = 93\text{MeV}$ and $D_\mu U = \partial_\mu U + ieA_\mu[Q, U]$.

To get the axion–pion potential expand the non–derivative part of Eq.(1.78), consider:

$$2B_0\frac{f_\pi^2}{4}\,\text{Tr}\left(UM_a^\dagger + M_a U^\dagger\right) = B_0 f_\pi^2(m_u + m_d) - \frac{1}{2}B_0(m_u + m_d)\pi^2$$
$$- \frac{i}{4}B_0\frac{f_\pi^2}{f_a}a\,\text{Tr}(U\{Q_a, M_q\}) + \text{h.c.} + \dots$$

(1.81)

Usually one takes $Q_a = M_q^{-1}/\text{Tr}\left(M_q^{-1}\right)$. This choice cancels any coupling between an axion and an arbitrary number of pions. Such a coupling is generated by the term

$$\left(\frac{i}{4}B_0\frac{f_\pi^2}{f_a}a\,\text{Tr}(U\{Q_a, M_q\}) + \text{h.c.}\right)\bigg|_{Q_a = M_q^{-1}/\text{Tr}\left(M_q^{-1}\right)}$$
$$= i\frac{f_\pi^2}{f_a}2(m_u + m_d)a\,\text{Tr}\left[\mathbb{1}\cos\frac{\pi}{f_\pi} + i\frac{\sigma^a\pi^a}{\pi}\sin\frac{\pi}{f_\pi}\right].$$

(1.82)

Substituting Eq.(1.80) in Eq.(1.82) one can see that the whole contribution is zero, either because $\text{Tr}[\sigma^a] = 0$ for odd numbers of π or because the contribution is purely imaginary and the Hermitean conjugate will put it to zero. This choice of Q_a eliminates the axion–pion mixing from the theory, while the expansion in Eq.(1.81) makes the $SU(2)$ symmetric pions masses $m_\pi^2 = B_0(m_u + m_d)$ at LO in the chiral expansion. The axion–pion potential can be computed exactly with this choice of Q_a:

$$
\begin{aligned}
V(a, \pi) &= -2B_0 \frac{f_\pi^2}{4} \text{Tr}\big(U M_a^\dagger + M_a U^\dagger\big) \\
&= -\frac{m_\pi^2 f_\pi^2}{m_u + m_d} \left\{ \left[m_u \cos\left(\frac{m_d}{m_u + m_d} \frac{a}{f_a}\right) + m_d \cos\left(\frac{m_u}{m_u + m_d} \frac{a}{f_a}\right) \right] \cos\left(\frac{\pi}{f_\pi}\right) \right. \\
&\quad \left. + \frac{\pi^0}{\pi} \left[m_u \sin\left(\frac{m_d}{m_u + m_d} \frac{a}{f_a}\right) - m_d \sin\left(\frac{m_u}{m_u + m_d} \frac{a}{f_a}\right) \right] \sin\left(\frac{\pi}{f_\pi}\right) \right\}.
\end{aligned}
$$
$$(1.83)$$

To obtain the axion mass value expand Eq.(1.83) to order two in $\frac{a}{f_a}$, the first order in $\frac{a}{f_a}$ is zero for construction. The axion–pion potential, up to order two is

$$
V(a, \pi) = -m_\pi^2 f_\pi^2 \cos\left(\frac{\pi}{f_\pi}\right) + \frac{1}{2} \frac{m_u m_d}{(m_u + m_d)^2} \frac{m_\pi^2 f_\pi^2}{f_a^2} a^2 \cos\left(\frac{\pi}{f_\pi}\right) + \mathcal{O}\left(\frac{a^3}{f_a^3}\right)
$$
$$(1.84)$$

Setting the pion field to its ground state, $\pi = 0$, yields the axion mass squared

$$
m_a^2 = \frac{m_u m_d}{(m_u + m_d)^2} \frac{m_\pi^2 f_\pi^2}{f_a^2} \implies m_a \simeq 5.7 \left(\frac{10^{12} \text{GeV}}{f_a}\right) \mu\text{eV}, \qquad (1.85)
$$

so for QCD–axions the mass and the Peccei–Quinn scale are not two independent parameters. An alternative expression for the axion–pion potential, corresponding to the choice $Q_a = \frac{1}{2}\text{diag}(1, 1)$, discussed in [29], gives

$$
V(a, \pi^0) = -m_\pi^2 f_\pi^2 \sqrt{1 - \frac{4 m_u m_d}{(m_u + m_d)^2} \sin^2\left(\frac{a}{2f_a}\right)} \cos\left(\frac{\pi^0}{f_\pi} - \phi_a\right), \quad (1.86)
$$

where $\tan \phi_a = \frac{m_u - m_d}{m_u + m_d} \tan(a/(2f_a))$. The minimum now is clearly given by

the point in field space $(a, \pi^0) = (0, 0)$. Moreover along the pion ground state $\pi^0 = f_\pi \phi_a$ the axion potential is

$$V(a, \pi^0) = -m_\pi^2 f_\pi^2 \sqrt{1 - \frac{4m_u m_d}{(m_u + m_d)^2} \sin^2 \left(\frac{a}{2f_a} \right)}. \qquad (1.87)$$

Expanding this solution at leading order and the "single instanton" one, the $\cos \theta$ in Eq.(1.56), one sees that for small values of a the approximations are converging. For larger values of a different non–perturbative effects enter the potential and the semiclassical dilute–instanton gass approximation breaks down as topologically non trivial configuration will give non zero contribution in the path integral.

1.5   UV Complete Axion Models

In Sec. 1.4.1 a number of model independent properties were discussed, based purely on the structure of QCD, on the anomaly coefficients and on the matter content of the theory. It is nevertheless important to study some UV complete axion models to prove that at least one exists and to study how the coupling of the high energy theory are related to the phenomenological ones. This section will explore the two benchmarks UV completion for the axion effective Lagrangian of Eq.(1.72). The simplest implementation of the Peccei–Quinn symmetry is given by the Weinberg–Wilczek (WW) model [22, 23], whre the QCD anomaly of the $U(1)_{\mathrm{PQ}}$ current is generated by SM quarks charged under the PQ symmetry. The scalar sector is enlarged with an extra Higgs doublet carrying the additional $U(1)_{\mathrm{PQ}}$. In the WW model the axion decay constant is of the order of the electroweak scale $v \simeq 246$ GeV. Indeed f_a is found to be $f_a = v/6 \sin(2\beta)$, where $\beta = \arctan(v_u/v_d)$. This model was not suppressed enough and was quickly ruled out by beam dump experiments and rare meson decays [30, 31]. This led to the so called "invisible axion" models where the PQ symmetry breaking is decoupled from the electroweak scale via the introduction of a Standard Model singlet scalar field, acquiring a VEV at very high scales $v_a \ f_a \gg v$. Then the axion's interactions are as suppressed as $\frac{1}{f_a}$, see Eqs(1.69–1.70).

UV completion of the axion effective Lagrangian comes down to two separated classes. The Kim-Shifman-Vainshtein-Zakharov (KSVZ) [32, 33] type requires new heavy coloured fermions to carry the anomaly, while Dine-Fischler-Srednicki-Zhitnitsky (DFSZ) [34, 35] type embeds the anomaly onto the Standard Model quarks, similarly to the WW–model.

1.5.1 KSVZ axion

The KSVZ model extends the Standard Model field content with a vector–like fermion $\mathcal{Q} = \mathcal{Q}_L + \mathcal{Q}_R$ in the fundamental of colour, singlet of $SU(2)_L$ and neutral under hypercharge: $\mathcal{Q}$ $(3, 1, 0)$, and a Standard Model Singlet complex scalar Φ $(1, 1, 0)$. The Lagrangian of the KSVZ model is

$$\mathcal{L}^{\text{KSVZ}} = |\partial_\mu \Phi|^2 + \bar{\mathcal{Q}} i \slashed{D} \mathcal{Q} - (y_\mathcal{Q} \bar{\mathcal{Q}}_L \mathcal{Q}_R \Phi + \text{h.c.}) - V(\Phi) \tag{1.88}$$

and it has the $U(1)_{\text{PQ}}$ symmetry

$$\Phi \to e^{ia}\Phi, \qquad \mathcal{Q}_L \to e^{ia/2}\mathcal{Q}_L, \qquad \mathcal{Q}_R \to e^{-ia/2}\mathcal{Q}_R. \tag{1.89}$$

The $U(1)_{\mathcal{PQ}}$ symmetric, spontaneous symmetry–breaking–ready potential is

$$V(\Phi) = \lambda_\Phi \left(|\Phi|^2 - \frac{v_a^2}{2} \right)^2, \tag{1.90}$$

with v_a as the order parameter. Considering polar coordinates for the scalar field

$$\Phi = \frac{1}{\sqrt{2}}(v_a + \rho_a)e^{ia/v_a}, \tag{1.91}$$

the axion field a correspond to the massless, at tree level, Goldstone boson, while the radial mode ρ_a picks up a mass $m_{\rho_a} = \sqrt{2\lambda_\Phi} v_a$. In the condesed phase the fermions $\mathcal{Q}$ will get a mass from the "Yukawa–like" term $m_\mathcal{Q} = y_\mathcal{Q} v_a / \sqrt{2}$. The Lagrangian

$$\mathcal{L} = -m_\mathcal{Q} \bar{\mathcal{Q}}_L \mathcal{Q}_R e^{ia/v_a} + \text{h.c.}, \tag{1.92}$$

is responsable for the generation of the $aG\tilde{G}$ operator. To see this one can perform an axion dependent chiral rotation of the $\mathcal{Q}$ fields

$$\mathcal{Q} \to e^{-i\frac{a}{2v_a}\gamma^5}\mathcal{Q}. \tag{1.93}$$

Indeed the transformation in Eq.(1.93) is anomalous under $SU(3)_c$, given that the $\mathcal{Q}$'s are in the colour fundamental, as such one gets a contribution from the non–invariance of the path integral measure [6]

$$\delta\mathcal{L}^{\text{KSVZ}} = \frac{g_s^2}{32\pi^2}\frac{a}{v_a}G\tilde{G}. \tag{1.94}$$

In this case one can identify $f_a = v_a$ and the only "portal" to SM fields is the $aG\tilde{G}$ term. Nonetheless such a term can generate radiatively all the coupling to the SM fields, given that the vector–like fermions can be as many as one likes, the coupling are not guaranteed to be small, even if they are loop generated.

1.5.2 DFSZ axion

In DFSZ models the field content includes two Higgs doublets, $H_u \sim (1, 2, -\frac{1}{2})$ and $H_d \sim (1, 2, \frac{1}{2})$, and a complex scalar Standard Model singlet $\Phi \sim (1, 1, 0)$. The latter field extends the WW model, allowing the PQ symmetry–breaking scale to be decoupled from the electroweak scale. The potential of the model is

$$V(H_u, H_d, \Phi) = \tilde{V}(|H_u|, |H_d|, |H_uH_d|, |\Phi|) + \lambda H_u H_d \Phi^{\dagger 2} + \text{h.c.}. \tag{1.95}$$

where $\tilde{V}$ depends only on the moduli of the fields and it preserves the re–phasing symmetry. On the contrary the term proportional to λ explicitly breaks this symmetry to two indipendent $U(1)$ factors, i.e.

$$U(1)_{H_u} \times U(1)_{H_d} \times U(1)_\Phi \to U(1)_Y \times U(1)_{\text{PQ}}, \tag{1.96}$$

so that one has hypercharge and PQ symmetry left. The action of the PQ symmetry is taken to be the same for all the generations and is determined

by the assigning the charges thanks to the following Yukawa Lagrangian, in the case of DFSZ-I model,

$$\mathcal{L}^{\text{DFSZ-I}} = -Y_U \bar{q}_L u_R H_u - Y_D \bar{q}_L d_R H_d - Y_E \bar{\ell}_L e_R H_d + \text{h.c.} \tag{1.97}$$

Alternatively one can couple $\tilde{H}_u = i\sigma^2 H_u^*$ in the lepton sector, DFSZ-II model, so that

$$\mathcal{L}^{\text{DFSZ-II}} = -Y_U \bar{q}_L u_R H_u - Y_D \bar{q}_L d_R H_d - Y_E \bar{\ell}_L e_R H_u + \text{h.c.} \tag{1.98}$$

The potential in Eq.(1.95) gives a non–zero VEV to the fields that can be parametrised, neglecting the radial components, as

$$H_u = \frac{v_u}{\sqrt{2}} e^{ia_u/v_u} \begin{pmatrix} 1 \\ 0 \end{pmatrix}, \quad H_d = \frac{v_d}{\sqrt{2}} e^{ia_d/v_d} \begin{pmatrix} 0 \\ 1 \end{pmatrix}, \quad \Phi = \frac{v_\Phi}{\sqrt{2}} e^{ia_\Phi/v_\Phi}, \tag{1.99}$$

where $v_\Phi \gg v_{u,d}$ in order to escape the WW model's exclusion. The next important task is to distinguish the axion field between all the possible combinations of the three scalar field defined in Eq. (1.95). To identify the axion one can use the Goldstone theorem, first build the associated PQ current

$$J_\mu^{\text{PQ}} = -i\chi_\Phi \Phi^\dagger \overleftrightarrow{\partial_\mu} \Phi - i\chi_{H_u} H_u^\dagger \overleftrightarrow{\partial_\mu} H_u - i\chi_{H_d} H_d^\dagger \overleftrightarrow{\partial_\mu} H_d + \cdots \supset$$

$$J_\mu^{\text{PQ}}\big|_a = \sum_{i=\Phi,u,d} \chi_i v_i \partial_\mu a, \tag{1.100}$$

where the dots are the contributions from the fermionic fields and the χ_i's are the fermion's–PQ charges. $J_\mu^{\text{PQ}}\big|_a$ is defined to get contributions only from the DFSZ–model fields. The axion field is defined as

$$a = \frac{1}{v_a} \sum_i \chi_i v_i a_i, \qquad v_a^2 = \sum_i \chi^2 v_i^2, \tag{1.101}$$

so that $J_\mu^{\text{PQ}}\big|_a = v_a \partial_\mu a$ and $\langle 0| J_\mu^{\text{PQ}}\big|_a |a\rangle = iv_a p_\mu$. Note that under a PQ transformation $a_i \to a_i + k\chi_i v_i$ the axion field transforms as $a \to a + kv_a$. The PQ charges in the scalar sector can be determined by requiring: *i)* PQ

invariance of the operator $H_u H_d \Phi^{\dagger 2}$, which implies $\chi_{H_u} + \chi_{H_d} - 2\chi_\Phi = 0$, and *ii*) orthogonality between $J_\mu^{\mathrm{PQ}}\big|_a$ in Eq.(1.100) and the corresponding contribution to the hypercharge current $J_\mu^{\mathrm{Y}}\big|_a = \sum_i Y_i v_i \partial_\mu a_i$, which implies $\sum_i 2Y_i \chi_i v_i^2 = -\chi_{H_u} v_u^2 + \chi_{H_d} v_d^2 = 0$. The latter condition ensures that there is no kinetic mixing between the physical axion and the Z boson. All charges are hence fixed up to an overall normalisation that can be fixed by choosing a conventional value for χ_Φ:

$$\chi_\Phi = 1, \quad \chi_{H_u} = 2\cos^2 \beta, \quad \chi_{H_d} = 2\sin^2 \beta, \tag{1.102}$$

where we have defined $v_u/v = \sin\beta$, $v_d/v = \cos\beta$, with $v \simeq 246$ GeV. Substituting in Eq.(1.101) we obtain:

$$v_a^2 = v_\Phi^2 + v^2 (\sin 2\beta)^2, \tag{1.103}$$

and given that $v_\Phi \gg v$ we have $v_a \simeq v_\Phi$. The axion coupling to SM fermions can be derived by inverting the first relation in Eq.(1.101) to express $a_{u,d}$ in terms of a and select the a dependent terms. This accounts to the substitutions $a_u/v_u \to \chi_{H_u} a/v_a$, $a_d/v_d \to \chi_{H_d} a/v_a$ and yields

$$\mathcal{L}^{\mathrm{DFSZ-I}} \subset -m_U \bar{u}_L u_R e^{i\chi_{H_u} a/v_a} - m_D \bar{d}_L d_R e^{i\chi_{H_d} a/v_a} - m_E \bar{e}_L e_R e^{i\chi_{H_d} a/v_a} \mathrm{h.c.} + \cdots \tag{1.104}$$

The axion field can be now removed from the mass terms by redefining the fermion fields according to the field–dependent axial transformations:

$$u \to e^{-i\gamma^5 \chi_{H_u} a/(2v_a)} u, \quad d \to e^{-i\gamma^5 \chi_{H_d} a/(2v_a)} d, \quad e \to e^{-i\gamma^5 \chi_{H_d} a/(2v_a)} e, \tag{1.105}$$

which, because of the QCD and EM anomalies, induce an axion coupling to both $G\tilde{G}$ and $F\tilde{F}$. Let us note in passing that since the fermion charges satisfy the relations $\chi_{u_L} - \chi_{u_R} = \chi_{H_u}$, $\chi_{d_L} - \chi_{d_R} = \chi_{H_d}$, and $\chi_{e_L} - \chi_{e_R} = \chi_{H_d}$, as dictated by PQ invariance of the Yukawa couplings, the transformations Eq.(1.105) are equivalent to redifine the LR chiral field with a phase transformation proportional to their PQ charges. The contribution to the anomalies

to the DFSZ-I case are

$$
\begin{aligned}
N &= n_g \left(\frac{1}{2}\chi_{H_u} + \frac{1}{2}\chi_{H_d} \right) = 3, \\
E &= n_g \left(3\left(\frac{2}{3}\right)^2 \chi_{H_u} + 3\left(-\frac{1}{3}\right)^2 \chi_{H_d} + (-1)^2\chi_{H_d} \right) = 8,
\end{aligned}
\tag{1.106}
$$

where $n_g = 3$ is the number of SM fermion generations while $\chi_{H_{u,d}}$ are given in Eq.(1.102). The anomalous part of the axion effective Lagrangian is

$$
\delta\mathcal{L}^{\text{DFSZ-I}} = \frac{\alpha_s}{8\pi}\frac{a}{f_a}G\tilde{G} + \frac{\alpha}{8\pi}\frac{E}{N}\frac{a}{f_a}F\tilde{F},
\tag{1.107}
$$

with $f_a = v_a/(2N)$, while $E/N = 8/3$. The field-dependent axion transformation do not leave the fermion kinetic terms invariant, and their variation corresponds to derivative couplings of the axion to the Standard Model fermionic fields:

$$
\delta(\bar{u}i\slashed{\partial}u) \;=\; \chi_{H_u}\tfrac{\partial_\mu a}{2v_a}\bar{u}\gamma^\mu\gamma^5 u \;=\; \left(\frac{1}{3}\cos^2\beta\right)\frac{\partial_\mu a}{2f_a}\bar{u}\gamma^\mu\gamma^5 u,
\tag{1.108}
$$

$$
\delta(\bar{d}i\slashed{\partial}d) \;=\; \chi_{H_d}\tfrac{\partial_\mu a}{2v_a}\bar{d}\gamma^\mu\gamma^5 d \;=\; \left(\frac{1}{3}\sin^2\beta\right)\frac{\partial_\mu a}{2f_a}\bar{d}\gamma^\mu\gamma^5 d,
\tag{1.109}
$$

$$
\delta(\bar{e}i\slashed{\partial}e) \;=\; \chi_{H_d}\tfrac{\partial_\mu a}{2v_a}\bar{e}\gamma^\mu\gamma^5 e \;=\; \left(\frac{1}{3}\sin^2\beta\right)\frac{\partial_\mu a}{2f_a}\bar{e}\gamma^\mu\gamma^5 e,
\tag{1.110}
$$

at this point one can read out the axion–fermion coupling c_ψ^0 in Eq.(1.71). Note that they are generation diagonal.

1.6 Axion Quality Problem

In Sec. 1.4.2 the axion potential has been derived. The striking feature of the model is that the of QCD dynamics will drive the value of $\bar{\theta}$ to zero in a natural way, given that the periodic potential has a minimum for that value, solving the strong CP problem. For a particular choice of charges the

potential for small $\bar{\theta}$ can be take to be

$$V_{\text{QCD}}(\bar{\theta}) = (m_a^i)^2 f_{\text{PQ}}^2 (1 - \cos\bar{\theta}), \qquad (1.111)$$

where the $\bar{\theta}$ parameter and the axion field a can be considered interchangable. For the model to be consistent the vacuum should be stable as one goes to the UV. It can be argued that higher–dimensional symmetry–violating operators expected to be induced at the Planck scale by quantum–gravity effects will spoil the Peccei–Quinn solution [36–40]. Indeed it is believed that Planck–scale physics will eventually violate all the global symmetries. As an example a black–hole scattering process with a global charge in the initial state will not conserve it due to Hawking evaporation [41]. At low–energies, with respect to the Planck mass, these effects are described by higher–dimensional operators in an effective field theory of light modes. These effects will in general favour a solution $\bar{\theta} \neq 0$. To avoid reintroducing a non–zero CP violating parameter the Quantum Gravity effects must be strongly suppressed with respect to the QCD ones driving $\bar{\theta}$ to zero. To solve this issue one has to consider either: (1) exponentially small couplings for the symmetry–breaking operators at the Planck scale or (2) the higher–dimensional potential coincidentally also has a minimum for $\bar{\theta} = 0$.

Consider a potential for the $U(1)_{\text{PQ}}$ scalar field of the form

$$V_0(\Phi) = \lambda\left(|\Phi|^2 - \frac{f_a^2}{2}\right)^2. \qquad (1.112)$$

Thanks to dimensional analysis one can asses the scale dependence of higher dimensional operators. These must be suppressed by positive powers of the Planck mass. Indeed a general symmetry–breaking operator of dimension $2m + n$ with PQ charge n will have the form:

$$V_g(\Phi) = \frac{g}{M_{\text{Pl}}^{2m+n-4}}|\Phi|^{2m}\Phi^n + \text{h.c.} + c, \qquad (1.113)$$

where $g = |g|e^{i\delta}$ is a complex coupling with $|g|$ not necessarily small and c a constant chosen so that V has a minimum in zero. The complex phase δ does not need to be generated from additional CP violation induced by Quantum

Gravitational effects but can be simply come from the chiral rotation in the mass sector $\delta \propto \arg \det(M)$. After spontaneous symmetry breaking this term generates a low–energy contribution:

$$V_g(\bar{\theta}) = (m_a^g)^2 f_a^2 \left(1 - \cos \left(n\frac{a}{f_a} + \delta \right) \right), \qquad (1.114)$$

where the gravitationally induced axion mass is

$$(m_a^g)^2 = |g|^2 M_{\text{Pl}}^2 \left(\frac{f_a}{\sqrt{2}M_{\text{Pl}}} \right)^{2m+n-2}. \qquad (1.115)$$

The total potential will then be

$$V(a) = f_a^2 \left[(m_a^g)^2 \left(1 - \cos \left(n\frac{a}{f_a} + \delta \right) \right) + (m_a^i)^2 \left(1 - \cos \frac{a}{f_a} \right) \right]. \qquad (1.116)$$

Some nuances are not explicitly discussed, e.g. δ should be replaced by $\bar{\delta}$ after the field–dependent chiral transformation to put $aG\tilde{G}$ to zero, and the coupling g has to run down from the Planck scale gaining a factor $\log M_{\text{Pl}}/m_a \approx 50$ that will not be important in what follows. To solve the strong CP–problem the minimum of the potential in Eq.(1.116) must be for $a \leq 10^{-10}$. To satisfy this bound, put $n = 1$ for simplicity, one must have

$$\frac{|\sin \delta|}{\sqrt{1 + r^2 + 2r \cos \delta}} \lesssim 10^{-10}, \qquad (1.117)$$

where $r \equiv (m_a^i)^2/(m_a^g)^2$. Therefore, if $\sin \delta$ is of order one, r is pushed up to be of order 10^{10}. If we demand that the coupling constant $|g| < 10^{-2}$, and assumes a symmetry–breaking operator of dimension 5 we find that in order to consistently solve the strong CP–problem we must have

$$f_a \lesssim 10 \, \text{GeV}, \qquad (1.118)$$

which corresponds to $m_a \geq 100$KeV. Axions with such masses coming purely from the anomaly and strong–interaction physics have been ruled out by *laboratory* experiments [42, 43]. Since in this regime $m_a^g \ll m_a^i$, the standard

phenomenology of the axion will remain essentially unaltered by the Planck–scale physics discussed here and as such the limits extracted from experiments are perfectly valid. The whole mechanism described essentially forces the axion theory space to be small and already disallowed by observation. Of course one can make the couplings of the symmetry–violating operator to be exponentially small. Consider the Peccei–Quinn mechanism for $m_a^i \sim 10^{-5}$ eV, corresponding to $f_{\mathrm{PQ}} \sim 10^{12}$ GeV. Such a symmetry–breaking scale, the coupling of a dimension–5 symmetry–breaking operator induced by Planck–scale physics must be

$$|g| \lesssim 10^{-55}. \tag{1.119}$$

So one exchanges a fine–tuning problem on $\bar{\theta}$ for a fine–tuning problem at the Planck scale.

The lesson here is that PQ symmetry is quite fragile under the effects of higher dimensional symmetry–breaking operators, and so it could hopefully arise as an accidental symmetry due to a combination of fundamental principles. In this way the effects of some of the first irrelevant operator might simply be zero, as it happens for B number violating operators at $d \leq 5$. Without substantial modifications the level of "accidental cancellation" of higher–dimensional operators is concerning as it should be of the order of $d \sim 10$. Many different mechanisms have been put forth to amend this problematic aspect of the theory of axion.

- **Low f_a**. Lowering the PQ scale to $f_a \geq 10^3$ GeV requires the disappearance only of the dim–5 symmetry–breaking operator to preserve a small enough value of $\langle \bar{\theta} \rangle$. In this set up the WW model works quite well as the first gauge–invariant PQ–breaking operator is a dimension 6 one, given by $(H_u H_d)^3$. Super–heavy axion models can escape most of the astrophysical constraints modyfing the QCD relation between m_a and the PQ scale f_a. These models can have f_a of the order of tens of TeVs.

- **Gauge protection.** New local symmetries can lead to an accidental PQ symmetry protected from higher-order PQ breaking operators, up to some fixed order. One can look into discrete symmetries, Abelian and non–Abelian etc... [37, 44–49]

- **Accidentality.** It should not be ruled out the case of an accidental high quality symmetry, similar to the B number violating operators, but there must be some theoretical mechanism to drive this case.

1.6.1 Axion–like particles

The theory and phenomenology of axions is to a large extent shared with any other pNGBs which have a low mass and very weak couplings coming from a spontaneously broken symmetry at very high energy scales. These **Axion–Like particles** are light scalars or pesudo–scalar fields arising from spontaneously broken symmetries at some scale f_a, much like the axion, but are not necessarily tied to the strong CP problem and will not get their masses from QCD effects but from some other dynamics that break explicitly the global symmetry. They emerge in GUTs or String Theory models via the breaking of accidental global U(1) symmetries that appear as low energy remnants of exact symmetries of the high energy theory. ALPs tipically, but are not exclusively, emerge as additional pNGBs perpendicular in field space to the spin–0 particle that couples to the topological charge density in QCD $G\tilde{G}$, and drives $\bar{\theta}$ to zero. This aspects allows them to be "decoupled" from some of the required features to solve the strong CP problem, such as the anti proportionality between their mass and the symmetry breaking scale. The parameters appearing in an ALP Lagrangian can be taken to be independent offering an appealing quality in terms of their phenomenological viability. Nonetheless the pNGBs nature gives some constraints on the form of the Lagrangian. Shift symmetry must be imposed on the interactions and symmetry breaking effects are of the soft kind [50]. In a more pragmatic sense ALPs will have similar interactions and effective Lagrangians as the ones discussed for axion fields, namely anomalous couplings to gauge fields and derivative ones to fermions but with the added advantage of having in principle independent parameters.

Chapter 2

Effective Lagrangians For Axions and ALPs

The literature on ALPs searches at colliders at and fixed-target experiments is rapidly growing and the interested reader is refferred to the seminal papers [51–58]. Inspired by these works the following Chapter is devoted to the study of the Effective Field Theory (EFT) of the SM with a new light pseudo–scalar-Nambu-Goldstone-Boson gauge singlet valid up to the cutoff scale $\sim f_a$ and truncated at dimension–5. The theory is in the spontaneously broken phase of a high scale $U(1)$, realised at these energies by the flat direction in the potential for the Goldstone boson a. This symmetry is also explicitly broken by the mass term and by the anomalous couplings to the gauge–vectors. The high scale $U(1)$, the Peccei–Quinn symmetry, can be made anomalous by construction to solve the Strong CP problem, although this is not necessary in general to the study of ALP phenomenology. The implementation of the Effective Theory at this stage is similar to the approach of a SMEFT where all the model dependence is contained in the higher–dimensional operator's coefficients. The leading order correction to the renormalizable Lagrangian is considered, and so the Laurent effective expansion in the cutoff is truncated at order f_a^{-1}. From now and in the rest of the manuscript ALPs and axions will be called ALPs collectively, unless explicitly stated.

2.1 Effective Lagrangian at the UV scale

An Effective Theory is formally defined by the model's field content and the symmetry group one imposes onto the theory. In the case of the ALP Standard Model EFT, field content and gauge–symmetries are inherited from the SM with the addition of a pseudo–scalar gauge singlet endowed with the shift symmetry, $a \to a + c$, anomalously broken by the gauge boson's couplings of the notorious $aX\tilde{X}$ form, and softly by a mass term. Global symmetries are to be considered accidental and non–renormalizable operator might break them. In any practical application the EFT's Laurent series has to be truncated at some order and a non–redundant complete operator basis must be chosen. The word chosen here is critical in the sense that typically more than a single basis will have these characteristics and a sensible choice can produce a simpler phenomenological study of the theory.

In this manuscript the Lagrangian will always be considered at NLO in the inverse f_a expansion, i.e. only non–renormalizable operators of dimension–5 are considered, indeed any operator of dimension higher than 5 will be suppressed by additional powers of f_a^{-1}. The question of the choice of basis is instead more involved and requires some attention. A recent review on the subject, including the complete one–loop corrections of the theory, can be found in [28, 59–61]. To start, consider the complete and non-redundant NLO ALP effective Lagrangian [59] defined below the UV scale f_a defined by

$$\mathcal{L}_{\text{ALP}} = \mathcal{L}_{\text{SM}} + \mathcal{L}_a^{CP} + \mathcal{L}_a^{CPV}. \tag{2.1}$$

where all the additional CP violating effects are induced by $\mathcal{L}_a^{CPV}$. The SM Lagrangian is

$$\mathcal{L}_{\text{SM}} = -\frac{1}{4}W_{\mu\nu}^{\alpha}W^{\alpha\mu\nu} - \frac{1}{4}B_{\mu\nu}B^{\mu\nu} - \frac{1}{4}G_{\mu\nu}^{a}G^{a\mu\nu} + i\sum_f \bar{\psi}_f \slashed{D}\psi_f + |D_\mu H|^\dagger |D^\mu H|$$

$$- \left[\bar{Q}_L\mathbf{Y}_d H d_R + \bar{Q}_L\mathbf{Y}_u \tilde{H} u_R + \bar{L}_L\mathbf{Y}_e H e_R + \text{h.c.}\right] - V(H^\dagger H),$$
$$\tag{2.2}$$

where the $\mathbf{Y}$'s are the SM Yukawa matrices and ψ_f is the set of chiral fermion fields $\{Q_L, d_R, u_R, L_L, e_R\}$ representing 3–dimensional flavor space vectors. H

is the Higgs doublet, V is its potential and $X^{a\mu\nu}$ are the field strengths associated to vectors bosons of the gauge group $\mathcal{G} = SU(3)_c \otimes SU(2)_L \otimes U(1)_Y$, as customarily defined. Here and in the rest of the manuscript neutrinos are considered massless and no right–handed neutrino is introduced.

The ALP–fermion operators of mass dimension 5 that preserve the local symmetry group $\mathcal{G}$ and the global Peccei–Quinn symmetry $U(1)_{PQ}$ (here realised as the shift–symmetry $a \to a + c$) are:

$$\mathbf{O}_u \equiv \frac{\partial_\mu a}{f_a}(\bar{u}_R\gamma^\mu u_R), \quad \mathbf{O}_d \equiv \frac{\partial_\mu a}{f_a}(\bar{d}_R\gamma^\mu d_R), \quad \mathbf{O}_Q \equiv \frac{\partial_\mu a}{f_a}(\bar{Q}_L\gamma^\mu Q_L),$$

$$\mathbf{O}_L \equiv \frac{\partial_\mu a}{f_a}(\bar{L}_L\gamma^\mu L_L), \quad \mathbf{O}_e \equiv \frac{\partial_\mu a}{f_a}(\bar{e}_R\gamma^\mu e_R), \tag{2.3}$$

where the matrix indices are left implicit. In particular all of these operators are matrices in flavor space and the flavor indices are realised as

$$\mathbf{O}_L^{ij} = \frac{\partial_\mu a}{f_a}\bar{Q}_L^i\gamma^\mu Q_L^j.$$

The most general mixed (including bosonic and fermionic couplings) CP conserving Lagrangian [28] is non unique and depends on the choice of basis. Many different complete and non redundant bases have been discussed in [59]. A particular choice of basis for the CP conserving Lagrangian, truncated at the first non trivial order in the Laurent expansion, of the EFT is

$$\mathcal{L}_a^{CP} = \frac{1}{2}(\partial_\mu a)^2 + \frac{m_a^2}{2}a^2 + c_W\frac{\alpha_2}{4\pi}O_W + c_B\frac{\alpha_1}{4\pi}O_B + c_G\frac{\alpha_s}{4\pi}O_G$$

$$+ \sum_{f=u,d,e}\mathbf{c}_f\mathbf{O}_f + \sum_{f=Q,L}\mathbf{c}_f\tilde{\mathbf{O}}_f, \tag{2.4}$$

where $O_W = -\frac{a}{f_a}W_{\mu\nu}^\alpha\tilde{W}^{\alpha\mu\nu}$, $O_B = -\frac{a}{f_a}B_{\mu\nu}\tilde{B}^{\mu\nu}$, and $O_G = -\frac{a}{f_a}G_{\mu\nu}^a\tilde{G}^{a\mu\nu}$ are the shift anomalous gauge couplings, note that in the previous chapter c_G was set to one, as customary when one considers QCD–axions. Nonetheless one can recover it either by redefining the PQ scale as $f_a \to f_a/c_G$, or e.g. for the DSFZ-I model by the equation $\frac{c_G}{f_a} = -\frac{N}{v_a}$. The next parameter to discuss is the hermitian flavor matrix $\mathbf{c}_f$. Under the CP conserving assumption $\mathbf{c}_f$ must

be taken symmetric. The matrix product in Eq.(2.4) is defined element by element and not as a typical row by column product. Finally in Eq.(2.4) there is a separation between R–handed operators and L–handed ones. Indeed the terms indicated by $\tilde{\mathbf{O}}_f$ for $f = Q, L$, involve only L–handed fermionic fields. The tilde operators are defined to avoid redundancies and are:

$$\tilde{\mathbf{O}}_L = \mathbf{O}_L - \text{diag}\{\mathbf{O}_L\}, \qquad \tilde{\mathbf{O}}_Q = \mathbf{O}_Q - \delta_{11}\text{diag}\{\mathbf{O}_Q\}. \qquad (2.5)$$

In $\tilde{\mathbf{O}}_L$ the diagonal is cancelled while for $\tilde{\mathbf{O}}_Q$ only the element 11 is set to zero. In general the model described in Eq.(2.4) has a total number of parameters equal to

$$3(\text{vectors}) + 2(m_a, f_a) + 5 \times \text{par}(\mathbf{c}_f) - N \qquad (2.6)$$

where N is the number of redundancies and $\text{par}(\mathbf{c}_f)$ is the number of real parameters contained in a single matrix $\mathbf{c}_f$. The $\mathbf{c}_f$'s are hermitian and as such they can be parametrised as

$$\mathbf{c}_f = \mathbf{a} + i\mathbf{b}, \qquad (2.7)$$

where $\mathbf{a}$ is symmetric while $\mathbf{b}$ is symmetric and traceless. For a generic number of flavors n_g the dimensions of $\mathbf{a}$ and $\mathbf{b}$ are $n_g(n_g+1)/2$ and $n_g(n_g-1)/2$ respectively; adding the CP conserving condition $\mathbf{c}_f = \mathbf{c}_f^T$ results in $\mathbf{b} = 0$. The redundancies are taken care by the elimination of the 4 operators discussed in Eq.(2.5). The total number of CP conserving independent parameters in the model of Eq.(2.4) is 31. The redundancies associated to the operators in Eq.(2.3) are related to classical global symmetries of baryon and lepton family number conservation, these are to be discussed in Sec.2.1.2.

2.1.1 Bases and Field Reparametrizations

The issue of bases and field redefinitions in Effective Field Theories are of course tied to one another and are a rather delicate subject to discuss. The equivalence of different choices has been proven in the Equivalence Theorem [62], so the issue of finding a "complete basis", intended as a minimal set of gauge–invariant operators closed under renormalization, is an issue of convenience. Indeed in principle there are no difficulties in considering a

redundant basis but complete ones will have a reduced number of Wilson coefficients and are in general simpler to work with. The important lesson of the theorem is that the local field dependent transformation will modify the theory's Lagrangian but leave the physical quantities, i.e. the S–matrix, invariant. The theorem states that any transformation $\phi \to \varphi + f(\phi)$ between regulated theories, i.e. without divergences, will not modify the S–matrix elements. This implies that the specific form of an interaction term in the Lagrangian can be changed and its physical effect will be distributed elsewhere. These field reparametrizations can be used to modify the interactions term of the Lagrangian, to rearrange or to cancel certain contributions, to facilitate calculations etc... It is not possible however to render a free–theory an interacting one or to de–interact completly a theory [63].

As a relevant example consider a unitary ALP dependent transformation of the Higgs doublet $H \to H e^{ic\frac{a(x)}{f_a}}$, under which a generic dimension–5 Effective Lagrangian

$$\mathcal{L}_{\mathrm{SM}}(HH^\dagger) + \mathcal{O}_a(H, H^\dagger), \tag{2.8}$$

where $\mathcal{O}_a(H, H^\dagger)$ is a generic higher dimensional operator depending on the Higgs field unrelated to the operators in Eq.(2.4), will change at linear order in $\frac{1}{f_a}$ after the expansion

$$\mathcal{L}_{\mathrm{SM}} + \mathcal{O}_a + ic\frac{\delta \mathcal{L}_{\mathrm{SM}}}{\delta H}H\frac{a(x)}{f_a} + ic\frac{a(x)}{f_a}\frac{\delta \mathcal{O}}{\delta H}H + \dots, \tag{2.9}$$

where the dots are the equivalent term due to the change in $H^\dagger$ and any eventual anomalous effect. The polynomial nature of the Lagrangian protects gauge invariance and the Equivalence Theorem assures that the physics description is the same. Consider the ALP–dependent fields redefinitions

$$\psi_f \to \exp\left(i\frac{a}{f_a}\mathbf{Q}_f\right)\psi_f, \qquad H \to \exp\left(i\frac{a}{f_a}Q_H\right)H, \tag{2.10}$$

where f describes the set of all the chiral fermions in the theory and $\mathbf{Q}_f$'s are tensors in flavor space. The field redefinitions in Eq.(2.10) must be unitary, and as such the rotation parameters Q_H and $\mathbf{Q}_f$ are real and hermitian

respectively, it turns out that $\mathbf{Q}_f$ has to be symmetric to preserve the hermitianity of the Lagrangian. Once these hypotheses are verified any Lagrangian obtained from the original via the transformation of Eq.(2.4) will have a different form of interaction but will describe the same physical results.

2.1.2   Redundancies and Operators Identities

Sec.2.1.1 tackles the reparametrization freedom of Effective Field Theory and its consequences. The most notable one is the presence of equivalent representations of the theory with an inequivalent number of parameters, or rather the existence of a class of equivalent Lagrangians by field redefinitions. The ones that have the minimum number of parameters and are at the same time closed under renormalization have a special role, they posses a "complete basis". In principle when discussing an EFT's Lagrangian one should include all possible terms allowed by the symmetry of the model, it is however clear [28] that there are gauge and shift invariant operators not included in Eqs.(2.4). These are the three left–handed leptonic operators $\frac{\partial_\mu a}{f_a} L_L^i \gamma^\mu L_L^i$, the left–handed quark operator $\frac{\partial^\mu a}{f_a} Q_L^1 \gamma_\mu Q_L^1$ and finally the ALP–Higgs interaction

$$O_{aH} = \frac{\partial^\mu a}{f_a} \left(H^\dagger \overleftrightarrow{D}_\mu H \right). \tag{2.11}$$

These five gauge and shift invariant operators are not included in Eq.(2.4) because of their redundancy. But why are these redundant? What is the formal procedure to remove them starting from a general EFT Lagrangian? To answer these questions consider the rotations in Eq.(2.10) and their effect on $\mathcal{L}_{\mathrm{SM}}$ to first order in the Laurent expansion parameter f_a^{-1}. The net shift

for the most general rotation is [59]

$$\Delta\mathcal{L}_{\text{SM}} = -Q_H O_{aH} - \sum_f \mathbf{Q}_f \mathbf{O}_f + \big[(\mathbf{Q}_L \mathbf{Y}_e - \mathbf{Y}_e \mathbf{Q}_e - Q_H \mathbf{Y}_e)\mathbf{O}_{eH}$$

$$+ (\mathbf{Q}_Q \mathbf{Y}_d - \mathbf{Y}_d \mathbf{Q}_d - Q_H \mathbf{Y}_d)\mathbf{O}_{dH} + (\mathbf{Q}_Q \mathbf{Y}_u - \mathbf{Y}_u \mathbf{Q}_u + Q_H \mathbf{Y}_u)\mathbf{O}_{dH} + \text{h.c.}\big]$$

$$+ \frac{g'^2}{32\pi^2} O_B \, \text{Tr}\left[\frac{1}{3}\mathbf{Q}_Q - \frac{8}{3}\mathbf{Q}_u - \frac{2}{3}\mathbf{Q}_d + \mathbf{Q}_L - 2\mathbf{Q}_e\right] + \frac{g^2}{32\pi^2} O_W \, \text{Tr}[3\mathbf{Q}_Q + \mathbf{Q}_L]$$

$$+ \frac{g_s^2}{32\pi^2} O_G \, \text{Tr}[2\mathbf{Q}_Q - \mathbf{Q}_u - \mathbf{Q}_d],$$

$$(2.12)$$

where the L and R pedices have been abandoned to lighten the notation and the operators $\mathbf{O}_{eH}$, $\mathbf{O}_{uH}$ and $\mathbf{O}_{dH}$ are defined as

$$\mathbf{O}_{eH} = i\frac{a}{f_a}\bar{L}_L H e_R, \qquad \mathbf{O}_{uH} = i\frac{a}{f_a}\bar{Q}_L \tilde{H} u_R, \qquad \mathbf{O}_{dH} = i\frac{a}{f_a}\bar{Q}_L H d_R \quad (2.13)$$

Remember that the Lagrangian shift obtained in Eq.(2.12) due to the transformations of Eq.(2.10) comes entirely from $\mathcal{L}_{\text{SM}}$ while $\mathcal{L}_a^{\text{CP}}$ is conserved. The first two terms in Eq.(2.12) come from the kinetic term shift of the Higgs field and the fermions, respectively. The three terms proportional to $\mathbf{O}_{eH}$, $\mathbf{O}_{uH}$ and $\mathbf{O}_{dH}$ are a consequence of the change of Yukawa interaction terms, and are sometimes dubbed as chirality–flipping interactions. Finally the last three operators are generated thanks to the anomalous contributions of the axial transformations performed. It is easy to recover these contributions by using Eq.(1.30), where the anomalous current carries the flavor charges $T_A^{(b)} = \{\mathbf{Q}_f, Q_H\}$ are given by Eq.(2.10) while the relevant gauge charges $T_V^{(a)}$ are the well known ones of the gauge group $\mathcal{G}$. The trace is intended over the flavor space indices. Finally products of matrices are to be performed following the usual internal product, while product of matrices and operators are instead defined as

$$\mathbf{MO} = \mathbf{M}_{ij}\mathbf{O}_{ij}. \qquad (2.14)$$

At this point one is free to take any value for $\mathbf{Q}_f$ or Q_H in Eq.(2.12) and in doing so it is possible to cancel the redundant operators that appear in $\mathcal{L}_a^{\text{CP}}$.

Field dependent rotations allows one to modify the parameters regulating

the interactions, and in doing so one can choose a particular form of the Lagrangian without modifying the physics described by the theory. So in order to remove a contribution in the Lagrangian of the form $c_{aH}O_{aH}$ one is instructed to rotate the Higgs field by a $Q_H = c_{aH}$ amount. The price of removing the Higgs–ALP interaction is in the introduction of the chirality flipping operators. In Eq.(2.12) the chirality flipping operators proportional to Q_H introduce the identity

$$O_{aH} = \mathbf{Y}_u \mathbf{O}_{uH} - \mathbf{Y}_d \mathbf{O}_{dH} - \mathbf{Y}_e \mathbf{O}_{eH} + \text{h.c.}. \tag{2.15}$$

The bosonic nature of O_{aH} disallows for any additional Flavor Violation to be induced by it. As such the flavor structure of the chirality flipping interactions is determined by the Standard Model's flavor structure, i.e. by the Yukawa matrices. At this point one can fix the quantities $\mathbf{Q}_f$ to exactly cancel the coefficients of $\mathbf{O}_{eH}, \mathbf{O}_{dH}$ and $\mathbf{O}_{uH}$, effectively trading O_{aH} for the chirality conserving operators of Eq.(2.3). Indeed if one takes only R handed fields, the coefficients of the chirality flipping operators can be eliminated by the choice $\mathbf{Q}_d = \mathbf{Q}_e = -\mathbf{Q}_u = c_{aH}\mathbb{1}$. This proves that the operator O_{aH} was always a redundant one as plugging this choice of parameters in Eq.(2.12) results in the condition

$$O_{aH} = \text{Tr}[\mathbf{O}_e + \mathbf{O}_d - \mathbf{O}_u]. \tag{2.16}$$

Note that in this particular case the anomalous contributions cancel exactly but will not be true for other choices of $\mathbf{Q}_f$.

Collecting all the terms proportional to $\mathbf{Q}_f$ in Eq.(2.12) it is possible to obtain relations between the fermionic operators. Writing flavor indices explicitly one gets

$$\mathbf{O}_Q^{ij} = \left[\mathbf{O}_{dH}^{ik}(\mathbf{Y}_d)_{jk} + \mathbf{O}_{uH}^{ik}(\mathbf{Y}_u)_{jk} + (\mathbf{O}^\dagger)_{dH}^{kj}(\mathbf{Y}_d^\dagger)_{ki} + (\mathbf{O}^\dagger)_{uH}^{kj}(\mathbf{Y}_u^\dagger)_{ki} \right]$$
$$+ \delta^{ij} \left[\frac{g'^2}{96\pi^2} O_B + \frac{3g^2}{32\pi^2} O_W + \frac{g_s^2}{16\pi^2} O_G \right], \tag{2.17}$$

$$\mathbf{O}_u^{ij} = \Big[- \mathbf{O}_{uH}^{kj} (\mathbf{Y}_u)_{ki} - (\mathbf{O}^\dagger)_{uH}^{ik} (\mathbf{Y}_u^\dagger)_{jk} \Big] - \delta^{ij} \left[\frac{g'^2}{12\pi^2} O_B + \frac{g_s^2}{32\pi^2} O_G \right], \quad (2.18)$$

$$\mathbf{O}_d^{ij} = \Big[- \mathbf{O}_{dH}^{kj} (\mathbf{Y}_d)_{ki} - (\mathbf{O}^\dagger)_{dH}^{ik} (\mathbf{Y}_d^\dagger)_{jk} \Big] - \delta^{ij} \left[\frac{g'^2}{48\pi^2} O_B + \frac{g_s^2}{32\pi^2} O_G \right], \quad (2.19)$$

$$\mathbf{O}_e^{ij} = \Big[- \mathbf{O}_{eH}^{kj} (\mathbf{Y}_e)_{ki} - (\mathbf{O}^\dagger)_{eH}^{ik} (\mathbf{Y}_e^\dagger)_{jk} \Big] - \delta^{ij} \frac{g'^2}{16\pi^2} O_B, \quad (2.20)$$

$$\mathbf{O}_L^{ij} = \Big[\mathbf{O}_{eH}^{ik} (\mathbf{Y}_e)_{jk} + (\mathbf{O}^\dagger)_{eH}^{kj} (\mathbf{Y}_e^\dagger)_{ki} \Big] + \delta^{ij} \left[\frac{g'^2}{32\pi^2} O_B + \frac{g^2}{32\pi^2} O_W \right], \quad (2.21)$$

where the sum over k is understood. Now consider the sum of Eq.(2.17–2.19) and take the trace of the result. Unpacking the notation one recognizes the operator built in this way, i.e.

$$\frac{\partial_\mu a}{f_a} J_B^\mu = \mathrm{Tr} \left[\frac{\mathbf{O}_Q + \mathbf{O}_u + \mathbf{O}_d}{3} \right] = \frac{n_g}{32\pi^2} (g^2 O_W - g'^2 O_B), \quad (2.22)$$

the ALP–baryonic current coupling. Finally take the diagonal part of the sum of Eq.(2.20–2.21). Once more explicitly writing the indices one obtains

$$\frac{\partial_\mu a}{f_a} J_{L_i}^\mu = [\mathbf{O}_L + \mathbf{O}_e]_{ii} = \frac{1}{32\pi^2} (g^2 O_W - g'^2 O_B), \quad (2.23)$$

the ALP–lepton current couplings. The relations in Eqs.(2.22–2.23) provide one constraint on the diagonal elements of quark currents, and n_g constraints on the diagonal elements of leptonic–currents operator. As such a single diagonal operator in the quark currents becomes redundant while n_g for leptonic currents. The basis presented in Sec.2.1 has these four redundant operator removed via the definitions of the $\tilde{\mathbf{O}}_{L,Q}$ operators.

2.2 Alternative Bases

The ALP–dependent field redefintions of Eq.(2.10) induce, to order $(1/f_a^{-1})$, the transformation laws in Eq.(2.12). This freedom allows one to change the Lagrangian and the specific form of the interactions. As such the Lagrangian $\mathcal{L}_a^{\mathrm{CP}}$ is not uniquely defined by Eq.(2.4) but rather changes with different choices of a basis. Any basis is fine as long as the total number of independent parameters is consistently maintained. A valid option is to include all the possible operators made out of left–handed fields, including all the diagonal couplings. To maintain the total number of parameters unchanged one would have to cancel all the right–handed flavor diagonal couplings in the leptonic sector and one of the flavor diagonal coupling of right–handed quark currents.

As shown in Eqs.(2.17–2.21) one can trade shift–invariant fermionic operators with a combination of chirality flipping operators and anomalous ones. Chirality flipping operators are of course not invariant per se under the required shift symmetry $a \to a + c$. Only in some particular cases the chirality–flip couplings are tradable for generic chirality–preserving ones (plus appropriate redefinitions of the anomalous couplings). This happens in Minimal Flavor Violation (MFV) Effective Field Theory models where all the flavor violation stems from the Standard Model Yukawa matrices, where the chirality–flipping coefficients have to be proportional to the Yukawa Matrices. In general the two descriptions are not equivalent, indeed it is enough to show that the two description have in general a different number of parameters. Shift invariant operators have hermitian matrices of coefficients while chirality-flipping ones have generic $n_g \times n_g$ matrices. In the CP–even case the number of purely shift invariant fermionic parameters amounts to $n_g(5n_g + 3)/2 - 1$, while for chirality flipping operators the generic number of parameters is $3n_g^2$. In practice any shift–invariant operators can be expressed as a sum of chirality-flipping ones and anomalous ones, but the relation is not invertible in general.

2.2.1 Anomalous Operators and Anomalous Currents

Naively, considering only classical symmetry invariance, one might expect to be able to express all the shift–invariance of the theory via the fermionic

chirality conserving operators. It should be clear that the anomalous operator are instead required by the quantum effects. This fact must be reflected in the transformation law of Eq.(2.12) given that a shift can not remove all the anomalous couplings leaving only the classical chirality conserving operators. To cancel the anomalous coupling the rotation parameters must satisfy

$$\frac{g'^2}{32\pi^2} \text{Tr}\left[\frac{1}{3}\mathbf{Q}_Q - \frac{8}{3}\mathbf{Q}_u - \frac{2}{3}\mathbf{Q}_d + \mathbf{Q}_L - 2\mathbf{Q}_e\right] = -c_B$$

$$\frac{g^2}{32\pi^2} \text{Tr}[3\mathbf{Q}_Q + \mathbf{Q}_L] = -c_W \tag{2.24}$$

$$\frac{g_s^2}{32\pi^2} \text{Tr}[2\mathbf{Q}_Q - \mathbf{Q}_u - \mathbf{Q}_d] = -c_G.$$

These can be solved by the $\mathbf{Q}_f$ but chirality-flipping operators are introduced in doing so. To get rid of them one should solve simultaneously the three conditions in Eq.(2.24) along with the system

$$\mathbf{Q}_Q\mathbf{Y}_u - \mathbf{Y}_u\mathbf{Q}_u = 0,$$
$$\mathbf{Q}_Q\mathbf{Y}_d - \mathbf{Y}_d\mathbf{Q}_d = 0, \tag{2.25}$$
$$\mathbf{Q}_L\mathbf{Y}_e - \mathbf{Y}_e\mathbf{Q}_e = 0.$$

It turns out that is is not possible to satisfy the conditions in Eqs.(2.24)–(2.25). Indeed one can get rid of the anomalous operators but quantum induced chirality-flipping terms must appear along with classical shift invariant fermionic operators. A solution for the anomalous operators in terms of fermionic ones can be obtained as long as one relaxes two of the conditions appearing in Eq.(2.25). One example is

$$O_B = -\frac{16\pi^2}{g'^2 n_g}[\text{Tr}\,\mathbf{O}_e + (\mathbf{Y}_e\mathbf{O}_{eH} + \text{h.c.})],$$

$$O_W = \frac{32\pi^2}{g^2 n_g}\left[\text{Tr}\left(\mathbf{O}_L + \frac{1}{2}\mathbf{O}_e\right) - \left(\frac{\mathbf{Y}_e}{2}\mathbf{O}_{eH} + \text{h.c.}\right)\right], \tag{2.26}$$

$$O_G = \frac{32\pi^2}{g_s^2 n_g}\left[\text{Tr}\left(-\mathbf{O}_d + \frac{1}{3}\mathbf{O}_e\right) - \left(\frac{\mathbf{Y}_d}{2}\mathbf{O}_{dH} - \frac{1}{3}\mathbf{O}_{eH} + \text{h.c.}\right)\right].$$

It is important to note that the combination $g^2 O_W - g'^2 O_B$ corresponds to the results in Eq.(2.22–2.23). Indeed consider the combinations

$$\frac{\partial_\mu a}{f_a}(J_B^\mu - \sum_i J_{L_i}^\mu) = 0 \tag{2.27}$$

and

$$\frac{\partial_\mu a}{f_a}(J_B^\mu + \sum_i J_{L_i}^\mu) = \frac{n_g}{16\pi^2}(g^2 O_W - g'^2 O_B). \tag{2.28}$$

These last two equations corresponds to the conservation of the $U(1)_{B-L}$ quantum number and to the non–conservation of the global anomaly associated to $U(1)_{B+L}$ respectively.

2.3 Phenomenological parameters

The ALP EFT discussed in terms of $SU(3)_c \times SU(2)_L \times U(1)_Y$ gauge invariant operators leads to multiple experimental signals. The ultimate goal is to detect or to constraint from data the set of fundamental independent variables

$$\{c_W, c_B, c_G, \mathbf{c}_f\},$$

which are to be treated as free Lagrangian parameters. The three anomalous gauge couplings O_W, O_B and O_G induce five distinct physical interactions with gluons, photons, W and Z bosons. These are typically codified as

$$\begin{aligned}
\mathcal{L}_a \supset &- c_G \frac{\alpha_s}{4\pi} \frac{a}{f_a} G_{\mu\nu}^a \tilde{G}^{a\mu\nu} - c_\gamma \frac{\alpha}{4\pi} \frac{a}{f_a} F_{\mu\nu} \tilde{F}^{a\mu\nu} - c_{\gamma Z} \frac{\alpha}{2\pi s_w c_w} \frac{a}{f_a} F_{\mu\nu} \tilde{Z}^{\mu\nu} \\
&- c_Z \frac{\alpha}{4\pi s_w^2 c_w^2} \frac{a}{f_a} Z_{\mu\nu} \tilde{Z}^{\mu\nu} - c_W \frac{\alpha}{2\pi s_w^2} \frac{a}{f_a} W_{\mu\nu}^+ \tilde{W}^{-\mu\nu},
\end{aligned} \tag{2.29}$$

where s_w and c_w are the sine and cosine of the Weinberg mixing angle respectively, c_w is defined at tree-level by

$$c_w = \frac{M_W}{M_Z}.$$

Thus the electroweak sector generates four interactions from the two anomalous couplings

$$\{c_W, c_B\} \rightarrow \{c_\gamma, c_Z, c_W, c_{\gamma Z}\}, \tag{2.30}$$

that are in principle independent. This fact allows one to overconstrain the electroweak gauge sector of the parameter space by imposing internal consistency.

In all cases the fermionic sector is instead described directly by the EFT coupling matrices $\mathbf{c}_f$ in a complete basis. For practical purposes one can define vector and axial couplings between the ALP and the fermionic current instead of chiral ones. To do so consider only quarks for simplicity and write everything in the vector/axial-vector form

$$\mathcal{L}_a^{\text{CP}} \supset \frac{\partial_\mu a}{2 f_a} \big(\bar{u} \gamma^\mu (\mathbb{1} + \gamma^5) \mathbf{c}_u u + \bar{d} \gamma^\mu (\mathbb{1} + \gamma^5) \mathbf{c}_d d + \bar{Q} \gamma^\mu (\mathbb{1} - \gamma^5) \mathbf{c}_Q Q \big) =$$

$$= \frac{\partial_\mu a}{2 f_a} \big(\bar{Q} \gamma^\mu \mathbf{C}_V Q + \bar{Q} \gamma^\mu \gamma^5 \mathbf{C}_A Q \big), \tag{2.31}$$

where $\mathbf{C}_V$ and $\mathbf{C}_A$ are defined as

$$\mathbf{C}_V = (\mathbf{c}_u \oplus \mathbf{c}_d) + \mathbf{c}_Q, \qquad \mathbf{C}_A = (\mathbf{c}_u \oplus \mathbf{c}_d) - \mathbf{c}_Q, \tag{2.32}$$

where the direct sum is the same as the one used in Eq.(2.31). The diagonal part of $\mathbf{C}_V$ is zero because of vector current conservation, while the diagonal part of $\mathbf{C}_A$ can be expressed in a basis independent way as

$$\begin{aligned}
c_u &\equiv (\mathbf{c}_u - \mathbf{c}_Q)^{11}, & c_c &\equiv (\mathbf{c}_u - \mathbf{c}_Q)^{22}, & c_t &\equiv (\mathbf{c}_u - \mathbf{c}_Q)^{33}, \\
c_d &\equiv (\mathbf{c}_d - \mathbf{V}^\dagger \mathbf{c}_Q \mathbf{V})^{11}, & c_s &\equiv (\mathbf{c}_d - \mathbf{V}^\dagger \mathbf{c}_Q \mathbf{V})^{22}, & c_b &\equiv (\mathbf{c}_d - \mathbf{V}^\dagger \mathbf{c}_Q \mathbf{V})^{33}, \\
c_e &\equiv (\mathbf{c}_e - \mathbf{c}_L)^{11}, & c_\mu &\equiv (\mathbf{c}_e - \mathbf{c}_L)^{22}, & c_\tau &\equiv (\mathbf{c}_e - \mathbf{c}_L)^{33},
\end{aligned} \tag{2.33}$$

where $\mathbf{V}$ is the CKM mixing matrix. If one takes the basis discussed in Sec.2.1 the notation is simpler given that $\mathbf{c}_Q^{11} = \mathbf{c}_L^{i=j} = 0$.

2.3.1 Minimal Flavor Violation

It is important to discuss what exactly Minimal Flavor Violation (MFV) means and to some extent what it entails, to do so here we follow the derivation found in [60]. The MFV Ansatz commands that the flavor violation stems from the Standard Model parameters and from nothing else. These means that any flavor–breaking hierarchical structure in the ALP EFT model has to come from the Yukawa matrices [64]. Under this hypothesis the matrices $\mathbf{c}_f$ can be expanded to first order in the spurion parameter ϵ as

$$
\begin{aligned}
\mathbf{c}_Q &= c_Q^0\mathbb{1} + \epsilon\left(c_Q^1\mathbf{Y}_u\mathbf{Y}_u^\dagger + c_Q^2\mathbf{Y}_d\mathbf{Y}_d^\dagger\right) + \mathcal{O}(\epsilon^2), \\
\mathbf{c}_u &= c_u^0\mathbb{1} + \epsilon c_u^1\mathbf{Y}_u^\dagger\mathbf{Y}_u + \mathcal{O}(\epsilon^2), \\
\mathbf{c}_d &= c_d^0\mathbb{1} + \epsilon c_d^1\mathbf{Y}_d^\dagger\mathbf{Y}_d + \mathcal{O}(\epsilon^2).
\end{aligned}
\tag{2.34}
$$

Similar results are valid for the leptonic sector. To study the effects of the MFV Ansatz it is instructive to look at the mass–basis. In this basis the change to the parameter matrices are better expressed by separating up and down fields in Q_L. One has

$$
\begin{aligned}
\mathcal{L}_a^{\mathrm{CP}} &\supset \frac{\partial^\mu a}{f_a}(\bar{U}_L\gamma_\mu\mathbf{c}_Q U_L + \bar{D}_L\gamma_\mu\mathbf{c}_Q D_L + \bar{u}_R\gamma_\mu\mathbf{c}_u u_R + \bar{d}_R\gamma_\mu\mathbf{c}_d d_R) = \\
&\frac{\partial^\mu a}{f_a}(\bar{U}_L\gamma_\mu\mathbf{c}_Q U_L + \bar{D}_L\gamma_\mu\mathbf{V}^\dagger\mathbf{c}_Q\mathbf{V} D_L + \bar{u}_R\gamma_\mu\mathbf{c}_u u_R + \bar{d}_R\gamma_\mu\mathbf{c}_d d_R),
\end{aligned}
\tag{2.35}
$$

where between the first and second line one performs a transformation to basis for which all the transition matrices are the identity except for the one associated to D_L, i.e. $\mathbf{U}_D^L = \mathbf{V}$, here $\mathbf{Y}_u$ is diagonal and $\mathbf{Y}_d^{\mathrm{diag}} = \mathbf{V}\mathbf{Y}_d$, where once again $\mathbf{V}$ indicates the CKM matrix. At this stage one needs to separate up and down coupling matrices for the L–handed fields, sometimes in the literature these matrices have been called $\mathbf{K}_U$ and $\mathbf{K}_D$. In the case discussed here $\mathbf{K}_U = \mathbf{c}_Q$, while $\mathbf{K}_D = \mathbf{V}^\dagger\mathbf{c}_Q\mathbf{V}$. Finally Eq.(2.34) in this basis with the

addition of $\mathbf{K}_U$ becomes

$$
\begin{aligned}
\mathbf{c}_Q &= c_Q^0 \mathbb{1} + \epsilon \left(c_Q^1 (\mathbf{Y}_u^{\text{diag}})^2 + c_Q^2 \mathbf{V}(\mathbf{Y}_d^{\text{diag}})^2 \mathbf{V}^\dagger \right) + \mathcal{O}(\epsilon^2), \\
\mathbf{K}_D &= c_Q^0 \mathbb{1} + \epsilon \left(c_Q^1 \mathbf{V}^\dagger (\mathbf{Y}_u^{\text{diag}})^2 \mathbf{V} + c_Q^2 (\mathbf{Y}_d^{\text{diag}})^2 \right) + \mathcal{O}(\epsilon^2), \\
\mathbf{c}_u &= c_u^0 \mathbb{1} + \epsilon c_u^1 (\mathbf{Y}_u^{\text{diag}})^2 + \mathcal{O}(\epsilon^2), \\
\mathbf{c}_d &= c_d^0 \mathbb{1} + \epsilon c_d^1 \mathbf{V}^\dagger (\mathbf{Y}_d^{\text{diag}})^2 \mathbf{V} + \mathcal{O}(\epsilon^2).
\end{aligned}
\tag{2.36}
$$

In Eq.(2.36) it is clear that any flavor violating effect comes from Standard Model parameters, in particular from products of Yukawas with elements of the CKM matrix. Finally one can get a good approximation by taking $\mathbf{Y}_d^{\text{diag}} = 0$ and $\mathbf{Y}_u^{\text{diag}} = \text{diag}(0, 0, y_t)$. This implies that any flavor violating effect will be induced by $\mathbf{K}_D$, and it will be proportional to y_t times elements of the CKM matrix:

$$
\begin{aligned}
\mathbf{c}_Q &= c_Q^0 \mathbb{1} + y_t^2 \epsilon c_Q^1 + \mathcal{O}(\epsilon^2), \\
(\mathbf{K}_D)_{ij} &= c_Q^0 \delta_{ij} + y_t^2 \epsilon V_{3j} V_{3i}^* c_Q^1 + \mathcal{O}(\epsilon^2), \\
\mathbf{c}_u &= c_u^0 \mathbb{1} + y_t^2 \epsilon c_u^1 + \mathcal{O}(\epsilon^2), \\
\mathbf{c}_d &= c_d^0 \mathbb{1} + \mathcal{O}(\epsilon^2).
\end{aligned}
\tag{2.37}
$$

2.4 Renormalization Group Flow

The Effective Field Theory discussed in Sec.2.1 is well defined in the energy range contained between f_a and v. At energies close to f_a the EFT approach breaks down and all the terms in the Laurent series contribute the same amount. On the other hand at energies below the electroweak phase transitions the effective degrees of freedom describing the interactions are different than the ones defined at high energies. The obvious example is given by the Higgs field effectively disappearing from the spectrum below the electroweak scale. If the energies of experiments are well below the masses of the heavy bosons mediating the weak interaction the theory can be simplified even further by removing the non–propagating particles with a second expansion in inverse mass scales given by the masses of the weak vector bosons.

In considering processes at different scales than the ones at which the

theory is defined quantum effects will induce a trajectory in theory space for the parameters of the Lagrangian. These corrections to the classical scaling will drive the solution away from the particular perturbative fixed point as the separation gets bigger. In the case of the ALP Effective Field Theory a combination of threshold effects and operator running play a role in the low–energy observables measured in experiments. This has recently motivated a number of articles on the subject of Renormalization Group flow and one loop corrections to the ALP coupling [59, 60, 65] that are discussed, in the needed measure, below.

2.4.1   Non-renormalization theorems

It is well known [66] that CP–odd anomalous gauge couplings within the SM, i.e. Lagrangian terms of the generic form $\alpha X \tilde{X}$ where X is a generic gauge field strength and α its fine structure constant, are not multiplicatively renormalized at any order in perturbation theory. The reason is their topological character, discussedd in Chapter 1, which ensures anomaly matching conditions. The combinations $\alpha/2\pi X \tilde{X}$ appear in the Lagrangian multiplied by "θ" angles which are periodic variables with periodicity of 2π, and cannot thus be multiplicatively renormalized. In the case of the ALP–gauge anomalous couplings, the ratio $\frac{a}{f_a}$ plays the role of the effective angle. The non-renormalization theorems thus apply as well to ALP couplings of the form $\alpha/2\pi X \tilde{X}$, where $2\pi f_a$ is the periodicity of a. In consequence, no UV divergent terms can result from corrections to the combinations $\alpha_1/2\pi O_W$, $\alpha_2/2\pi O_B$ and $\alpha_s/2\pi O_G$, this result has been discussed in [65]. This simply means that

$$\beta_{c_B} = \frac{d}{d\log\mu}c_B = 0, \qquad \beta_{c_W} = \frac{d}{d\log\mu}c_W = 0, \qquad \beta_{c_G} = \frac{d}{d\log\mu}c_G = 0.$$
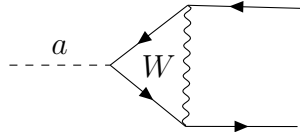$$(2.38)$$

Matching effects to the ALP-gluon and ALP-photon couplings c_G and c_γ could in principle arise from loop graphs containing top quarks and heavy electroweak gauge bosons. The corresponding effects were calculated in [67] and it was shown that for a light ALP these effects decouple like m_a^2/m_t^2 and m_a^2/m_W^2, respectively. For a light ALP far below the weak scale there are

thus no matching contributions to the effective low-energy Lagrangian

$$\Delta c_G = 0, \qquad \Delta c_\gamma = 0. \qquad (2.39)$$

2.4.2 Renormalization of Fermionic couplings

The case of fermionic couplings is much more involved than that of the anomalous ones. The beta functions for the ALP–fermion couplings have been obtained using a variety of bases [60, 65, 68] and a complete one–loop analysis including finite effects is present for generation diagonal couplings only [59]. While the beta functions and matching have been obtained with in a redundant basis in [60]. The relevant discussion, at least for the phenomenological analysis presented in this manuscript, is the one regarding top–induced flavor changing effects. As discussed in [60, 67] these are the result of top–enhanced penguin type diagrams, and can be mapped, in the leading log approximation, onto a low–energy flavor violating effective Lagrangian [69]. This effect is a NLO correction to the 3–point function $\left\langle \frac{\partial_\mu a}{f_a} \bar{\psi}_i \gamma^\mu \gamma^5 \psi_j \right\rangle$ mostly relevant for external down–type quarks. Assuming a large enough separation of scales, $f_a \gg v$, one can use the leading log approximation to evaluate the diagram:

$$\simeq -\frac{q_\mu}{8 f_a} \frac{G_F}{\sqrt{2}} \bar{Q}_i \gamma^\mu \gamma^5 \left(\sum_k V_{ki}^* V_{kj} \mathbf{C}_{kk}^A m_k^2 \log\left(\frac{f_a}{m_k}\right)^2 \right) Q_j$$

$$(2.40)$$

where the sum runs over the internal loop quarks and the extra mass term is from a mass insertion. The dimensionless quantity regulating the magnitude of the contribution is $G_F m_k^2 V_{ki}^* V_{kj} \log\left(\frac{f_a}{m_k}\right)^2$, and as such a combination of mass and Cabibbo suppression will determine the strength of this effect. One should expect the top–quark to dominate the loop contribution, nonetheless some interesting phenomenology is induced by internal down–type quarks too. A through analysis is presented in Sec.5.1 and in Tab.5.1. Consistently with the literature on ALP–fermion phenomenology and the discussion pre-

sented here, the parameters regulating flavor changing neutral currents mediated by the ALP are defined at low energy by the effective Lagrangian

$$\delta\mathcal{L}^a_{\text{eff}} = -c_{ij}\frac{\partial_\mu a}{f_a}\bar{d}_i\gamma^\mu P_L d_j + \text{h.c.} \tag{2.41}$$

with an analogue for external up–type quarks. The parameter c_{ij} is typically defined by equating Eqs.(2.40) and (2.41) to each other.

2.5 Phenomenological parameters below the electroweak scale

It is necessary to choose a complete set of phenomenologically viable parameters, similarly to what have been discussed in Sec.2.3, viable at low–energies. Indeed Eq.(2.31) is a perfectly good starting point. As discussed in Sec.2.4.1 the gauge anomalous parameters do not run nor receive matching contribution from integrating out the heavy chiral fermion fields $t_{L,R}$ neither from the heavy gauge bosons W and Z. The fermionic case, discussed in Sec.2.4.2 is different and requires some more careful considerations. A perfectly fine way to discuss the low–energy theory is to define the couplings and the parameters that one measures at the scale at which one measures them. This eliminates the issue of quantum–induced running and the matching procedure altogether. As a relevant example consider the Lagrangian in Eq.(2.31), a complete set of couplings is $\{c_\gamma, c_G, \mathbf{C}_V, \mathbf{C}_A\}$. Of course in Eq.(2.31) the top field t is still considered dynamical. To simplify the theory further consider the construction of Sec.2.3.1 along with the discussion in Sec.2.4.2, i.e. consider a Minimal Flavor Violation Ansatz for the theory. This will ensure that all the flavor violation is proportional to the top Yukawa times a combination of elements of the CKM. The Lagrangian considered in the phenomenological analysis of Chapters 4 and 5 is defined as

$$\begin{aligned}\mathcal{L}^{\text{CP}}_a = &- c_G\frac{\alpha_s}{4\pi}\frac{a}{f_a}G^a_{\mu\nu}\tilde{G}^{a\mu\nu} - c_\gamma\frac{\alpha}{4\pi}\frac{a}{f_a}F_{\mu\nu}\tilde{F}^{a\mu\nu}\\ &+ \frac{\partial_\mu a}{2f_a}\left(\bar{Q}\gamma^\mu\mathbf{C}_V Q + \bar{Q}\gamma^\mu\gamma^5\mathbf{C}_A Q\right),\end{aligned} \tag{2.42}$$

where $\mathbf{C}_V$ and $\mathbf{C}_A$ have been discussed in Sec.2.3 and are to be considered in the mass basis. Following [69] and Sec.2.4.2 the RG effect is captured in a logarithm dependence introduced in the down–quarks off–diagonal couplings.

2.5.1 Weak Chiral Lagrangian Couplings

In Sec.1.4.2 we obtained an expression for the Chiral Lagrangian for the QCD–Axion, the same can be done for ALPs too without changing much. Following what has been pointed out in a recent paper [61] where the authors discuss a contribution that has been missed in the literature one can recover the terms that mediate flavor–changing non-leptonic decays in the Kaonic sector. The problem arises in the first place if one argues that having no coupling in the partonic phase between the W bosons and the L–handed current would yield no coupling in the condensed phase. The reasoning seems sound at face value but once the fields condense the L and R part are mixed via the mass term, thus inducing an ALP–meson coupling even when only the R–handed fermions couple with the ALP in the partonic phase.

The Lagrangian responsable for flavor–changing non-leptonic decays in $s \to d$ transitions is

$$\mathcal{L}_\chi = -\frac{4G_F}{\sqrt{2}} V_{ud}^* V_{us} \left(g_8 \mathcal{O}_8 + g_{27}^{1/2} \mathcal{O}_{27}^{1/2} + g_{27}^{3/2} \mathcal{O}_{27}^{3/2} \right) \tag{2.43}$$

where the effective chiral operators are classified according to their transformation properties under $SU(3)$ and isospin. The $SU(3)$ octet operator $\mathcal{O}_8$ mediates weak transitions with isospin change $\Delta I = \frac{1}{2}$, while the 27–plet operators $\mathcal{O}_{27}^{1/2}$ and $\mathcal{O}_{27}^{3/2}$ mediate the transitions with $\Delta I = \frac{1}{2}$ and $\Delta I = \frac{3}{2}$, respectively. These operators can be expressed in terms of products of the left–handed operators J_μ^a, corresponding to the chiral representation of the chiral quark currents $\bar{q}^i \gamma_\mu P_L q^j$. One finds that the operators are:

$$\begin{aligned} \mathcal{O}_8 &= \sum_i (J^a)_{3i} (J^a)_{2i}, \\ \mathcal{O}_{27}^{1/2} &= (J^a)_{32}(J^a)_{11} + (J^a)_{31}(J^a)_{12} + 2(J^a)_{32}(J^a)_{22} - 3(J^a)_{32}(J^a)_{33}, \\ \mathcal{O}_{27}^{3/2} &= (J^a)_{32}(J^a)_{11} + (J^a)_{31}(J^a)_{12} - (J^a)_{32}(J^a)_{22}, \end{aligned} \tag{2.44}$$

where the contraction over Lorentz indices is implied. The coefficient of the octet operator $|g_8| \approx 5$ [70], is larger than the coefficient $|g_{27}^{3/2}|$ by about a factor of 30, and in the $SU(3)$ symmetry limit the coefficient $|g_{27}^{1/2}|$ is smaller than $|g_{27}^{3/2}|$ by a factor of 5. The enhancement of the $\Delta I = 1/2$ transition is known as the $\Delta I = 1/2$ selection rule.

2.6 CP–violating ALP couplings

A surprisingly less explored sector of light pseudo–scalar particles phenomenology are the CP–Violating ALP interactions. To introduce CP violation in the PQ broken phase one is simply required to consider the operators:

$$\mathcal{L}^{CPV} = c_\gamma^{CPV} \frac{\alpha}{4\pi} \frac{a}{f_a} FF + c_G^{CPV} \frac{\alpha_s}{8\pi} \frac{a}{f_a} GG + g_{af}^S \phi H \bar{f} f. \qquad (2.45)$$

These terms can introduce new–forces, such as scalar–scalar (monopole–monopole) and scalar–pseudo-scalar (monopole–dipole) interactions [71]. The non–relativistic limit of the scalar–scalar interaction in Eq.(2.45) for two nucleons N_1 and N_2 can be computed as in the inverse Born approximation

$$V(r) = -\frac{g_{N_1}^S g_{N_2}^S}{4\pi r} e^{-m_a r}. \qquad (2.46)$$

For light–ALPs the couplings are subject to strong limits, as one can test precise Newton's inverse square law. Instead monopole–dipole interactions can test combination of couplings of the type $g_{aN}^S g_{aN}$, that will be tested in the ARIADNE and QUAX experiments [72, 73]. It has been shown [74] that CPV signatures at low–energy require shift and CP symmetry–breaking effects in the UV. These effects will be inherited to the IR dynamics via some mechanism that is yet to be specified. An interesting parallel can be found in mesonic interactions where the π_0 is the analogue of the ALP, mediating CP conserving and CP violating interactions whenever $\theta \neq 0$.

CP-violating scalar ALP couplings to nucleons are generated whenever the potential does not exactly relax the ALP VEV to zero. In the presence of extra sources of CP violation in the UV it is expected that $\theta_{\text{eff}} = \langle a \rangle / f_a \neq 0$

and one can pose a limit on the scalar coupling

$$g_{aN}^{S} = \theta_{\text{eff}} \left(\frac{17\text{MeV}}{f_a} \right).$$

(2.47)

For a recent discussion on the subject, one is referred to [74, 75].

Chapter 3

Experimental Searches and Results

In the following we give a brief review of the different possible Axion and ALP parameter bounds extracted from experiments focusing on Beam Dump searches and flavor factories. Nonetheless, as one can see from Fig. 3.1, the ALP parameter space has been explored in many different ways, often with non zero overlap. This joint effort of astrophysical, cosmological and terrestrial probes gives the best chance of exploring the theory space in a meaningful way. For the sake of completeness a brief discussion is carried on the primary arguments of the different searches, along with a concise review of the indirect constraints on axions and ALPs from cosmology and astrophysics, for an in–depth look at these issues see [77–79]. Typically the bounds extracted from cosmological searches are often model–dependent and come from early–universe, inflation, reionisation, dark matter, dark radiation etc... Axions and ALPs might sometime improve the matching of observation with theoretical expectations, in this case one might see these results as **hints** towards a preferred model. With these highly indirect observations claiming a discovery is very hard due to the difficulty in establishing observational and systematic errors. The strategy is to accumulate hints of axion and ALPs existence from different searches to increase their individual significance.
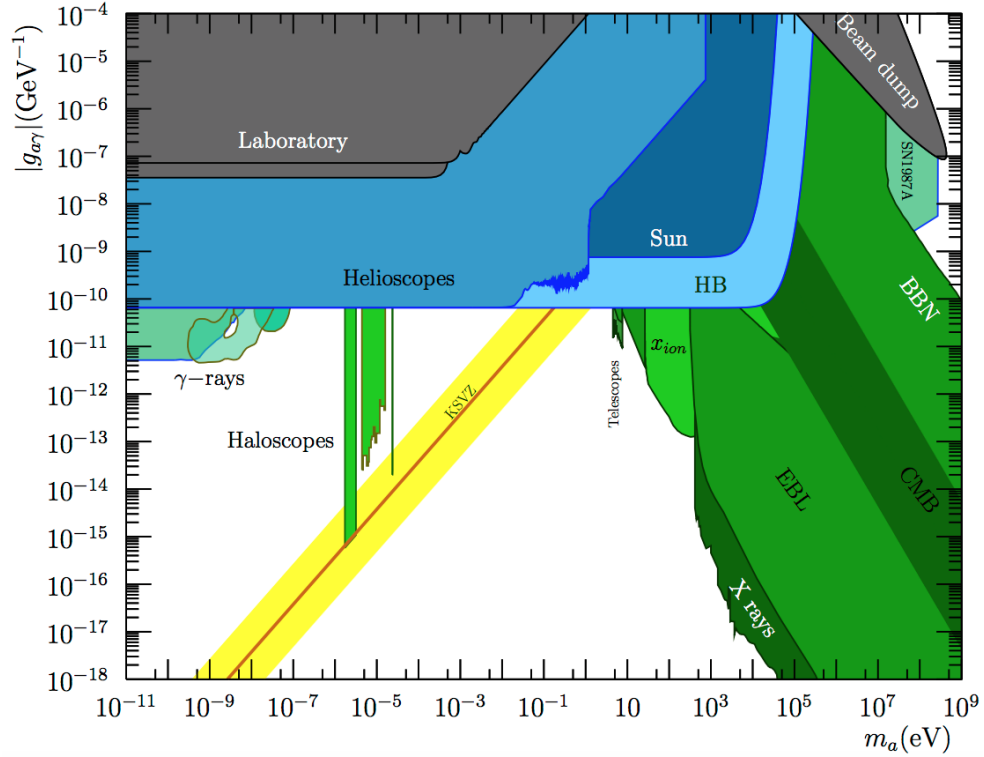
Figure 3.1: In the figure its presented a review of the overall constraints in the (m_a, g_γ) plane. The yellow/orange area represents the allowed parameter space of QCD–axion models while the rest is the theory space of ALPs. The bounds are colour coded: black/gray for purely laboratory results, bluish colors for helioscope experiments or bounds depending on stellar physics, and greenish for haloscopes or cosmology-dependent arguments. The picture is taken from the rewiew [76].

3.1 Cosmological Bounds

ALPs and axions are pseudo–Nambu–Goldstone–Bosons of a symmetry spontaneously broken at some high scale f_a. At energies higher than that scale ALPs are nowhere to be found, instead a different degree of freedom, typically identified with some scalar field S, would be dynamical and evolving. As the energy of the field S reaches scales that are comparable to f_a a phase transition must occur with the field VEV freezing to some value. Below the critical temperature of this transition a new degree of freedom, associated with a flat direction in the potential emerges, this is the QCD axion/ALP. Any deviation from a completely flat direction are associated with explicit breaking of the global shift symmetry of the ALPs, in particular the mass operator. Of course as long as the ALP mass is small with respect to the scale f_a at the phase transition the ALP will be in a state of indifferent stability, meaning that in different causally disconnected "patches" of the Universe different equivalent vacuua will be occupied. If the ALP field is periodic than one cannot avoid string formation due to the Kibble mechanism [80]. In the string cores, the order parameter cannot break the PQ symmetry restricted by topology and a huge energy density is stored $\sim f_a^4$. The string network eventually evolves emitting low–momentum ALPs and decreasing its length. At the phase transition ALP interactions to the thermal bath are not expected to be small, and so a thermalized ALP populations is expected on top of the smooth field. The VEV will have a wavelength the size of the horizon t, while the thermal fluctuations are $t(T/M_{\rm Pl}) \ll 1$ where T is the temperature. In this picture one has $T \sim f_a \ll M_{\rm Pl}$ so that there is a huge separation of scales between the long-wavelength ALPs and the thermal ones.

The picture that emerges up to this point is completely general and the main take away should be the fact that there are at least two ALP populations, cold and hot. Their role in the history of the Universe is well separated and un–correlated. The important separation is that cold ALPs are a candidate for cold dark matter, while hot ALPs population can account for hot dark matter and hot dark energy. In particular the effects due to the ALP–SM couplings can always be as small as one can push f_a in the UV, while some other constraints are harder to avoid, e.g. its gravitational sig-

nature. Suppose that the ALP production takes place during the radiation dominated era, where the production rate are high thanks to high temperature, and suppose that the ALP thermalizes with the SM bath. Under this assumption is possible to compare the ALP radiation density to today's CMB photon density. Depending on the masses one can distinguish either cold or hot dark matter, and eventually dark radiation for very light ALPs. Hot dark matter threshold is typically at 10KeV. The latter scenario affects structure formation and can be constrained via CMB anisotropies. There is also the possibility of non–thermal production where Dark Radiation ALPs and Hot DM ALPs are produced in galaxy clusters producing soft–X–rays by photon conversion. In this case a strong bound on photon coupling can be enforced $g_\gamma \sim 10^{-12}$. If the ALPs/Axions are light enough their preferred decay channel has to be via photons and will induce signatures based on when the DM ALP decays. If the decay happens before the CMB decoupling the huge photon injection can distort the predicted spectrum. If one considers DM decaying after recombination there should be some monochromatic line broadened by cosmic expansion, that can be constrained by the flux of extragalactic background light (EBL in Fig.3.1) or by direct line searches in the X-ray and gamma-ray region. At high energies the UV cross section of H photoionisation is so large that these photons can alter the history of the Hydrogen ionisation fraction is modified. If one then assumes a high enough reheating temperature one has the constraints shown as BBN, CMB, X–rays and *x*ion [78]. Assuming that ALPs account for all the observable cold DM, the ensuing constraints are shown in Fig. 3.1 labelled as "Telescopes".

Another interesting way of implementing bounds in the ALP parameter space is via inflation. The ALP potential is flat and to have UV validity it has to be protected by radiative corrections and higher order effects. Some models have been proposed, called "natural–inflation" with interesting potentials such as $\Lambda^4(1 - \cos\theta)$. Given the nature of inflation the low–energy phenomenology is typically decoupled from the specific of the UV theory.

3.2 Astrophysics

Thanks to their couplings with light matter fields ALPs can be thermally produced inside stars. The dense and hot surrounding along with the possibility of emission from the whole star, core included, compensates well the weakness of these parameters. It is well known that the total emission can compete with photon surface emission and with thermal neutrino emission. This means that stars are the best ALPs and axions factories in the Universe and effects of such a huge production should yield some kind of signature of their presence, unless their couplings are extremely small. In this sense astrophysical bounds are perfect for probing the light ALPs theory space via a number of mechanisms. Particular attention is dedicated to the ALP coupling to photons in the literature, the coefficient of the operator $aF\tilde{F}$.

In the contest of stellar evolution, the most relevant process is the Primakoff conversion. This consist in the conversion of thermal photons, due to external electrostatic fields, into ALPs:

$$\gamma + Ze \rightarrow a + Ze. \tag{3.1}$$

It turn out that the energy–loss rate per unit mass via ALPs radiation of a star becomes relevant for low density and high temperature cores. These conditions are found in the Horizontal Branch (HB) evolution phase of a Red Giant. The indirect limit extracted from these observation can be seen in Fig. 3.1 denominated as "HB". The data has been collected on 39 Globular Clusters (GCs) [81, 82] and measures the ratio of Horizontal Branch to Red Giants in the GC. The ratio decreases as the HB phase is accelerated due to ALPs overproduction. The Sun is also a great laboratory for ALP–photon coupling, and its proximity allows one to be very sensitive to these light particles flux. In particular the bounds extracted from Sun physics are due to neutriuno flux and helioseismology [83]. Another, more "direct" way of using the Sun's Axion flux to probe the ALPs parameter space is via Helioscopes. These work using the inverse Primakoff effect where an ALP interact with an external magnetic field and is converted to a photon. These Helioscopes have mass ranges of m_a [meV,eV], and essentially are concerned with Dark Radiation ALPs. Limits have also been extracted from the Supernova data

SN1987A.

As discussed in Sec.2.6 the introduction of CPV couplings can induce monopole–monopole forces between baryons that can compete with gravity at distances $1/m_a$. These have been studied in highly precise experiments. The direct measurements on dipole–dipole interactions are much weaker than the astrophysical limits on the same parameters, both for nucleons and electrons couplings.

3.3   Bounds from Flavor Physics

This section finally introduces the main argument of the manuscript: flavor induced bounds on ALP–fermion couplings. These searches are relevant in virtually any model in which the ALP is implemented. As discussed in [60] the PQ–symmetry can exhibit flavor–violation at the UV scale or not, the low–energy couplings will always get a radiatively induced flavor–violating part. Flavor violation opens up the possibility to study ALPs in rare, flavor–changing processes that are among the most sensitive tests for light new–physics. The nature of pseudo–Nambu-Goldstone-Bosons provide a window into energy scales well beyond the capabilities of LHC with machines that operate at a fraction of the energy.

Flavor violating processes are typically, but not exclusively, mediated by couplings to fermionic fields, and provide powerful and sensitive tools in the exploration of the ALP theory–space. Among the 5–dimensional portal between ALPs and SM the most important structure, in this context, is the ALP–fermion coupling in Sec2.3.1. In what follows model–independent couplings are considered and no UV structure is assumed. In this sense all the limits derived are, if not explicitly said so, on the low–energy parameters of the theory.

This theoretical picture allows one to look at Flavor Factories and Beam Dump data, taken at energies up to a few GeV's, and project limits on ALP–fermion interactions from flavor–violating processes. Quark flavor phenomenology of Axion–Like Particles has mesonic decays in its primary roles, for a recent review see [84, 85]. Indeed most of the studies and the advances in this sector come from Kaon physics or B-physics.
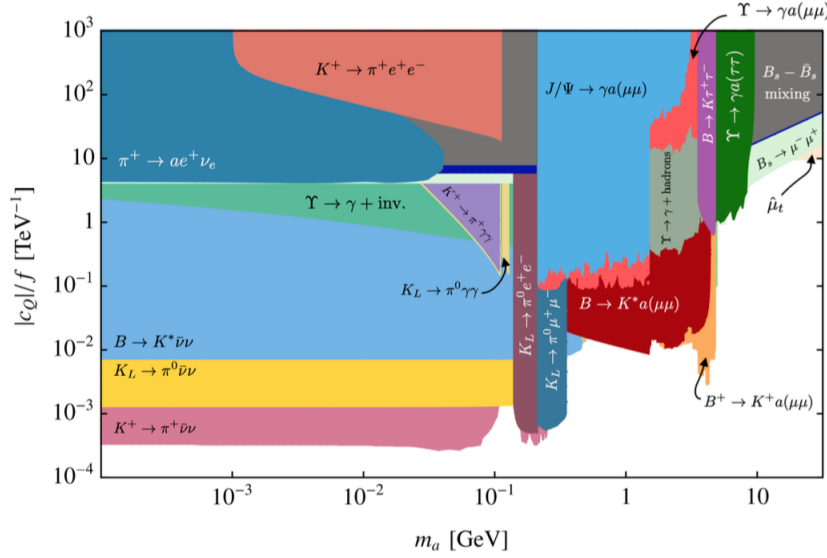
Figure 3.2: Flavor bounds on universal ALP couplings to quark doublets with $\mathbf{c}_Q = c_Q \mathbb{1}$, and all other coefficients set to zero at the scale $f_a = 1\text{TeV}$. The picture is taken from the review [84].

As a simplifying model–dependent case study take all the ALP couplings as Universal and to the quark doublets. The constraint from flavor physics are shown in Figure 3.2. In this scenario any isospin conserving ALP coupling comes from the running and matching from the high energy scale to the low–energy one. Moreover isospin breaking ALP couplings enhance the ALP–photon couplings and in this hypothesis the final visible state $\gamma\gamma$ will experience suppression. The strongest bounds are from invisible channels or muonic signatures.

The flagship process of flavor searches for ALPs is the $K \to \pi a$ signature. It arises from a $s \to d\, a$ quark level transition, with the new physics particle escaping the detector. Kaon physics is thus in the spotlight and many different current and future experiments are probing these rare Kaon decays. In particular the NA62 experiment at CERN is looking for a signal of the type $K^+ \to \pi^+ a$. The experiment has collected 3×10^{16} pot in Run 1 and is aiming for 10^{18} pot by the end of Run 2. Using the complete Run 1 dataset, the NA62 experiment established upper limits on $\mathcal{B}(K \to \pi a)$ with a invisible at

the level of 10^{-11} in the mass ranges of 0–110 MeV and 155–260 MeV [86, 87] The search represents a direct extension of the $K^+ \to \pi^+ \bar{\nu} \nu$ measurement, which determines the range scanned for m_a. The event selection requires a K^+ in the initial state and a π^+ in the final state, in the absence of any other in–time activity in the detector. The largest (and irreducible) background is due to the $K^+ \to \pi^+ \bar{\nu} \nu$ decay. The two-body decay of these channel is characterised by a peak in the reconstructed missing mass distribution, with a width of $\mathcal{O}\left(10^{-3}\right)$ GeV^2 determined by the experimental resolution, on top of the contiuous $K^+ \to \pi^+ \bar{\nu} \nu$ spectrum. The NA62 experiment has also established upper limits on $\mathcal{B}(K \to \pi a)$ with invisible a, at the level of $\mathcal{O}\left(10^{-9}\right)$ in the 110–115 MeV mass range, in the vicinity of the π_0 mass, from a dedicated analysis based on the 10% of the Run 1 minimum bias dataset [88]. Measurements of the $K_L \to \pi^0 \bar{\nu} \nu$ decay naturally provide limits on $\mathcal{O}\left(K_L \to \pi^0 a\right)$. Once again the dominant background is given by the $\pi \bar{\nu} \nu$ final state. In this experiment no missing mass reconstruction is performed, so there is no reduction in the acceptance for the ALP to be in the π^0 mass region. The KOTO experiment [89] has reported a limit on $\mathcal{B}(K^0 \to \pi^0 a)$ down to 2.4×10^{-9} at 90% CL with the 2015 dataset. Recently new preliminary results have shown three signal candidate over a 50% predicted background. In the short term KOTO sensitivity is expected to improve.

The B physics sector has also a fundamental impact on flavor searches limiting the ALP–fermion couplings space. LHCb [90, 91] BaBar and Belle [69, 92–99] have studied visible and invisible signatures of b–decays. Belle experiment had conducted searches for $B \to h \bar{\nu} \nu$ for many different mesonic states. These searches are conducted with the full Belle data sample produced by the KEKB collider at the $\Upsilon(4S)$ center-of-mass energy with an integrated luminosity of 711 fb^{-1}, $(772 \pm 11) \times 10^6$ $B\bar{B}$ pairs. The three–body $B \to h \bar{\nu} \nu$ decay, with two invisible particles in the final state can not convey enough kinematic information. Indeed the experiment has to fully reconstruct the accompanying B meson in the semileptonic decay channels decaying to D's or D^* and a lepton–neutrino couple.

Another class of decays usefull in probing ALP–fermion physics is given by monogamma final states. Υ resonant searches exploiting decays such as $\Upsilon(nS) \to \Upsilon(1S)\pi^+\pi^-$ can be used to directly probe $\Upsilon(1S)$ decays [100].

Also low background channels like $B^0 \to \gamma a$ or $K_L^0 \to \gamma a$ can be used to probe quark couplings at low–energies. These searches have been carried on at BaBar [101] and at the Belle [102] experiment.

Chapter 4

Hadronization Techniques

It will be useful to spend some time discussing hadronization and composite-object couplings to ALP current ($a_\mu^{(a)} = (\partial_\mu a)/f_a$) to understand the approximation considered and build some physical intuition. Such a discussion, to the authors knowledge, is missing in the literature at least for the case of a massive ALP, while a general discussion can be found in [103–105]. For elementary particles the coupling is a model dependent parameter coming from a "charge" matrix sometimes denoted $\mathbf{C_Q}$. For extended objects, exactly like the case of protons form factors, it will be replaced by a momentum-dependent function reflecting the distribution of the masses and velocities of partons, and in turn the bound state's internal structure [106, 107]. Once again in the case of elementary particles coupling to ALPs it is understood that the current will couple to fermions proportionally to their momenta, or in an equivalent base, to their masses. In a similar fashion one expects extended objects to have a sort of effective coupling mass that will depend on the total momentum and on its distribution between the internal degrees of freedom. Finally the nature of the hadronic state will play a fundamental role in its relativistc behaviour. The perturbative treatment of these processes assumes a partonic description of the hadrons involved in the transition. The general discussion is very similar to that of inclusive hadron processes, such as deep–inelastic scattering, with the premise that in some limit the amplitudes can be written as a product of three probabilties that separate long–distance and short-distance physics.
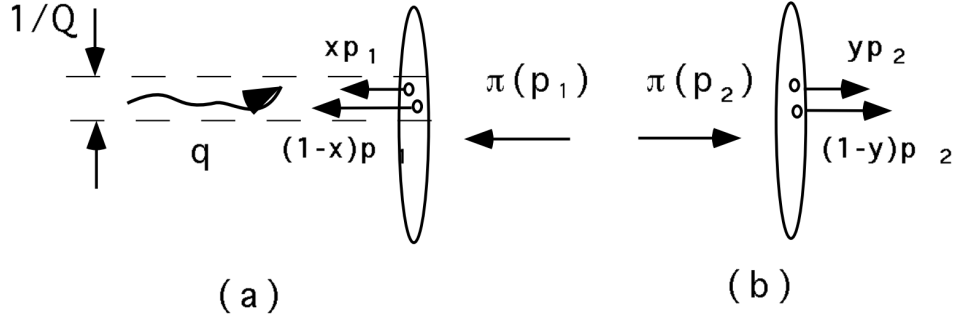
Figure 4.1: The valence quark state of a pion interacting with an external current carrying momentum Q. The valence couple must be localized in $1/Q$ in the transverse direction while in the longitudinal one Lorentz contraction assures the particles to be close. The picture is taken from [105].

Despite the fact that in their rest frame mesons are complex non-static objects, a highly relativistic particle would ony see the dominant valence quark content justifing a simplified description of these non–perturbative states [103–105]. In the case at hand[1] the important observation is that the final state particles recoiling back to back, the ALP and the daughter meson, must have a nearly light-like relative velocity, i.e. they must be emitted in a highly relativstic state. Under this condition the strong quantum effects that bind the constituents of the involved meson are highly time-dilated in the rest frame of the escaping ALP. Moreover the lifetime of these states are stretched and the partonic content looks frozen to the escaping particle. For relative speeds near the speed of light the two recoiling particles are in contact for very short times decreasing as $1/\gamma = (1 - v^2/c^2)^{1/2}$. The relevant interactions can only happen on small time scales and short distances, relative to typical mesonic sizes and masses, where QCD is perturbative. As such the short–distance dynamics and the long–distance ones will have no interference. This incoherence between soft and hard physics implies that one can consider each meson to consist of a definite partonic state during the entire interaction, allowing for the simplification discussed at the start of the section. The long time dynamics of the initial state are described by

---

[1]A version of the hadronization technique discussed here with a massless ALP was discussed first in [108].

the valence quarks distribution ϕ_{in}, these quarks undergo a short–distance process described by a hard–scattering skeleton diagram. At a later time, they reform the outgoing meson via a wave function ϕ_{out}. The amplitude is written as the product of three probabilities: 1) the probability of finding the valence quarks of the incoming meson with a certain momentum distribution, namely ϕ_{in}, 2) the hard amplitude T_H for the partons to emit an ALP and undergo a flavour change producing the quarks in the final state, see Fig.4.4, and finally 3) the amplitude for that same final state to recombine in the meson, given by ϕ_{out}. These three pieces are then convoluted into a single amplitude describing the process in this approximation. At energies well below the electroweak symmetry breaking the process appears as if a flavor changing external ALP current, proportional to $G_F V^{\text{CKM}} \partial_\mu a / f_a$, induces the hadronic process considered. In this sense the analogy with an electroweak form factor is saturated. From a more practical point of view the amplitudes are represented by the product

$$\int_0^1 dx \delta \left(1 - \sum_i x_i \right) \int_0^1 dy \phi_{\text{out}}^*(y_i, \mu) T_H(x_i, y_i, Q, \mu) \phi_{\text{in}}(x_i, \mu) \delta \left(1 - \sum_i y_i \right),$$
(4.1)

where T_H is the hard scattering computed perturbatively, Q is the exchanged momentum and μ is the renormalization scale (entering via the couplings). The μ dependence in the ϕ's is induced to render Eq.(4.1) independent of the particular value of the renormalization scale. A natural choice is $Q = \mu$ making perturbative calculation consistent as long as $\alpha_s(Q)$ is perturbative, i.e. for large Q's. The length associated to this momentum exchange is $b = 1/Q$ and it represents the localization of the valence quarks couple in the transverse plane, relative to the mesons motion as shown pictorically in Fig.4.1. If the partons are separated more than $b = 1/Q$ that particular state will not contribute to the amplitude. So the information needed is on the state is of the order Q/M_M where M_M is the meson mass. Three particle states, e.g. with an extra gluon, will be suppressed by extra factors of $1/Q$, since as Q grows the probability of finding more than the minimum number of particles bunched up in $1/Q$ decreases. The classical dimension of T_H is of $(\text{mass})^{-2}$ and since the dependence has to come from external momenta

the approximate form can be $T_H \sim 1/(xyQ^2) + 1/((1-x)(1-y)Q^2)$. The extremes $x, y \simeq 0, 1$ known as "end–points" are problematic as they violate the localization assumption and generate unphysical singularities. Indeed in the limit $x, y \simeq 0, 1$ the hard scattering function T_H spreads out in transverse space and it will not be concentrated around $1/Q$. One has to finally define the position space equivalent of the wave function. The definition is carried in the light–cone coordinates for a mesonic state. The amplitude for the valence quark of such a state to annihilate in the vacuum in position space is,

$$\Psi(z \cdot p, z^2) = \langle 0| \, \bar{q}(0)\gamma^+\gamma^5 Q(z) \, |M(p)\rangle \,, \tag{4.2}$$

where p is taken in the plus direction, $\gamma^{\pm} = \frac{1}{\sqrt{2}}(\gamma^0 \pm \gamma^3)$, z are the light–cone coordinate and the distance between the valence quark fields z^2 is taken as space–like. The Dirac structure $\gamma^+\gamma^5$ projects out the zero helicity combination of the valence quarks. For $\phi(x, \mu)$ the convention is to fix the quark momentum fraction to be xp along the mesonic direction of motion and to integrate freely on the rest transverse momenta. The coordinate system is then fixed to have $z_+ = z_T = 0$, and the Fourier transform taken with respect of z^-,

$$\phi(x, \mu) = \int_{-\infty}^{\infty} \frac{dz^-}{2\pi} e^{iz^- p^+ x} \Psi(z^- p^+, z^2 \to 0), \tag{4.3}$$

here the limit onto the light–cone, $z^2 = 0$, is singular and a dependence on the renormalization scale is introduced, remember that if one chooses μ to be of the order of Q and Q is the inverse of typical size of the localization of the valence couple, $Q \sim 1/b$, it follows that the renormalization scale is of the order of transverse momenta of the valence couple.

4.1   Brodsky–Lepage prescription

It is instructive to construct the zero–th order Brodsky–Lepage prescription, some times called the leading–twist wave functions, for the pion and the D meson distribution amplitude, to compute them one can follow [103, 109–111].
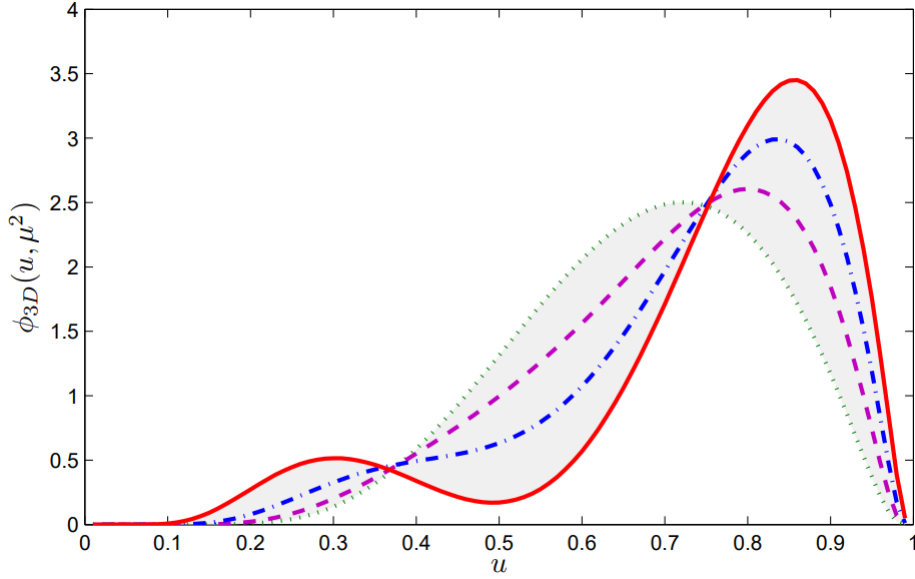
Figure 4.2: The D meson Distribution Amplitude $\phi_D(x, \mu^2)$ at 1 GeV. The dotted, the dashed, the dash-dot and the solid lines are for different values of the Gegenbauer momentum $B_D = 0, 0.20, 0.40$ and 0.60 respectively. The numerical results obtained in the manuscript will always consider $B_M = 0$, i.e. Eq.(4.7). The plot is taken from [109].

Consider the spatial part of pion Wave–Function

$$\Psi_\pi(x, \mathbf{p}_\perp) = A_\pi \varphi_\pi(x) \exp\left(-\frac{\mathbf{p}_\perp^2 + m_q^2}{8\beta_\pi^2 (1-x)x}\right), \tag{4.4}$$

where A_π is an normalization constant and β_π is a mass scale regulating the spread in the transverse plane of Ψ. Integrating out the transverse momentum down to the scale μ, or otherwise up to distances $\sim 1/Q$, produces the pion's distribution amplitude:

$$\phi_\pi(x, \mu^2) \propto \beta_\pi A_\pi \sqrt{x(1-x)} \varphi_\pi(x)$$
$$\times \left(\text{Erf}\left[\sqrt{\frac{m_q^2 + \mu^2}{8\beta_\pi^2 x(1-x)}}\right] - \text{Erf}\left[\sqrt{\frac{m_q^2}{8\beta_\pi^2 x(1-x)}}\right] \right), \tag{4.5}$$

where $\varphi_\pi(x) = \left(1 + B_\pi C_1^{3/2}(2x-1)\right)$ is defined in terms of the Gegenbauer expansion. A similar expression can be obtained for the D meson with the substitution in Eq.(4.4) for the argument of the exponential function

$$\frac{\mathbf{k}_\perp^2 + m_q^2}{8\beta_\pi^2(1-x)x} \rightarrow \frac{\mathbf{k}_\perp^2 + m_q^2}{8\beta_\pi^2(1-x)} + \frac{\mathbf{k}_\perp^2 + m_Q^2}{8\beta_\pi^2 x}. \tag{4.6}$$

The resulting wave functions $\phi_{H,L}(x,\mu)$ describing the meson's quark momenta distribution for heavy and light mesons are very well approximated by their asymptotic form, i.e. the limit $\mu \sim Q \to \infty$, respectively by:

$$\phi_H(x) \propto \left[\frac{\xi^2}{1-x} + \frac{1}{x} - 1\right]^{-2} \quad , \qquad \phi_L(x) \propto x(1-x). \tag{4.7}$$

The parameter ξ in $\phi_H(x)$ is a small parameter typically of $O(m_q/m_Q)$, being q and Q the light and heavy quark in the meson. The mass function $g_P(x)$ is usually taken to be a constant varying from $g_H(x) \approx 1$ and $g_L(x) \ll 1$ for a heavy or a light meson. This is a theorem for Q high enough to completely decouple QCD running effects [103, 104, 112], while it must be taken as a **model** for lower[2] values of Q. Unless stated differently in the rest of the paper this model is assumed. The exceptions are the kaonic sector, a detailed discussion dedicated to the subject of the employed model can be found in [115] and in Sec.5.2, and for lighter D mesons. Coming back to regular gamma matrices one can extend Eq.(4.2) and define the meson decay constants f_M as:

$$\langle 0 | \bar{q}\,\gamma^\mu\,\gamma_5\,Q\,|P\rangle \;\; = i f_P P_P^\mu\,, \tag{4.8}$$

$$\langle 0 | \bar{q}\,\gamma^\mu\,Q\,|V\rangle \;\;\; = f_V M_V \epsilon^\mu(P_V)\,, \tag{4.9}$$

where the vector structures on the RHS are forced by Lorentz invariance. Finally one has to define the spin structure of the Wave–Functions for the

---

[2] The so-called Sudakov resummation [113,114] allows one to formulate precise predictions for even lower values of Q.

ground state of a meson M [103, 108, 116, 117]:

$$
\begin{aligned}
\Psi_P(x) =& \frac{\phi(x)}{4}\gamma^5(\slashed{P}_P + M_P g_P(x)) \\
\Psi_V(x) =& \frac{\phi(x)}{4}(M_V\gamma^\alpha + i\sigma^{\alpha\beta}P_{V\beta})\epsilon_\alpha(P_V)
\end{aligned}
\tag{4.10}
$$

while $\phi(x)$'s here are to be considered normalized to 1. In Eq. (4.10), with x one typically denotes the fraction of the momentum carried by the heaviest quark in the meson. In Eqs. (4.7–4.13), a slightly different notation with respect to the referred literature is used. In particular the functions $\phi(x)$ have been normalized to one, in such a way that in Eq. (4.13) the mesonic form factor can be explicitly factorized.

4.1.1 Limits and Criticalities

An essential part of the discussion of the results obtained has to do with their limitations and their applicability. Although an in–depth discussion regarding the validity of the approximation used throughout this work has been presented in Sec.4 and 4.1 there are still some interesting points to raise. The most important one is probably the so called end–point behaviour of the distribution amplitude. This is the asymptotic form of the probability distribution in Eq.(4.3) as one of the valence quark gets all the available energy in the system, signaled by $x_i \to 1$. It has been shown in [118, 119] that the $x_i \to 1$ limit that as long as $1 - x_i \gg \delta_M$ the partonic distribution amplitude vanishes with a power law $(1 - x_i)^\nu$ with $\nu > 1$, assuring the convergence of the distribution. Consequently the integrations in the variables x_i, representing the fraction of the meson's 4–momenta carried by the i–th valence quark, are well behaved, as long as $1 - x_i \gg \delta_M$. The region where $1 - x_i \le \delta_M$ has to be analyzed separately. Here δ_M is defined as a process dependent cutoff, excluding the unphysical bare singularities. These end–point effects are under control if the emitted ALP is massless but introduce non–trivial complications in amplitudes where the emitted particle has a non–zero mass. The role of this cutoff is discussed in Sec.5.2 and its numerical impact on the results is negligible. Contributions from these regions can be taken into

account, and are typically more suppressed than bulk contributions, but require a modification of the distribution amplitudes, e.g. Drell–Yan–West did it for the first time [118] and considered $(1 - x_i)^3$ in the limit $x \to 1$, in accord (roughly) to experiments and theoretical expectations[3].
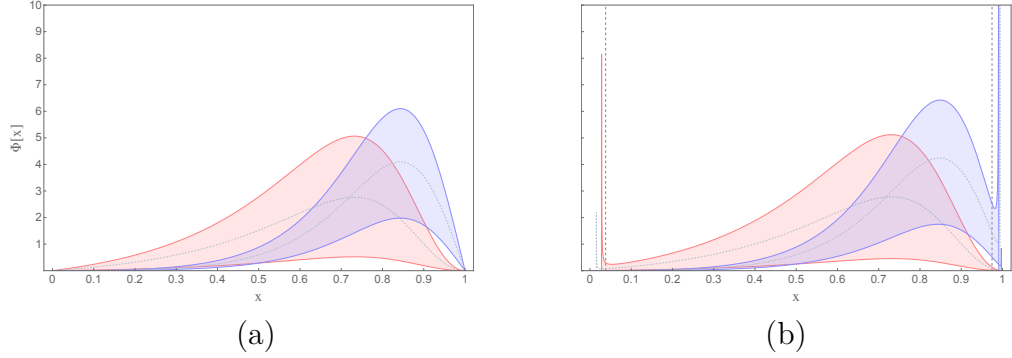

(a)   (b)

Figure 4.3: End–point behavior for both the heavy (pink) and light (blue) contributions to the hadronized amplitudes discussed in Eq.(5.11). In (a) the $D_s \to \mu \bar{\nu} a$ process with $m_a = 0$ is shown to be regular and integrable, while in (b) the $D_s \to \mu \bar{\nu} a$ process is discussed in the case $m_a = 0.1$ GeV. The shaded area correspond to the allowed values for the Mandelstam variable u. The dotted curve corresponds to its mean value.

The lesson one can learn here is that the issue of end point singularities, $x_i, y_i \to 1$ in Eq.(4.1), has to be discussed process by process. Some processes will have regular and integrable functions, e.g. emission of a massless particle, while other processes can develop simple poles near the boundaries of the integration interval[4]. This exact situation is encountered in the $\Phi_M^{(Q,q)}(m_a^2)$ discussed in Eq.(5.11). The form of the cutoff should clarify that this effect in the present context is generated only if a massive particle is emitted in the final state. These poles have been addressed [103, 118] by modifying the mesonic Distribution Amplitudes in the $x \to 1$ limit. To reabsorb these

---

[3]A more comprehensive discussion on the asymptotic behavior for $x \to 1$ can be found in [119]

[4]In the case presented here the issue seems related to the emitted particle mass but in general this is not true as the same problems emerge in the context of DIS.
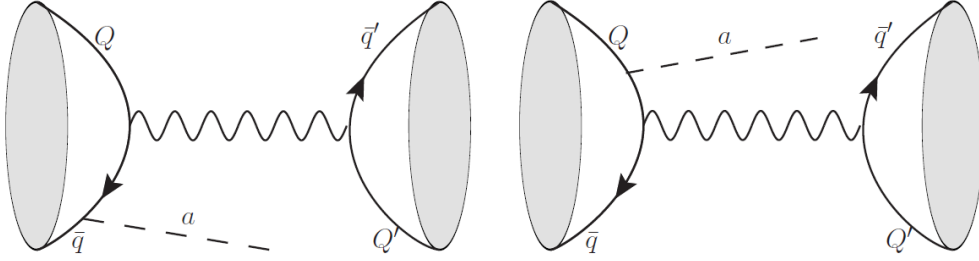
Figure 4.4: Tree-level s-channel of a charged $(\bar{q}Q)$–meson decaying into a charged $(\bar{Q}'q')$ meson and an ALP. Diagrams where the ALP is emitted from the final state meson can be easily obtained.

simple poles, generated by the appearance of extra $(1-x)$ in the propagators of the internal valence quarks, one is instructed to add a term $(1-x)$ in the numerator, thus curing the simple pole.

4.2 Factorization in the s–channel

Following the Brodsky Lepage method the factorization of an amplitude going through a mesonic vacuum state is discussed. This is the simplest non–trivial possible application of the techniques discussed in Sec.4. The process studied is shown in Fig.4.4. Looking at the picture the factorization emerges naturally. The amplitude is a product of two uncorrelated vector currents obtained by cutting the diagram along the weak boson leg connecting the hadronic external states. One of the two currents gives a trivial hadronization contribution given by Eq.(4.8) while the other has to be calculated using Eq.(4.1) but with a trivial "out" state. Let the initial mesonic state be $\bar{q}Q$ and the final one $\bar{Q}'q'$ and consider that, thanks to the intermediate vacuum state, one can factorize the contributions as

$$\langle 0 | \, (\bar{q}\Gamma_{\mu}^{(i)}Q) \, | M_I \rangle \, \langle M_F | \, (\bar{Q}'\gamma^{\mu}P_L q') \, | 0 \rangle + \langle 0 | \, (\bar{q}\gamma^{\mu}P_L Q) \, | M_I \rangle \, \langle M_F | \, (\bar{Q}'\Gamma_{\mu}^{(f)}q') \, | 0 \rangle \, .$$
(4.11)

where i, (f), stand for initial, (final), state production and M_I and M_F are the initial and final mesonic states. One is tasked with the computation of $\langle 0 | \, (\bar{q}\Gamma_{\mu}^{i,f}Q) \, | M \rangle$, where $(\bar{q}\Gamma_{\mu}^{i,f}Q)$ is the hard scattering process that has to

be extracted from the Feynman diagrams depicted in Fig.4.4. The diagram where the ALP is emitted from the W internal line automatically vanishes, being the W^+W^-–ALP coupling proportional to the fully antisymmetric 4D tensor. The hard-scattering calculation produces the result

$$
\begin{aligned}
\Gamma_\mu^{(i)} &= \frac{4G_F}{\sqrt{2}f_a} V^{CKM} \left(c_q m_q \frac{\gamma^5 \slashed{k} \gamma_\mu P_L}{m_a^2 - 2k \cdot P_q} - c_Q m_Q \frac{\gamma_\mu P_L \slashed{k} \gamma^5}{m_a^2 - 2k \cdot P_Q} \right) \\
\Gamma_\mu^{(f)} &= \frac{4G_F}{\sqrt{2}f_a} V^{CKM} \left(c_{Q'} m_{Q'} \frac{\gamma^5 \slashed{k} \gamma_\mu P_L}{m_a^2 + 2k \cdot P_{Q'}} - c_{q'} m_{q'} \frac{\gamma_\mu P_L \slashed{k} \gamma^5}{m_a^2 + 2k \cdot P_{q'}} \right).
\end{aligned}
\tag{4.12}
$$

where c_q and c_Q are the ALP–fermion coupling of the q and Q quarks. Now one applies Eq.(4.1) with a single mesonic out state:

$$
\langle 0 | (\bar{q} \Gamma_\mu Q) | M \rangle = i f_M \int_0^1 dx \, \mathrm{Tr}[\Psi_M(x) \Gamma_\mu].
\tag{4.13}
$$

The different possible nature of the mesons M are implemented via Ψ_M. Here are presented the cases of pseudo–scalar and vector mesons in all the possible permutations. It is convenient to divide the results in Initial State Production (ISP) and Final State Production (FSP). Indeed such a choice will facilitate the evaluation of relative magnitudes, based on the masses of the emitting mesons, and the general computation of the signal due to the set up proposed in Section 4. One should start by looking at the familiar pseudo-scalar to pseudo-scalar decay, where quantities with I and F subscript are relative to initial and final state mesons respectively. This class of transitions has been thoroughly studied in ALP phenomenology [69,94,115] due to the importance of the NA62 search on the rare decay $K \to \pi \nu \bar{\nu}$ [87,120] and the Belle and BaBar searches for the equivalent B physics signal [121]. These processes have been associated to 1-loop effective observables but in a recent analysis [115] the authors have shown the potential information loss in choosing to ignore tree-level contribution to these observables, in particular one can have correlations between the parameters of the amplitude, and even bound the lighter quarks coupling constants. Here are presented the pseudo–scalar to

pseudo–scalar transitions:

$$
\mathcal{A}_{\text{ISP}}^{(s)} = \frac{G_F f_I f_F k \cdot P_F}{\sqrt{2} f_a} V M_I
$$
$$
\int dx g_I(x) \left[\frac{c_q m_q}{m_a^2 - 2k \cdot P_I (1-x)} - \frac{c_Q m_Q}{m_a^2 - 2k \cdot P_I x} \right] \phi_I(x)
$$

(4.14)

and

$$
\mathcal{A}_{\text{FSP}}^{(s)} = \frac{G_F f_I f_F k \cdot P_I}{\sqrt{2} f_a} V M_F
$$
$$
\int dx g_F(x) \left[\frac{c_{Q'} m_{Q'}}{m_a^2 + 2k \cdot P_F x} - \frac{c_{q'} m_{q'}}{m_a^2 + 2k \cdot P_F (1-x)} \right] \phi_F(x).
$$

(4.15)

The next interesting channel is pseudo-scalar to vector. An important example is the search for $B \to K^* a$ [121]. Once again we separate in ISP and FSP. Here we have for the s–channel

$$
\mathcal{B}_{\text{ISP}}^{(s)} = i \frac{G_F f_I f_F k_\mu \epsilon^\mu (P_F)}{\sqrt{2} f_a} V M_I M_F
$$
$$
\int dx g_I(x) \left[\frac{c_q m_q}{m_a^2 - 2k \cdot P_I (1-x)} - \frac{c_Q m_Q}{m_a^2 - 2k \cdot P_I x} \right] \phi_I(x)
$$

(4.16)

and

$$
\mathcal{B}_{\text{FSP}}^{(s)} = \frac{G_F f_I f_F}{\sqrt{2} f_a} V \epsilon^\alpha (P_F) P_F^\beta P_I^\mu \int dx \times
$$
$$
\left[\frac{c_{Q'} m_{Q'}}{m_a^2 + 2k \cdot P_F x} (\varepsilon_{\alpha\beta\mu\rho} k^\rho + ik^\beta g^{\alpha\mu} - ik^\alpha g^{\beta\mu}) \right.
$$
$$
\left. + \frac{c_{q'} m_{q'}}{m_a^2 + 2k \cdot P_F (1-x)} (\varepsilon_{\alpha\beta\mu\rho} k^\rho + ik^\alpha g^{\beta\mu} - ik^\beta g^{\alpha\mu}) \right] \phi_F(x).
$$

(4.17)

Finally the results on the other possible channels, vector-to-pseudo–scalar and vector-to-vector, are presented. Once again in the following Initial State

Emission (ISP) and Final State Production are discussed (FSP):

$$\mathcal{C}_{\text{ISP}}^{(s)} = -\frac{G_F f_I f_F}{\sqrt{2} f_a} V \epsilon^\alpha(P_I) P_I^\beta P_F^\mu \int dx \times$$
$$\left[\frac{c_q m_q}{m_a^2 - 2k \cdot P_I(1-x)} (\varepsilon_{\alpha\beta\mu\rho} k^\rho + ik^\alpha g^{\beta\mu} - ik^\beta g^{\alpha\mu}) \right. \tag{4.18}$$
$$\left. + \frac{c_Q m_Q}{m_a^2 - 2k \cdot P_I x} (\varepsilon_{\alpha\beta\mu\rho} k^\rho - ik^\beta g^{\alpha\mu} + ik^\alpha g^{\beta\mu}) \right] \phi_I(x).$$

and FSP

$$\mathcal{C}_{\text{FSP}}^{(s)} = -i \frac{G_F f_I f_F}{\sqrt{2} f_a} V \epsilon^\alpha(P_F) k_\alpha M_I M_F$$
$$\int g_F(x) dx \left[\frac{c_{Q'} m_{Q'}}{m_a^2 + 2k \cdot P_F x} - \frac{c_{q'} m_{q'}}{m_a^2 + 2k \cdot P_F(1-x)} \right] \phi_F(x). \tag{4.19}$$

Finally one has the vector-to-vector amplitudes:

$$\mathcal{D}_{\text{ISP}}^{(s)} = -i \frac{G_F f_I f_F}{\sqrt{2} f_a} V \epsilon^\mu(P_F) \epsilon^\alpha(P_I) M_F P_I^\beta$$
$$\int dx \left[\frac{c_q m_q}{m_a^2 - 2k \cdot P_I(1-x)} (\varepsilon_{\alpha\beta\mu\rho} k^\rho + ik^\beta g^{\alpha\mu} - ik^\alpha g^{\beta\mu}) + \right. \tag{4.20}$$
$$\left. \frac{c_Q m_Q}{m_a^2 - 2k \cdot P_I x} (\varepsilon_{\alpha\beta\mu\rho} k^\rho + ik^\alpha g^{\beta\mu} - ik^\beta g^{\alpha\mu}) \right] \phi_I(x).$$

and

$$\mathcal{D}_{\text{FSP}}^{(s)} = -i \frac{G_F f_I f_F}{\sqrt{2} f_a} V \epsilon^\mu(P_I) \epsilon^\alpha(P_F) M_I P_F^\beta$$
$$\int dx \left[\frac{c_{Q'} m_{Q'}}{m_a^2 + 2k \cdot P_F x} (\varepsilon_{\alpha\beta\mu\rho} k^\rho + ik^\beta g^{\alpha\mu} - ik^\alpha g^{\beta\mu}) + \right. \tag{4.21}$$
$$\left. \frac{c_{q'} m_{q'}}{m_a^2 + 2k \cdot P_F(1-x)} (\varepsilon_{\alpha\beta\mu\rho} k^\rho + ik^\alpha g^{\beta\mu} - ik^\beta g^{\alpha\mu}) \right] \phi_F(x).$$

4.3   Factorization in the t–channel

The same study done for the s–channel can be done for the t–, in the context of neutral processes. In this case the relevant diagrams are the ones
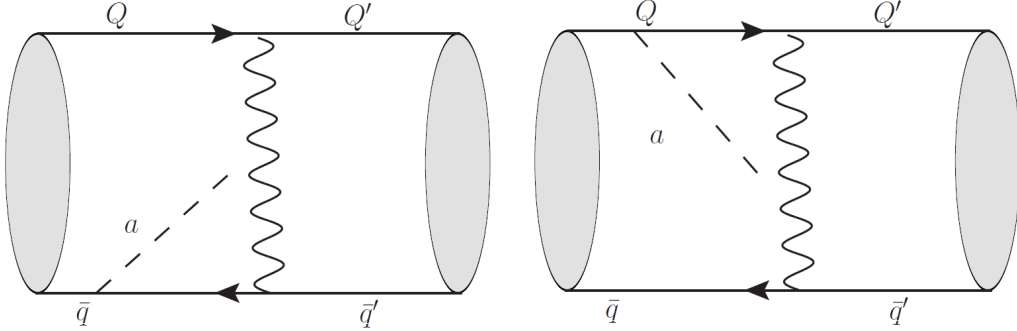
Figure 4.5: Tree-level t-channel of a neutral $(\bar{q}Q)$–meson decaying into a neutral $(\bar{Q}'q')$ meson and an ALP. Diagrams where the ALP is emitted from the final state meson can be easily obtained. Similar diagrams can be depicted for the CP conjugate process.

depicted in Fig.4.5. Once again the diagram where the ALP is emitted from the W internal line automatically vanishes, being the W^+W^-–ALP coupling proportional to the fully antisymmetric 4D tensor. To condense the computation one separates the emission based on the line it originates from, either fermionic or antifermionic. In this fashion the channel's factorization will be

$$\langle M_F | \, (\bar{Q}'\Gamma_\mu^{(Q)}Q)(\bar{q}\gamma^\mu P_L q') \, | M_I \rangle + \langle M_F | \, (\bar{Q}'\gamma^\mu P_L Q)(\bar{q}\Gamma_\mu^{(\bar{Q})}q') \, | M_I \rangle , \quad (4.22)$$

where $\Gamma^{(Q,\bar{Q})}$ stand for either particle or anti–particle emission. Note that this process, unlike what happens for the s–channel, does not present any trivial external state and so the full Brodsky–Lepage machinery is required to make sense of the amplitude. As before the hard scattering is computed perturbatively with the diagrams depicted in Fig.4.5, resulting in

$$\begin{aligned}
\Gamma_\mu^{(Q)} &= \frac{4G_F}{\sqrt{2}f_a} V^{CKM} \left(c_{Q'}m_{Q'} \frac{\gamma^5 \slashed{k}\gamma_\mu P_L}{m_a^2 + 2k\cdot P_{Q'}} - c_Q m_Q \frac{\gamma_\mu P_L \slashed{k}\gamma^5}{m_a^2 - 2k\cdot P_Q} \right) \\
\Gamma_\mu^{(\bar{Q})} &= \frac{4G_F}{\sqrt{2}f_a} V^{CKM} \left(c_q m_q \frac{\gamma^5 \slashed{k}\gamma_\mu P_L}{m_a^2 - 2k\cdot P_q} - c_{q'}m_{q'} \frac{\gamma_\mu P_L \slashed{k}\gamma^5}{m_a^2 + 2k\cdot P_{q'}} \right) .
\end{aligned} \quad (4.23)$$

Finally one recovers Eq.(4.1) for the process at hand

$$\langle M_F | (\bar{Q}' \Gamma_\mu Q)(\bar{q} \Gamma'^\mu q') | M_I \rangle = -\frac{f_{M_F} f_{M_I}}{\sqrt{2}} \int dx dy \, \text{Tr}[\Psi_{M_I}(x) \Gamma'^\mu \Psi_{M_F}(y) \Gamma_\mu],$$

(4.24)

where the nature of the meson will modify the amplitudes via the Ψ_M's. Once more let us consider the different set of processes available with a combination of pseudo–scalar and vector external states. The pseudo–scalar to pseudo–scalar, where ISP and FSP refer to Initial State Production and Final State Production (of an ALP), are

$$\mathcal{A}_{\text{ISP}}^{(t)} = \frac{G_F f_I f_F}{2 f_a} k \cdot P_F V M_I \times$$
$$\int dx g_I(x) \left[\frac{c_Q m_Q}{m_a^2 - 2k \cdot P_I x} - \frac{c_q m_q}{m_a^2 - 2k \cdot P_I (1-x)} \right] \phi_I(x)$$

(4.25)

and

$$\mathcal{A}_{\text{FSP}}^{(t)} = \frac{G_F f_I f_F}{2 f_a} k \cdot P_F V M_F \times$$
$$\int dx g_F(x) \left[\frac{c_{q'} m_{q'}}{m_a^2 + 2k \cdot P_F (1-x)} - \frac{c_{Q'} m_{Q'}}{m_a^2 + 2k \cdot P_F x} \right] \phi_F(x).$$

(4.26)

The pseudo–scalar to vector t–channel instead reads:

$$\mathcal{B}_{\text{ISP}}^{(t)} = i \frac{G_F f_I f_F}{2 f_a} V M_I M_V \epsilon^\alpha(P_F) k_\alpha \times$$
$$\int g_I(x) dx \left[\frac{c_Q m_Q}{m_a^2 - 2k \cdot P_I x} - \frac{c_q m_q}{m_a^2 - 2k \cdot P_I (1-x)} \right] \phi_F(x),$$

(4.27)

and

$$
\mathcal{B}_{\text{FSP}}^{(t)} = - \frac{G_F f_I f_F}{2 f_a} V \epsilon^\alpha (P_F) P_F^\beta \times
$$
$$
\int dx \Big[\frac{c_{Q'} m_{Q'}}{m_a^2 + 2k \cdot P_F x} (\varepsilon_{\alpha\beta\mu\rho} k^\mu P_I^\rho + ik^\alpha P_I^\beta - ik^\beta P_I^\alpha) +
$$
$$
\frac{c_{q'} m_{q'}}{m_a^2 + 2k \cdot P_F (1-x)} (\varepsilon_{\alpha\beta\mu\rho} k^\mu P_I^\rho - ik^\alpha P_I^\beta + ik^\beta P_I^\alpha) \Big] \phi_F(x).
$$

(4.28)

Finally the results on the other possible channels, vector-to-pseudo–scalar and vector-to-vector, are presented. Once again in the following Initial State Emission (ISP) and Final State Production are discussed (FSP). the t–channel vector-to-pseudo–scalar ISP is:

$$
\mathcal{C}_{\text{ISP}}^{(t)} = - \frac{G_F f_I f_F}{2 f_a} V \epsilon^\alpha (P_I) P_I^\beta \times
$$
$$
\int dx \Big[\frac{c_Q m_Q}{m_a^2 - 2k \cdot P_I x} (\varepsilon_{\alpha\beta\mu\rho} k^\mu P_F \rho + ik^\beta P_F^\alpha - ik^\alpha P_F^\beta) +
$$
$$
\frac{c_q m_q}{m_a^2 - 2k \cdot P_I (1-x)} (\varepsilon_{\alpha\beta\mu\rho} k^\mu P_F^\rho + ik^\alpha P_F^\beta - ik^\beta P_F^\alpha) \Big] \phi_I(x).
$$

(4.29)

and FSP

$$
\mathcal{C}_{\text{FSP}}^{(t)} = i \frac{G_F f_I f_F}{2 f_a} M_I M_F V \epsilon^\alpha (P_F) k_\alpha \times
$$
$$
\int g_F(x) dx \Big[\frac{c_{q'} m_{q'}}{m_a^2 + 2k \cdot P_F (1-x)} - \frac{c_{Q'} m_{Q'}}{m_a^2 + 2k \cdot P_F x} \Big] \phi_F(x).
$$

(4.30)

Finally one has vector-to-vector amplitudes in the t–channel

$$
\mathcal{D}_{\text{ISP}}^{(t)} = i \frac{G_F f_I f_F}{2 f_a} V \epsilon^\alpha (P_I) \epsilon^\delta (P_F) M_F P_I^\beta
$$
$$
\int dx \Big[\frac{c_Q m_Q}{m_a^2 - 2k \cdot P_I x} (\varepsilon_{\alpha\beta\delta\rho} k^\rho - ik^\beta g^{\alpha\delta} + ik^\alpha g^{\beta\delta}) +
$$
$$
\frac{c_q m_q}{m_a^2 - 2k \cdot P_I (1-x)} (\varepsilon_{\alpha\beta\delta\rho} k^\rho - ik^\alpha g^{\beta\delta} + ik^\beta g^{\alpha\delta}) \Big] \phi_I(x).
$$

(4.31)

and

$$
\begin{aligned}
\mathcal{D}_{\mathrm{FSP}}^{(t)} =\,&i\frac{G_F f_I f_F}{2f_a}V\epsilon^\delta(P_F)\epsilon^\alpha(P_I)M_I P_F^\rho \\
&\int dx\Big[\frac{c_{Q'}m_{Q'}}{m_a^2+2k\cdot P_F x}(\varepsilon_{\alpha\delta\rho\nu}k^\nu+ik^\rho g^{\alpha\delta}-ik^\delta g^{\alpha\rho})+ \\
&\frac{c_{q'}m_{q'}}{m_a^2+2k\cdot P_F(1-x)}(\varepsilon_{\alpha\delta\rho\nu}k^\nu+ik^\delta g^{\alpha\rho}-ik^\rho g^{\alpha\delta})\Big]\phi_F(x).
\end{aligned}
\tag{4.32}
$$

4.4   Penguin Hadronization

Some of the meson decays will receive contributions at one–loop level [67, 69, 94] by the flavor diagonal part of the fermion–ALP interactions of Eq. (2.31) from the diagrams shown in Fig. 4.6. In the following only the contribution arising from fermion–ALP interaction will be considered. In this kind of
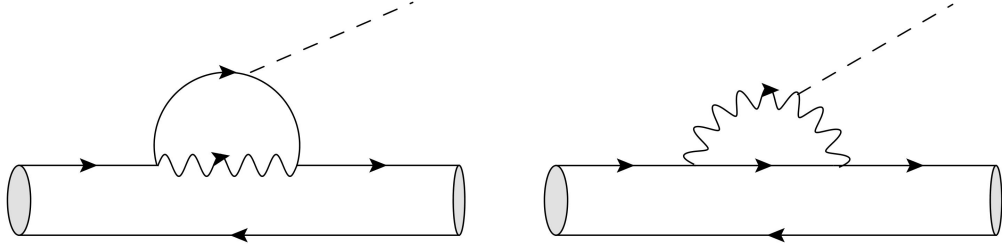

Figure 4.6: One-loop penguin contributions

processes, one quark line participates to the ALP emission while the other quark is a spectator. Customarily the hadronization of a matrix element between two pseudo-scalar meson mediated by a vector current, where one of the quark does not interact can be factorised as

$$
\langle M_F|\,\bar{q}_1\gamma^\mu Q_2\,|M_I\rangle = f_+(q^2)(P_{M_I}+P_{M_F})^\mu + f_0(q^2)\,q^\mu
\tag{4.33}
$$

with $q = P_{M_I} - P_{M_F}$. The form factors $f_{+,0}(0) = 1$ in the isospin symmetric limit, while the non approximated, q^2 dependent, form factors are obtained from LQCD calculation [122]. Consider only the flavor diagonal part of the Lagrangian in Eq.(2.31), where all the parameters are zero except the diagonal ones defined in Eq.(2.33). Using only this flavor conserving part

one can induce at one loop, via the processes depicted in Fig.4.6, an effective flavor violating coupling. Indeed from Eq. (4.33) the amplitude for the $M_I \to M_F\, a$ decay mediated by the 1–loop effective flavor–violating part is:

$$\mathcal{M}_{\mathrm{Ps}\to\mathrm{Ps}}^{L} = \frac{G_F\, m_t^2}{4\sqrt{2}\pi^2} \frac{M_I^2}{f_a} \left(1 - \frac{M_F^2}{M_I^2}\right) \left[f_+(q^2) + \frac{q^2}{M_I^2 - M_F^2} f_-(q^2)\right] \sum_{f=u,c,t} c_{ij}^{(f)}$$
(4.34)

where the coefficient

$$c_{ij}^{(q)} = V_{qi}V_{qj}^* \left[3\, c_W \frac{g(x_q)}{x_t} - \frac{c_q\, x_q}{4\, x_t} \ln\left(\frac{f_a^2}{m_q^2}\right)\right]$$
(4.35)

opportunely normalized in order to factorize out all the relevant scale dependences, is the induced effective coupling at 1–loop. The process mediating the decay in the UV regime has been discussed in Sec. 2.4.2 and. The penguin with the ALP emitted from the internal W line is included for completeness, even if in the following phenomenological analysis $c_W = 0$ will be assumed. If the quark changing its flavour is a down type quark than the dominant contribution coming from this amplitude is proportional to c_t, but in general one needs to look at it case by case, e.g. for the K meson decay, the charm contribution roughly accounting for 10% of the total contribution. One-loop diagrams, with the ALP emitted from the initial/final quarks can be safely neglected being suppressed by at least a factor m_i^2/m_W^2 with respect to the penguin contributions, as they arise at third order in the external momenta expansion. Therefore, no sensitivity on the ALP–quark couplings from the external legs can emerge in the decays from one loop diagrams.

In the case of a Vector to Pseudo-scalar transition the factorisation in terms of Form Factors is different [123, 124], namely

$$\langle V_F|\, \bar{q}_1\gamma^\mu(1-\gamma_5)Q_2\,|M_I\rangle = P_1^\mu\mathcal{V}_1(q^2) - P_2^\mu\mathcal{V}_2(q^2) - P_3^\mu\mathcal{V}_3(q^2) - P_P^\mu\mathcal{V}_P(q^2).$$
(4.36)

If one couples the Left-Handed current in Eq.(4.36) with the ALP the only non zero term is the one proportional to $\mathcal{V}_P$. Finally one can use the con-

ventions found in [123] to obtain

$$\mathcal{M}^{L}_{\text{Ps}\rightarrow\text{V}} = ic^{(f)}_{ij} \frac{G_F m_t^2}{2\sqrt{2}\pi^2 f_a} M_V A_0(q^2)\epsilon(P_V) \cdot q, \qquad (4.37)$$

where conventionally one takes $\mathcal{V}_P(q^2) = \frac{-2M_V A_0(q^2)}{q^2}$, and q is the momentum transferred.

Chapter 5

Invisible ALP Bounds From Flavor Physics

Meson to meson processes are the well-known protagonists in bounding the quarks–ALP couplings in the MeV–GeV mass range, mainly thanks to the Kaonic sector [86, 87, 89, 120, 125–128]. It is natural to ask if there are other potential candidates in this class of processes that may improve, or at least supplement, the limits discussed in Sec. 3.3. In this chapter a number of interesting results are presented to answer this question. At first the focus will be on ALP searches via rare meson decay of the form $M \to M'a$. Here the most promising candidates appear to be B–factories and B–physics in general [90, 91, 93, 96]. Recently many results and analysis have been published [61,68,69,94,99,115,129] on the subject but it is clear that B meson decays do not produce bounds as dominant as the ones from kaon rare decays. A thorough analysis shows that the difference is in the experimental precision achived. Another interesting mesonic sector is the D–sector, here any bound extracted would truly be "orthogonal" to the ones deduced in the other cases. Indeed D–mesons decays are typically are free from any c_t presence, and as such they probe directly the couplings to the valence quarks. Even though the signals are very weak these channels are intrinsically interesting. Finally light vector mesons provide a unique laboratory to test interferences and correlations between loop and tree level in the signal, similarly to the kaon channel. In general when tree-level and loop contributions are separated by

Channel	Tree–Level	Loop
$B_c^{\pm} \to D_s^{\pm} a$	1×10^{-8}	7×10^{-3}
$B_c^{\pm} \to D^{\pm} a$	1×10^{-9}	7×10^{-3}
$B_c^{\pm} \to K^{*\pm} a$	8×10^{-9}	n.a.
$B_c^{\pm} \to \rho^{\pm} a$	3×10^{-8}	n.a.
$B_c^{\pm} \to K^{\pm} a$	2×10^{-9}	n.a.
$B_c^{\pm} \to \pi^{\pm} a$	4×10^{-9}	n.a.
$B^{\pm} \to D_s^{\pm} a$	1×10^{-9}	n.a.
$B^{\pm} \to D^{\pm} a$	1×10^{-10}	n.a.
$B^{\pm} \to K^{*\pm} a$	1×10^{-9}	4×10^{-3}
$B^{\pm} \to \rho^{\pm} a$	1×10^{-9}	5×10^{-4}
$B^{\pm} \to K^{\pm} a$	1×10^{-10}	6×10^{-3}
$B^{\pm} \to \pi^{\pm} a$	5×10^{-10}	1×10^{-3}
$D_s^{\pm} \to K^{*\pm} a$	3×10^{-7}	3×10^{-9}
$D_s^{\pm} \to \rho^{\pm} a$	2×10^{-7}	n.a.
$D_s^{\pm} \to K^{\pm} a$	1×10^{-8}	3×10^{-8}
$D_s^{\pm} \to \pi^{\pm} a$	1×10^{-8}	n.a.
$D^{\pm} \to K^{*\pm} a$	3×10^{-7}	n.a.
$D^{\pm} \to \rho^{\pm} a$	3×10^{-7}	3×10^{-9}
$D^{\pm} \to K^{\pm} a$	3×10^{-9}	n.a.
$D^{\pm} \to \pi^{\pm} a$	2×10^{-9}	2×10^{-8}
$K^{*\pm} \to \rho^{\pm} a$	3×10^{-8}	4×10^{-7}
$K^{*\pm} \to K^{\pm} a$	3×10^{-8}	4×10^{-6}
$K^{*\pm} \to \pi^{\pm} a$	7×10^{-9}	4×10^{-7}
$\rho^{\pm} \to K^{\pm} a$	6×10^{-8}	5×10^{-7}
$\rho^{\pm} \to \pi^{\pm} a$	2×10^{-7}	5×10^{-8}
$K^{\pm} \to \pi^{\pm} a$	7×10^{-9}	4×10^{-7}

Table 5.1: Order of magnitude of charged amplitudes.

a factor between[1] $10^{-2} \approx 10^{-3}$ one can extract some interesting correlation between the couplings. Such a big window is justified by the hierarchical limits extracted on the parameters associated with the different channels,

---

[1]To be relevant the bigger amplitude must be the one associated with the more constrained parameter.

in [115] the authors discuss these features in the relevant case of the analysis of the NA62 signal.

5.1 Bounds from mesonic final states

Using the formulas discussed in Sec.4.1 and 4.4 a number of predictions on the order of magnitude of amplitudes is presented in Tab.5.1, where these results are obtained in the massless limit, and in units of the relevant coupling, i.e. having $c_i = 1$ and $f_a = 1$ TeV, using the form factors [122–124, 130–139], and the relevant Clebsch–Gordan decompositions. The channels considered in Tab.5.1 represent a sample of interesting processes where the approximation discussed in Chapter 4 has meaning, namely the particles produced in the final state are emitted at high relative velocities. In the CM frame the 3–momentum of the final state particles is

$$|\vec{p}_{\text{fin}}| = \frac{\sqrt{(M_M^2 - M_P^2)^2 + m_a^4 - 2m_a(M_M^2 + M_P^2)}}{2M_M}, \quad (5.1)$$

and as long as the relative velocity of the final particles is relativistic the approximation we are in is well defined. In the following the biggest in magnitude are discussed in descending mass order of the mother particle. The $B_c^\pm \to D_s^\pm (D^\pm) a$ channel appears clear from any correlation due to the smallness of its tree level. Moreover it has the biggest amplitude of the computed ones thanks to the smallness of the Cabibbo suppression, and has a decently large parameter space. Of course processes involving these exotic resonances are typically harder to control experimentally, nonetheless it is important to point out that a measurement of a Branching ratio $< 10^{-5}$ would be competitive with the bounds from the kaonic sector, with a much larger available parameter space. The dashed black line in Fig.5.1 is the expected limit from this scenario. Another important channel is the $B_c^\pm \to Va$ for both the final vector states considered as this decay appears to be dominated by tree-level contribution. Moreover the small ratio $M_{B_c}/M_{\rho,K^*}$ allows one to forget about final state emission producing a very clean, but somewhat small, signal proportional to down-type quarks coupling. One could potentially reach
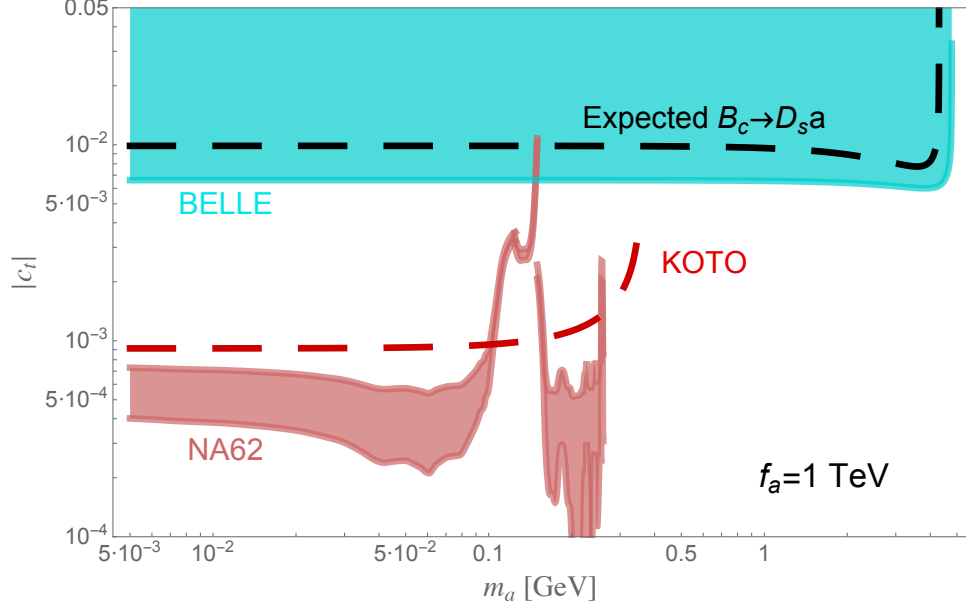
Figure 5.1: Summary on c_t bounds in the GeV ALP mass range.

perturbativity bounds with $BR < 10^{-5}$. Descending in mass one encounters B–physics and B factories with data from BaBar and BELLE [93, 96, 140] close to reaching the Kaon sector bounds but with branching ratios orders of magnitude higher. The bound in Fig. 5.1 is obtained using BELLE data on $B \rightarrow Ka$. As mentioned above the D_s/D–sector has unique and interesting properties. The NLO contribution for these channels are not top enhanced as the quarks running inside the loop correction are down–type. This produces interference in the signal, present in particular in $D_s^+ \rightarrow K^+a$ and in $D^+ \rightarrow \pi^+a$, where naive considerations suggest correlation between c_c and c_b. It is clear that these and the other channels in this sector allow for measurement on a typically difficult contribution to isolate, the one coming from the charm quark. Although the amplitudes are not the largest they offer an interesting window on charm quark physics otherwise precluded in the meson to meson ALP decays. The lighter mesonic resonances K^* and ρ can be considered in the same category due to similar Cabibbo suppressions and mass scales. All the processes allow simultaneous presence of tree level and

loop with similar magnitudes. This will produce a non zero interference between the two, offering a possible analysis of light couplings. The combined signal entering the measures has to be studied carefully in a fashion similar to that of the kaonic sector. The last channel present in Tab. 5.1 is the most important one and deserves a dedicated discussion postponed to Sec.5.2.

For neutral channels one has a similar story and all the results are shown in Tab.5.2. The most promising are of course $B^0 \to K^{*0}a$ for loop couplings and $D^0 \to K^{*0}a$ for tree-level couplings and finally a couple of channels will have strong correlations between the parameters. In particular $K^{*0} \to K^0 a$, $\rho^0 \to K^0 a$ and $\rho^0 \to \pi^0 a$ exhibit the largest correlation out of every channel considered in the analysis. Unsurprisingly it emerges even in the neutral sector, that the best way to probe tree-level channels is to look at the D sector where the penguins contributions are mediated by down type quarks and will experience large $\frac{m_b^2}{m_w^2}$ suppression. On the other hand these tree-level channels will have contributions coming from ISP, typically a charm quark or a lighter down type quark emission, in the former case additional suppression might be introduced depending on the model of the ALP-fermion coupling (e.g. if one chooses a up-type, down-type coupling as done in [115] or a universal coupling).

5.2 Kaonic sector

The kaonic sector deserves a special treatment for a number of reasons. It is without a doubt the channel with the most precise data and most number of studies. The extreme precision reached by terrestrial experiments allows for the most stringent bounds it and presents correlation effects between loop and tree–level. Nevertheless the amplitude associated with this process is not the biggest. The most interesting aspect, beside the potential to bound c_t, are the correlation effect discussed by the author in [115] and that will be shortly reviewed in Sec.5.2.2. Another interesting feature of this process is the non–trivial hadronization required, if one wants to keep track of both tree level and penguin contribution. Following what has been discussed in Sec.4.1 one obtains the tree level decay amplitude of the $K^+ \to \pi^+ a$ for

Channel	Tree–Level	Loop
$B_s^0 \to D_s^0 a$	n.a.	1×10^{-3}
$B_s^0 \to D^0 a$	2×10^{-6}	n.a.
$B_s^0 \to K^{*0} a$	n.a.	8×10^{-6}
$B_s^0 \to \rho^0 a$	1×10^{-7}	n.a.
$B_s^0 \to K_L^0 a$	n.a.	9×10^{-4}
$B^0 \to K^{*0} a$	n.a.	8×10^{-6}
$B^0 \to D^0 a$	7×10^{-7}	n.a.
$B^0 \to \rho^0 a$	4×10^{-8}	1×10^{-6}
$B^0 \to K_L^0 a$	n.a.	4×10^{-3}
$B^0 \to \pi^0 a$	3×10^{-8}	9×10^{-4}
$D^0 \to K^{*0} a$	5×10^{-6}	n.a.
$D^0 \to \rho^0 a$	4×10^{-6}	2×10^{-12}
$D^0 \to K_L^0 a$	1×10^{-7}	n.a.
$D^0 \to \pi^0 a$	1×10^{-8}	2×10^{-10}
$K^{*0} \to K^0 a$	2×10^{-8}	4×10^{-8}
$K^{*0} \to \pi^0 a$	5×10^{-9}	2×10^{-9}
$\rho^0 \to K^0 a$	5×10^{-8}	7×10^{-9}
$\rho^0 \to \pi^0 a$	1×10^{-7}	5×10^{-10}
$K_L^0 \to \pi^0 a$	6×10^{-12}	5×10^{-9}

Table 5.2: Order of magnitude of neutral amplitudes.

initial and final state ALP emission, namely Eqs.(4.14) and (4.15), to be:

$$
\mathcal{A}_{ISR}^{(s)} = \frac{G_F}{\sqrt{2}} (V_{us}^* V_{ud}) \, f_K \, f_\pi \, (k_a \cdot P_\pi) \frac{M_K}{f_a}
$$
$$
\int_0^1 \left\{ \frac{c_s \, m_s \, \theta(x - \delta_a^K)}{m_a^2 - 2\,x\,k_a \cdot P_K} - \frac{c_u \, m_u \, \theta(1 - x - \delta_a^K)}{m_a^2 - 2\,(1-x)\,k_a \cdot P_K} \right\} \phi_K(x) \, g_K(x) \, dx, \tag{5.2}
$$

and

$$
\mathcal{A}_{FSR}^{(s)} = \frac{G_F}{\sqrt{2}} (V_{us}^* V_{ud}) \, f_K \, f_\pi \, (k_a \cdot P_K) \frac{M_\pi}{f_a}
$$
$$
\int_0^1 \left\{ \frac{c_s \, m_s}{m_a^2 + 2\,x\,k_a \cdot P_\pi} - \frac{c_u \, m_u}{m_a^2 + 2\,(1-x)\,k_a \cdot P_\pi} \right\} \phi_\pi(x) \, g_\pi(x) \, dx \tag{5.3}
$$

with $\delta_a^K = m_a/(2M_K)$ an explicit cutoff introduced in the fractional momentum to remove the unphysical singularities appearing in the integrals. The most compelling aspect of Eqs.(5.2) and (5.3) is that for universal, or diagonal couplings, say $c_s = c_u = c$, a parametric cancellation appears in the amplitude. This is a general feature of all tree level process and does not depend on the particular channel parameters, masses decay constants etc. As a rule, if present the tree–level will always have a parametric cancellation for same signs couplings. Of course the individual signs are arbitrary and one might choose a different convention, but Eq.(2.31) looks like the most natural choice for a phenomenological model. The second interesting observation has to be that kaons are not properly heavy mesons nor light ones. The "heavyness" of a meson, in this context, is determined by the parameter $\xi = m_q/m_Q$ defined in Eq.(4.7) and measures how much of the total momentum distribution of the meson should be assigned to the heaviest parton. Small values of ξ indicate a large skew in the momentum distribution amplitude, typical of heavy meson, while $\xi \simeq 1/2$ suggests a light meson, with a symmetric distribution of momenta among the valence quarks. These correspond to two extreme cases that have an immediate approximated form. One can consider either, $SU(3)$ symmetry ($m_s \approx m_u$) thus consider the Kaon as light , or the opposite heavy meson treatment where $m_s \gg m_u$. At this point one has to assign a low–energy value to the valence quarks and introduce some level of model dependency. When $\xi = 1/2$ quarks in the valence state are assigned the same mass, namely $\hat{m}_s = \hat{m}_u = M_K/2$, and in the massless ALP limit one gets:

$$\mathcal{M}_{K^+}^L \approx -\frac{3\,G_F\,f_K\,f_\pi}{4\sqrt{2}}(V_{us}^*V_{ud})\frac{M_K^2}{f_a}\,g_K^L\,(c_s - c_u)\ . \tag{5.4}$$

Conversely, in the heavy meson approximation, one can assume $\hat{m}_u = \xi M_K$ and $\hat{m}_s = (1-\xi)M_K$, with $\xi = m_u/m_s$. Moreover, approximating $\phi_K(x) \approx \delta(1 - x - \xi)$ as suggested in [141], one obtains, in the $m_a = 0$ limit:

$$\mathcal{M}_{K^+}^H \approx -\frac{G_F\,f_K\,f_\pi}{2\sqrt{2}}(V_{us}^*V_{ud})\frac{M_K^2}{f_a}\,g_K^H\,(c_s - c_u)\ . \tag{5.5}$$

This simple example highlights the criticalities discussed below Eq.(5.3). The approximate formulas of Eq. (5.4) and (5.5) cancel completely when a universal coupling is chosen maximizing the parametric cancellation. This cancellation is still partially at work even when the full $\phi_K(x)$ is used and indicates a possible underestimation of the $\mathcal{M}_K$ amplitude (and consequently on the ALP-quark coupling limits) in the "universal" ALP–SM quark coupling scenario compared to the general case[2]. Moreover one can see the difference that considering a heavy or light meson in this model brings, in particular the ratio of these cases $\mathcal{M}_{K^+}^L/\mathcal{M}_{K^+}^H = (3/2)(g_K^L/g_K^H)$. From the approximate formulas of Eq. (5.4) and (5.5) one can estimate roughly the order of magnitude of the uncertainties introduced in the calculation by the hadronization procedure for the K meson. To reproduce the numerical results of the following section, an intermediate approach will be, instead, considered: the heavy meson function will be used, assuming[3] $g_K^H = 1$, and with the two partons defined as $\hat{m}_u = m_u + \Lambda$ and $\hat{m}_s = m_s + \Lambda$ with $\Lambda = (M_K - m_u - m_s)/2$ a parameter of order Λ_{QCD}. Conversely, for the estimation of the $\mathcal{M}_\pi$ amplitude, one can safely assume to parametrize the pion using the light meson wave-function. If one take $g_\pi(x) \approx 0$, as customarily suggested in the literature, the pion contribution automatically vanishes. A conservative estimate can however be obtained by setting, for example, $g_\pi/g_K \approx M_\pi/M_K$, which predicts the following upper bound to the ratio

$$R_{\pi K} = \left| \frac{\mathcal{M}_{\pi^+}}{\mathcal{M}_{K^+}} \right| \lesssim \left(\frac{M_\pi}{M_K} \right)^3 \simeq 1. \times 10^{-2}.$$

For this reason, even in the numerical calculation one can neglect the ALP-π emission as expected on a general ground, once same order ALP couplings to u, d and s quarks are assumed. Looking at Tab.5.1 one can see that the dominant part of the amplitude comes from the top enhanced loop. To compute it one follows Sec.4.4 to find the loop amplitude for the $K^+ \rightarrow \pi^+ a$:

---

[2]Being the sign of the ALP–fermion couplings completely arbitrary, depending on the conventions used this parametric cancellation can occur for $c_s = c_u$, when the Lagrangian in Eq. (2.31) is used, as done for example in [68, 99, 108].

[3]In the following section it will be commented on how to adapt the numerical results to account for different choices of g_K.

$$\mathcal{M}^L_{K^+ \to \pi^+ a} = \frac{G_F \, m_t^2}{4\sqrt{2}\pi^2} \frac{M_{K^+}^2}{f_a} \left(1 - \frac{M_{\pi^+}^2}{M_{K^+}^2} \right)$$
$$\left[f_+(m_a^2) + \frac{m_a^2}{M_{K^+}^2 - M_{\pi^+}^2} f_-(m_a^2) \right] \sum_{q=u,c,t} c_{sd}^{(q)} \tag{5.6}$$

with the coefficient

$$c_{sd}^{(q)} = V_{qi} V_{qj}^* \left[3 \, c_W \frac{g(x_q)}{x_t} - \frac{c_q \, x_q}{4 \, x_t} \ln \left(\frac{f_a^2}{m_q^2} \right) \right] \tag{5.7}$$

opportunely normalized in order to factorize out all the relevant scale dependences. The penguin with the ALP emitted from the internal W line is included for completeness, even if in the following phenomenological analysis $c_W = 0$ will be assumed. The dominant contribution from the penguin diagram is mostly proportional to the c_t coupling. For the K meson decay, with the charm contribution roughly accounting for 10% of the total contribution. One-loop diagrams, with the ALP emitted from the initial/final quarks can be safely neglected being suppressed by at least a factor $m_s^2/m_W^2 \approx 10^{-6}$ with respect to the penguin contributions, as they arise at third order in the external momenta expansion. Therefore, no sensitivity on the ALP–down quark couplings can emerge in the $K \to \pi a$ decays from one loop diagrams. An order of magnitude of the tree vs loop amplitude ratio is obtained from comparing Eqs. (5.4) and (5.6), giving:

$$R_{T/L} = \left| \frac{\mathcal{M}^T_{K^+}}{\mathcal{M}^L_{K^+}} \right| \approx 2 \, \pi^2 \frac{f_K \, f_\pi}{m_t^2} \left| \frac{V_{us}^* \, V_{ud}}{V_{ts}^* \, V_{td}} \right| \simeq 1. \times 10^{-2} \tag{5.8}$$

showing the expected level of suppression. Even if the tree vs loop ratio is at the per cent level, the tree level diagrams may have a non negligible impact in the measurement of the $K \to \pi a$ decays, as in principle they depend on different and less constrained, down quark–ALP couplings. The corresponding neutral amplitudes are obtained in a similar fashion using the appropriate results shown in Sec.4.3 and 4.4. The only subtlety is that the mass eigenstates of the neutral Kaon are misaligned with the flavour ones.

This requires a particular combination of amplitudes in the flavour basis to be considered as the experimental signal. The authors discuss this particular issue at length in section 3.3 in [115]. Moreover one can check in Tab. 5.1 that the one can safely ignore tree–level in the case of the K_L^0 decay.

5.2.1 Phenomenology of the $K \to \pi a$ channel

Armed with the tree–level and one–loop, charged and neutral, $K \to \pi\, a$ decays amplitudes, one can bound the ALP-fermion couplings using the experimental limits provided by the NA62 [86–88], E949 [125–127] and KOTO [89] experiments. The main assumption underlying the following phenomenological analysis is that the ALP lifetime is sufficiently long for escaping the detector (i.e. $\tau_a \gtrsim 100$ ps) or alternatively the ALP is mainly decaying in a, not better specified, invisible sector. Visible ALP decays have been studied, for example, in [67, 69, 75, 142]. The tree–level amplitudes of charged and neutral channels depend on the ALP couplings with s, d and u quarks, while the one–loop ones are typically dominated by the ALP coupling with the heaviest quark running in the loop, the t quark, being the c, u contributions suppressed by the $m_{u,c}/m_t$ mass ratio. Being the focus of this paper on ALP-fermion couplings, for the rest of the section $c_W = 0$ will be assumed. The interplay between the simultaneous presence of c_W and c_t has been discussed in detail in [69]. An analysis of the $K \to \pi\, a$ decay with completely general, but flavor conserving, ALP-quark couplings, would require to consider a five-parameters fit, $(c_u, c_d, c_c, c_s, c_t)$ beside the ALP mass m_a. In order to obtain meaningful information about the ALP-fermion couplings different simplifying assumptions have to be introduced. To study the phenomenology only two independent family universal ALP-fermion couplings, $c_\uparrow$ for the up quarks and $c_\downarrow$ for the down ones, will considered, for sake of simplicity[4]. Under this assumption, the interplay between the tree–level and loop contributions to the $K \to \pi\, a$ decay will be thoroughly discussed. Limits for the universal ALP–fermion coupling $c_{a\Phi}$ can be then obtained straightforwardly. As stated in the discussion above, the following results have been obtained

---

[4]The authors refer to [115] for a more detailed study of the contributions considered here.

using the heavy meson approximation for the K meson with $g_K^H = 1$, but with a modified parton mass definition, e.g. a value $g_K = 1/2$ could be reasonable considered the mixed nature of the K-meson. However, different assumptions on g_K can be simply obtained by accordingly rescaling the showed bounds on c_i: i.e. $c_i' = c_i/g_K$.

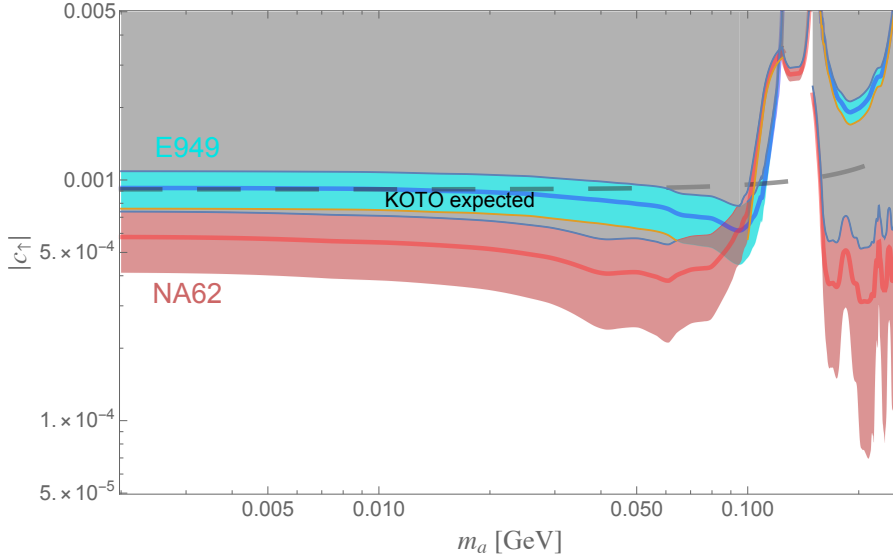## 5.2.2 Interplay between tree–level and one–loop contributions

Figure 5.2: Excluded parameter regions for an universal ALP–up quark coupling $c_\uparrow$ derived from NA62 (pink), E949 (cyan) and KOTO expected (dashed line) experiments.

To constrain, simultaneously, tree–level and one–loop contributions to the $K \to \pi a$ decay one has to adopt simplified frameworks. Following [69], one can consider the scenario of universal ALP-quark coupling, $c_{a\Phi}$. From the analysis of Sec. 4 one easily realizes that in this scenario, the top-penguin loop contribution dominates the charged and neutral K decay, once $c_W = 0$ is assumed. The full cyan and pink lines in Fig. 5.2, represent the limits on $c_{a\Phi}$ obtained from E949 and NA62 respectively as function of the ALP mass m_a.

The dashed gray line represents, instead, the $c_{a\Phi}$ limits from the expected KOTO upgrade. These results are in agreement with the bounds presented in [69] and show that K meson decays typically constrain $c_{a\Phi} \lesssim 10^{-3}$ in the sub-GeV ALP mass range.

In general MFV ALP frameworks, however, it may not be unconceivable to assign different, but flavor universal, PQ charges to the up and down quark sectors, see for example [143–145], that in the following will be denoted as $c_\uparrow$ and $c_\downarrow$, respectively. In this scenario, one–loop amplitudes only depend from $c_\uparrow$ while the tree–level amplitudes are practically proportional to a linear combination of $c_\uparrow$ and $c_\downarrow$, as evident for example in the simplified amplitudes of Eqs. (5.4) and (5.5). Indeed, to study the interplay between tree–level and one–loop the reference value $c_\downarrow = \pm 0.05$ has been chosen, somehow in the ridge of the parameters allowed from previous analysis on tree–level contributions [115]. The blue and brown shaded regions showed in Fig. 5.2 represent the variability of NA62 and E979 bounds on $c_\uparrow$ once $c_\downarrow$ is let varying in the $[-0.05, 0.05]$ range. The presence of the tree-level contribution can modify the bounds on $c_\uparrow$ extracted from penguin diagrams of roughly one order of magnitude, in all the m_a range. The expected KOTO limits on the $K_L^0 \rightarrow \pi^0 a$ decay is reported in Fig. 5.2 as a black dashed line, giving a practically constant bound $c_\uparrow \lesssim 1 \times 10^{-3}$ over all the m_a range of interest, yet not competitive with the charged sector one. Notice that, however, the neutral K decay sector does not suffer from any relevant interference from the tree–level processes, largely suppressed from the CP violating parameter $\tilde{\epsilon}$. A simultaneous measurement of the charged and neutral $K \rightarrow \pi a$ decays, may thus in a not too far future may give independent indications on the relative size of the ALP–light quark couplings. Finally, in Fig. 5.3, a summary on the combined bounds on $(c_\uparrow, c_\downarrow)$ is presented for two reference values of the ALP mass $m_a = 0$ GeV and $m_a = 0.2$ GeV. For the two upper plots $\text{sign}(c_\downarrow) = \text{sign}(c_\uparrow)$ has been taken. In the lower plots, where $\text{sign}(c_\downarrow) = -\text{sign}(c_\uparrow)$ has been considered, a partial cancellation between one–loop and tree-level contributions takes place. In this second scenario, the $c_\downarrow$ constraint from the $\Upsilon(ns)$ decays at Babar and Belle (full vertical black line) derived by [99] can contribute to close this flat direction.
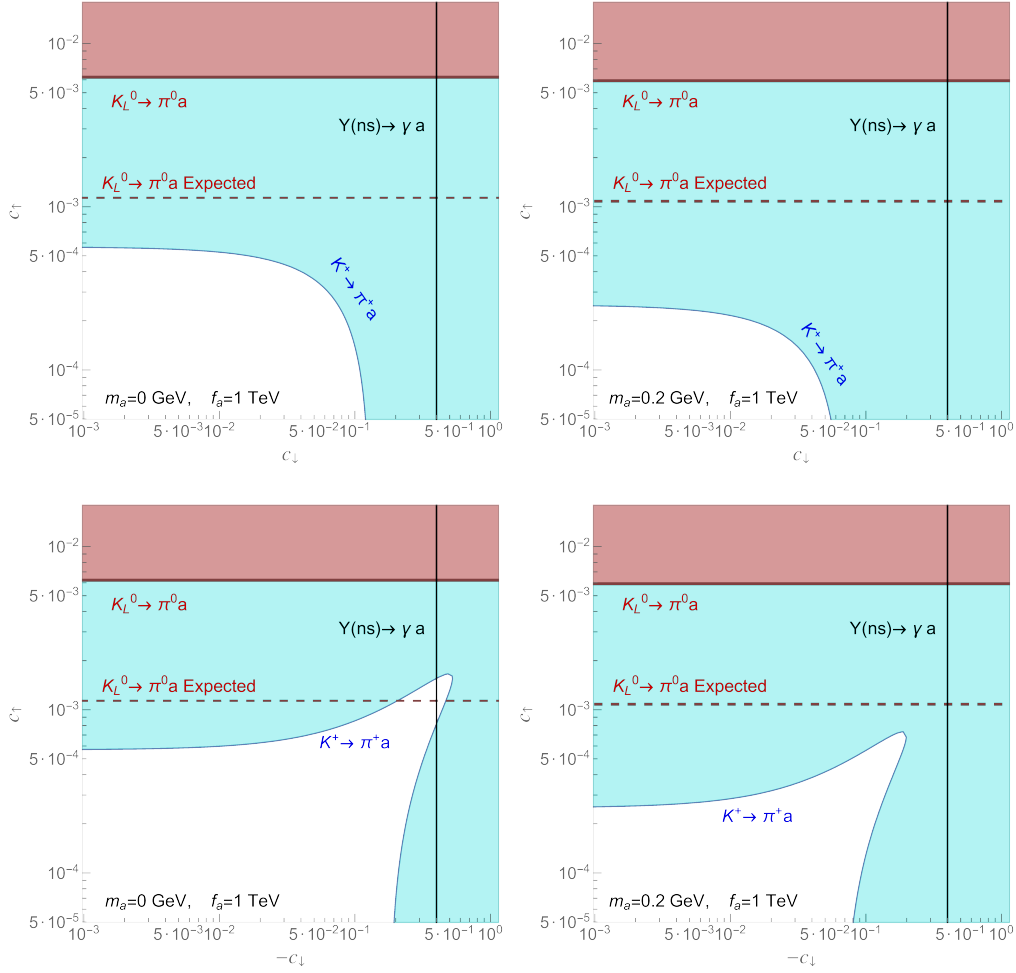
Figure 5.3: Excluded parameter regions for universal ALP–up and down quark couplings $c_\uparrow$ and $c_\downarrow$ derived from NA62 (cyan) and KOTO (pink and dashed pink line) and $Y(ns) \to \gamma a$ (full vertical black line) experiments. The upper plots refer to the $\text{sign}(c_\downarrow) = \text{sign}(c_\uparrow)$ case, while in the lower ones $\text{sign}(c_\downarrow) = -\text{sign}(c_\uparrow)$ has been chosen.

5.3 Leptonic Final States

In this section the authors consider the detailed analysis of pseudo–scalar meson leptonic decays, $M \to \ell\,\nu_\ell a$, with an ALP escaping the detector or
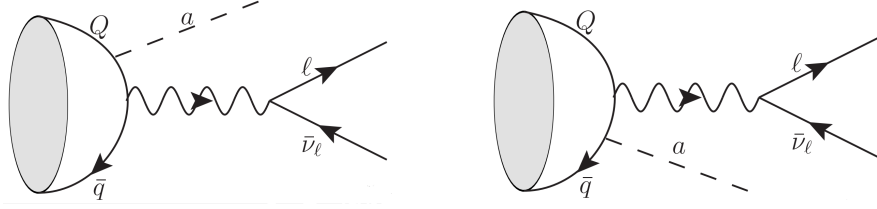
Figure 5.4: Tree level contributions to the $M \to \ell \, \nu_\ell \, a$ amplitude, with the ALP emitted from the M meson. The diagram where the ALP is emitted from the charged lepton is straightforward.

decaying into an "invisible" sector. These decay channels were previously analyzed in [108] for a massless ALP and for a universal ALP–fermion coupling, here instead the ALP mass and the fermion couplings are going to be considered generic and flavour–conserving. Therefore it will be possible to extract independent limits to both quarks and leptons couplings to ALP. The bounds obtained for the couplings of ALPs to leptons are the most stringent to date. Using the effective Lagrangian of Eq. (2.31) one can calculate the leptonic decay rates of pseudo–scalar mesons, $M \to \ell \nu_\ell \, a$, with the ALP sufficiently long-lived to escape the detector without decaying (or decaying into invisible channels). In such a case the only possible ALP signature is its missing energy/momentum. In the following, M_M and P_M will denote the mass and 4–momentum of the decaying meson, while leptons and ALP masses and 4–momenta will be indicated with m_ℓ, m_a, p_ℓ, p_ν and p_a respectively. Neutrinos will be assumed massless. These decays have a single allowed topology shown in Fig. 5.4, where only the diagrams where the ALP is emitted from the M–meson are shown. The diagram where the ALP is emitted from the charged lepton follow straightforwardly, while the one with the ALP emitted from the W^+ internal line automatically vanishes, being the $W^+ W^-$–ALP coupling proportional to the fully antisymmetric 4D tensor. In the following, the derivation of the decay amplitude for the channel in which the ALP is emitted from the initial quarks or from the final charged lepton are discussed separately, as they need two different hadronization treatments. The two diagrams depicted in Fig. 5.4 represent the contributions to the $M \to \ell \nu_\ell \, a$ decay in which the parent meson constituent quarks emit the ALP and then annihilate into a virtual W boson, producing the final leptons. The corre-

sponding amplitude[5] can be written as:

$$\mathcal{M}_h = \langle 0| \, \bar{q} \, \Gamma_h^\mu \, Q \, |M\rangle \left(\bar{\ell} \, \gamma_\mu P_L \, \nu_\ell \right) ,$$

with Γ_h^μ given by

$$\Gamma_h^\mu = -\frac{4G_F}{\sqrt{2}} V_{qQ} \left(\frac{c_q \, m_q}{f_a} \, \gamma^\mu P_L \, \frac{\not{p}_a - \not{p}_q + m_q}{m_a^2 - 2p_a \cdot p_q} \, \gamma_5 \right.$$
$$\left. - \frac{c_Q \, m_Q}{f_a} \, \gamma_5 \, \frac{\not{p}_a - \not{p}_q - m_Q}{m_a^2 - 2p_a \cdot p_Q} \, \gamma^\mu P_L \right). \tag{5.9}$$

In Eq. (5.9) p_q and p_Q are the initial quarks momenta, with c_q and c_Q the corresponding ALP–fermion couplings. Using the methods introduced in Eqs.(4.13–4.7) one obtains the following decay amplitudes for the meson ALP–emission process:

$$\mathcal{M}_h = \frac{4 \, i \, G_F \, V_{qQ} \, f_M}{\sqrt{2}} \, \frac{M_M^2}{f_a \, 2 \, p_a \cdot P_M} \left[c_Q \frac{m_Q}{M_M} \Phi_M^{(Q)}(m_a^2) \right.$$
$$\left. - c_q \frac{m_q}{M_M} \Phi_M^{(q)}(m_a^2) \right] \left(\bar{\ell} \, \not{p}_a \, P_L \, \nu_\ell \right). \tag{5.10}$$

where the functions $\Phi_M^{(q,Q)}(m_a^2)$ contain the integrals over the quark momentum fraction and are defined respectively as:

$$\Phi_M^{(q)}(m_a^2) = \int_0^{1-\delta_M} \frac{p_a \cdot P_M}{m_a^2 - 2\,(1-x)\,p_a \cdot P_M} \, \phi_M(x) \, g_M(x) \, dx$$
$$\Phi_M^{(Q)}(m_a^2) = \int_{\delta_M}^1 \frac{p_a \cdot P_M}{m_a^2 - 2\,x\,p_a \cdot P_M} \, \phi_M(x) \, g_M(x) \, dx . \tag{5.11}$$

The presence of the kinematical cutoff $\delta_M = m_a/(2M_M)$ prevents the appearance of unphysical bare singularities. The leptonic decay amplitude for the lepton ALP–emission process can be easily obtained by using the definition

---

[5]For definiteness, the leptonic current is written assuming a negative charged meson $M = \bar{q}Q$ state, being q a light up-type quark and Q an heavy down-type one.

of the meson form factors of Eq. (4.8), giving

$$\mathcal{M}_\ell \;=\; \langle 0 | \, \bar{q} \, \gamma_\mu P_L \, Q \, | M \rangle \left(\bar{\ell} \, \Gamma_\ell^\mu \, \nu_\ell \right) ,$$

with

$$\Gamma_\ell^\mu \;=\; -\frac{4 G_F}{\sqrt{2}} V_{qQ} \left(\frac{c_\ell \, m_\ell}{f_a} \, \gamma_5 \, \frac{\slashed{p}_a + \slashed{p}_\ell + m_\ell}{m_a^2 + 2 p_a \cdot p_\ell} \, \gamma^\mu P_L \right) . \tag{5.12}$$

In Eq. (5.12) p_ℓ dubs the momentum of the final charged lepton. By making use of all the Dirac matrices relations one obtains:

$$\mathcal{M}_\ell \;=\; -\frac{4 \, i \, G_F}{\sqrt{2}} V_{qQ} \frac{f_M}{f_a} \left[c_\ell \, m_\ell \left(\bar{\ell} \, P_L \, \nu_\ell \right) - \frac{c_\ell \, m_\ell^2}{m_a^2 + 2 \, p_a \cdot p_\ell} \left(\bar{\ell} \, \slashed{p}_a \, P_L \, \nu_\ell \right) \right] . \tag{5.13}$$

5.3.1 Differential Decay Rate

For the 3-body decay at hand, and assuming a massless neutrino, one can define the following Mandelstam variables:

$$s \;=\; (P_M - p_\ell)^2 = (p_\nu + p_a)^2 = M_M^2 + m_\ell^2 - 2 M_M \omega_\ell \tag{5.14}$$
$$t \;=\; (P_M - p_\nu)^2 = (p_\ell + p_a)^2 = M_M^2 - 2 M_M \omega_\nu \tag{5.15}$$
$$u \;=\; (P_M - p_a)^2 = (p_\ell + p_\nu)^2 = M_M^2 + m_a^2 - 2 M_M \omega_a \tag{5.16}$$

with the energy conservation providing the identity:

$$s + t + u = M_M^2 + m_\ell^2 + m_a^2 .$$

The differential 3-body decay rate of any scalar particle in its rest frame can be simply written as function of two independent final energies ω_i, or equivalently of the two independent Mandelstam variables, as

$$(d\Gamma_M)_{RF} = \frac{1}{(2\pi)^3} \frac{1}{8 M_M} |\overline{\mathcal{M}_M}|^2 \, d\omega_\ell \, d\omega_a = \frac{1}{(2\pi)^3} \frac{1}{32 M_M^3} |\overline{\mathcal{M}_M}|^2 \, ds \, du \tag{5.17}$$

with $\mathcal{M}_M = \mathcal{M}_\ell + \mathcal{M}_h$. The Feynman amplitude squared reads:

$$|\overline{\mathcal{M}_\ell}|^2 = C_M\, c_\ell^2\, \frac{m_\ell^2}{M_M^2} \left\{ \frac{p_\ell \cdot p_\nu}{M_M^2} - \frac{m_\ell^2}{M_M^2} \left(\frac{p_a \cdot p_\nu}{m_a^2 + 2\, p_a \cdot p_\ell} \right.\right.$$
$$\left.\left. + m_a^2\, \frac{p_\nu \cdot (p_a + p_\ell)}{(m_a^2 + 2\, p_a \cdot p_\ell)^2} \right) \right\} \tag{5.18}$$

$$|\overline{\mathcal{M}_h}|^2 = C_M \left[c_Q \frac{m_Q}{M_M} \Phi_M^{(Q)}(m_a^2) - c_q \frac{m_q}{M_M} \Phi_M^{(q)}(m_a^2) \right]^2$$
$$\times \frac{2(p_a \cdot p_\ell)(p_a \cdot p_\nu) - m_a^2\, p_\ell \cdot p_\nu}{(p_a \cdot P_M)^2} \tag{5.19}$$

$$\overline{\mathcal{M}_h \mathcal{M}_\ell^*} = C_M\, c_\ell\, \frac{m_\ell^2}{M_M^2} \left[c_Q \frac{m_Q}{M_M} \Phi_M^{(Q)}(m_a^2) - c_q \frac{m_q}{M_M} \Phi_M^{(q)}(m_a^2) \right]$$
$$\times \frac{m_a^2\, (p_a \cdot p_\nu + p_\ell \cdot p_\nu)}{(m_a^2 + 2\, p_a \cdot p_\ell)(p_a \cdot P_M)} \tag{5.20}$$

with the overall constant factor defined as:

$$C_M = 4\, G_F^2\, |V_{qQ}|^2 M_M^4 \frac{f_M^2}{f_a^2}\,.$$

One can notice from Eq. (5.20), that the mixed product is proportional both to the ALP and the charged lepton masses and, consequently, can be neglected either for a massless ALP or for meson decays to a light charged lepton. The total decay rate, for a general ALP mass, can be obtained by numerically integrating the differential decay rate of Eq. (5.17) in the kinematically allowed region. On the other hand, the massless ALP limit

can be easily integrated analytically. By setting $m_a = 0$ one obtains:

$$
\Gamma_{M \to \ell \nu_\ell a} = \left\{ \frac{G_F^2 \, |V_{qQ}|^2 M_M^5}{384\pi^2} \frac{f_M^2}{f_a^2} \left\{ c_\ell^2 \left(2\rho^2 + 3\rho^4 + 12\rho^4 \log \rho - 6\rho^6 + \rho^8 \right) \right. \right.
$$

$$
\left. \left. + \left[\frac{c_Q \, m_Q}{M_M} \Phi_M^{(Q)}(0) - \frac{c_q \, m_q}{M_M} \Phi_M^{(q)}(0) \right]^2 \left(1 - 6\rho^2 - 12\rho^4 \log \rho + 3\rho^4 + 2\rho^6 \right) \right\}.
$$

$$(5.21)$$

For $c_\ell = c_q = c_Q = 2$ one recovers an agreement with the leptonic part of the decay rate in Eq. (17) of Ref. [108], while the hadronic part is wrong and $1/4$ of the result in Eq. (5.21), consistently with what obtained from the Feynman amplitude check.

5.3.2 Bounds from Leptonic Final States

Pseudo–scalar leptonic decay experiments can be used to constraint flavour–diagonal ALP-fermion couplings of Eq. (2.31) via the ALP (invisible) decay rate derived in Sec.5.3.1 in Eqs.(5.17–5.20). Leptonic B-decays have been measured at B-factories, latest BELLE data for electron, muon and tau channel can be found in [146–148], respectively. Charmed meson decays have been measured at BESS (see [149–151] for D and [152, 153] for D_s decays respectively) and at BELLE [154]. Leptonic Kaon decays have been measured by KLOE and NA62 [155–157]. In Tab. 5.3 available experimental determinations for the leptonic pseudo–scalar decay branching ratios are summarized and the lowest order SM predictions are shown for comparison.

It is once again important to stress that the following phenomenological analysis assumes an ALP lifetime sufficiently long to escape detection (i.e. $\tau_a \gtrsim 100$ ps) or alternatively that the ALP is mainly decaying into a, not better specified, invisible sector. In both cases, the ALP signature is a missing energy/momentum, just as for neutrinos. In this scenario, the simplest way to constrain ALP–fermion couplings is then to saturate the $1–\sigma$ experimental limits on the corresponding leptonic branching ratio adding the leptonic ALP decay to the leptonic SM amplitude. No kinematical constraint (2-body vs 3-body decay) is used in the analysis at this stage. The derived bounds

Channel	SM Branching Ratio	Experiment	Ref.
$B^\pm \to e^\pm \bar{\nu}_e$	8.37×10^{-12}	$< 9.8 \times 10^{-7}$	[146]
$B^\pm \to \mu^\pm \bar{\nu}_\mu$	3.57×10^{-7}	$(5.3 \pm 2 \pm 0.9) \times 10^{-7}$	[147]
$B^\pm \to \tau^\pm \bar{\nu}_\tau$	7.95×10^{-5}	$(7.2 \pm 2.7 \pm 1.1) \times 10^{-5}$	[148]
$D^\pm \to e^\pm \bar{\nu}_e$	9.51×10^{-9}	$< 8.8 \times 10^{-6}$	[149]
$D^\pm \to \mu^\pm \bar{\nu}_\mu$	4.04×10^{-4}	$(3.71 \pm 0.19 \pm 0.06) \times 10^{-4}$	[150]
$D^\pm \to \tau^\pm \bar{\nu}_\tau$	1.08×10^{-3}	$(1.2 \pm 0.24 \pm 0.12) \times 10^{-3}$	[153]
$D_s^\pm \to e^\pm \bar{\nu}_e$	1.24×10^{-7}	$< 8.3 \times 10^{-5}$	[154]
$D_s^\pm \to \mu^\pm \bar{\nu}_\mu$	5.28×10^{-3}	$(5.49 \pm 0.17) \times 10^{-3}$	[151]
$D_s^\pm \to \tau^\pm \bar{\nu}_\tau$	5.15×10^{-2}	$(4.83 \pm 0.65 \pm 0.26) \times 10^{-2}$	[152]
$K^\pm \to e^\pm \bar{\nu}_e$	1.62×10^{-5}	$(1.582 \pm 0.007) \times 10^{-5}$	[157]
$K^\pm \to \mu^\pm \bar{\nu}_\mu$	0.629	0.6356 ± 0.0011	[157]

Table 5.3: Lowest order SM predictions and experimental constraints on the considered $M \to \ell\nu$ decay branching ratios.

on the $U(1)_{PQ}$ breaking scale f_a are shown in Tab. 5.4. These values have been obtained by setting the relevant ALP-fermion coupling to one, with all the others vanishing. The results are provided for two reference values of the ALP mass $m_a = 0$ GeV and $m_a = M_M/2$ GeV, showing the variability range that should be expected for a massive vs (almost) massless ALP. As an example, the first row in Tab. 5.4 should be read as follows: the "up–quark" columns represent the f_a limits obtained by setting $c_u = 1$ and $c_b = c_e = 0$ for the two reference values of m_a, the "down–quark" columns represent the limits obtained by setting $c_b = 1$ and $c_u = c_e = 0$, and finally the values in the "lepton" columns are obtained by setting $c_e = 1$ and $c_u = c_b = 0$.

For the heavy pseudo–scalar mesons, such as B, D and D_s, the formulas discussed in Sec.4.1 can be readily applied. These mesons are very well described by the heavy wave function $\phi_H(x)$ in Eq. (4.7), with $g_M = 1$. Constituent quark masses should be used for partons, instead of bare masses, i.e. $M_M = \hat{m}_Q + \hat{m}_q$ (being $\hat{m}_Q \approx m_Q$) with Q and q the heavy and light quark in the meson, respectively. The Kaon sector is more delicate as Kaons cannot be treated fully consistently neither as heavy or as light mesons [110]. The specifics of these contribution have been discussed in detail in Sec.5.2.

One can immediately realize that the f_a bounds shown in Tab. 5.4 from

Channel	f_a [GeV] u-quark		f_a [GeV] d-quark		f_a [GeV] lepton	
	$m_a=0$	$m_a=\frac{M_M}{2}$	$m_a=0$	$m_a=\frac{M_M}{2}$	$m_a=0$	$m_a=\frac{M_M}{2}$
$B^{\pm}\to e^{\pm}\bar{\nu}_e$	2.8	0.079	4	1.3	$5\cdot10^{-4}$	$1.3\cdot10^{-4}$
$B^{\pm}\to \mu^{\pm}\bar{\nu}_\mu$	6	0.16	8.3	2.7	0.2	0.06
$B^{\pm}\to \tau^{\pm}\bar{\nu}_\tau$	0.38	0.006	0.5	0.065	0.2	0.05
$D^{\pm}\to e^{\pm}\bar{\nu}_e$	6	2.1	5.7	0.86	0.02	$5.3\cdot10^{-4}$
$D^{\pm}\to \mu^{\pm}\bar{\nu}_\mu$	4	1.3	3.7	0.56	0.27	0.070
$D^{\pm}\to \tau^{\pm}\bar{\nu}_\tau$	0.007		0.007		0.006	
$D_s^{\pm}\to e^{\pm}\bar{\nu}_e$	8	3	8.2	1.9	0.002	$6.6\cdot10^{-4}$
$D_s^{\pm}\to \mu^{\pm}\bar{\nu}_\mu$	5.5	2	5.7	1.3	0.3	0.09
$D_s^{\pm}\to \tau^{\pm}\bar{\nu}_\tau$	0.02		0.01		0.02	
$K^{\pm}\to e^{\pm}\bar{\nu}_e$	249.	87	170	10	0.243	0.06
$K^{\pm}\to \mu^{\pm}\bar{\nu}_\mu$	1.7	0.5	1.2	0.05	0.32	0.06

Table 5.4: Limits on the $U(1)_{PQ}$ scale f_a derived from leptonic pseudo–scalar meson decays, setting the relevant ALP-fermion coupling equal to one, with all the other couplings vanishing.

up-type and down-type ALP-quark sectors are far from being competitive with the ones derived from FCNC processes, presented in Sec.5.2 in Figs. (5.1–5.3). For example, from Fig.5.2, one can read off a limit $f_a \gtrsim 10^{10}$ MeV stemming from the top-enhanced penguin contribution, assuming $c_t = 1$. Tree–level diagram contributions to FCNC processes can provide constraints on lighter quark sectors, Fig.(5.3) or Ref. [115], giving limits on f_a in the range $f_a \gtrsim 10^6 - 10^7$ MeV. From $\Upsilon(ns)$ decays on can obtain a constraint of the same order for the bottom sector [99]. The only pseudo–scalar meson leptonic channel that provide almost comparable bounds on the quark sector is the $K^{\pm} \to e^{\pm}\bar{\nu}_e$ decay, while most the other pseudo–scalar leptonic decays provide limits in the ballpark $f_a \gtrsim 10^3 - 10^4$ MeV for the light lepton decays and $f_a \gtrsim 10^1 - 10^2$ MeV for the τ ones.

Nonetheless, pseudo–scalar meson leptonic decays can be still very useful, as they provide the best present limits on the ALP–lepton sector for an ALP with m_a in the (sub)–GeV range, bounding $f_a \gtrsim 10^2 - 10^3$ MeV for most of the available channels. Typically, the muon sector gives better limits on f_a as it combines experimental data with relatively smaller errors and a not too
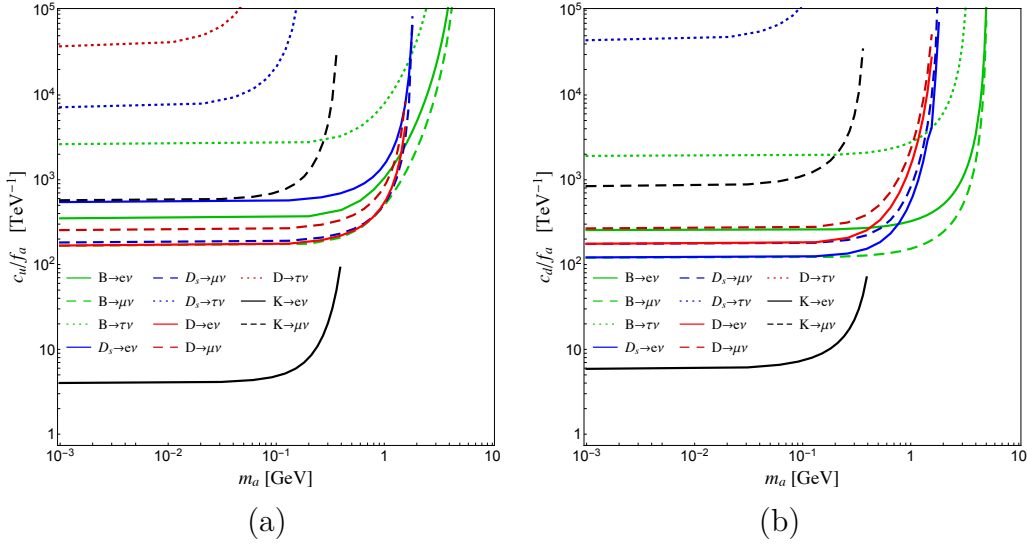
Figure 5.5: Limits on the coupling (a) c_u/f_a and (b) c_d/f_a derived from the leptonic meson decay indicated in the legend, as function of the ALP mass m_a.

large lepton mass suppression of the amplitude in Eq. (5.18). The electron sector suffers from a larger mass suppression and typically provides bounds on $f_a \gtrsim 10^5 - 10^6$ MeV, with the only exception of the $K^\pm \to e^\pm \bar{\nu}_e$ channel benefiting from its highly precise determination[6]. Furthermore, in this ALP mass range, the results presented here on the electron coupling c_e can be complementary with present and future ALP-DM searches like EDEL-WEISS [158] and LDMX [159] and reactor searches at CONNIE, CONUS, MINE, and ν-cleus [160].

The same information can be visually obtained from the plots in Fig. 5.5 and Fig. 5.6, where the dependence of the c_i/f_a bounds on the ALP mass is shown for the ALP couplings to up-type and down-type quarks (Fig. 5.5 (a) and Fig. 5.5 (b) respectively) and for the ALP couplings to charged leptons (Fig. 5.6 (a)). As previously noticed, the $K^\pm \to e^\pm \bar{\nu}_e$ channel is the most promising one, putting bounds on $c_{u,s}/f_a \lesssim 5$ TeV^{-1}, while most of the other

---

[6]Recall, however, that caution should be used when handling K data as a larger hadronic uncertainty has to be accounted for, unavoidably.

channels are providing limits $c_{u,c,s,b}/f_a \lesssim 10^2 - 10^3$ TeV^{-1}, still far from the perturbativity region for $f_a = 1$ TeV. Concerning the ALP-charged lepton coupling notice that the best limits come form μ decay channels, bounding $c_\mu/f_a \lesssim 10^3 - 10^4$ TeV^{-1}. Measurements of c_τ are still limited by worse experimental resolution providing bounds $c_\tau/f_a \lesssim 10^5$ TeV^{-1}. Sensitivity to the ALP-electron coupling c_e is obviously suppressed by the tiny electron mass giving $c_e/f_a \lesssim 10^6 - 10^7$ TeV^{-1}.

The results presented here represent an improvement of at least one order of magnitude compared with limits obtained in Tab. III of [108]. Three main reasons can be advocated: i) first of all, since the publishing of [108], experimental determination of pseudo–scalar leptonic decays has typically improved by roughly a factor ten, leading to more stringent bounds on f_a, ii) moreover, one has to recall that the leading hadronic contribution in Eq. (17) of [108] underestimates by 1/4 the ALP branching ratio, resulting again in lower f_a bounds, iii) finally, assuming a universal ALP-fermion coupling results in a parametric cancellation, clearly shown in Eq. (5.10) once $c_q = c_Q$ is assumed, causing a lost in sensitivity that numerically can be estimated in the 50%–70% range[7].

5.3.3   Spectrum analysis

All the bounds shown up to now have been extracted using exclusively information inferred from the total decay rate. One may think that stronger constraints should be derived from the differential decay rate $d\Gamma/d\omega_\ell$ (or equivalently $d\Gamma/ds$) obtained integrating Eq. (5.17) over the ALP energy ω_a (or over the Mandelstam variable u), thus exploiting the different leptonic energy distribution characterizing two–body vs three–body decays. The SM two-body decay distribution is peaked around vanishing missing mass $s = m_\nu^2 \approx 0$, and therefore any excess of events with $s > 0$ could be an indication of a three-body decay, once SM backgrounds (like $D_s \to \mu\,\nu_\mu\,\gamma$ with ω_γ below the detection energy threshold) have been opportunely accounted for. As an example, in Fig. 5.6(b), the comparison between the limits on the c_i/f_a coefficients obtained from the differential decay rate analysis for the $D_s \to \mu\,\nu_\mu$

---

[7]A detailed and more qualitative discussion of this effect can be found in [115]
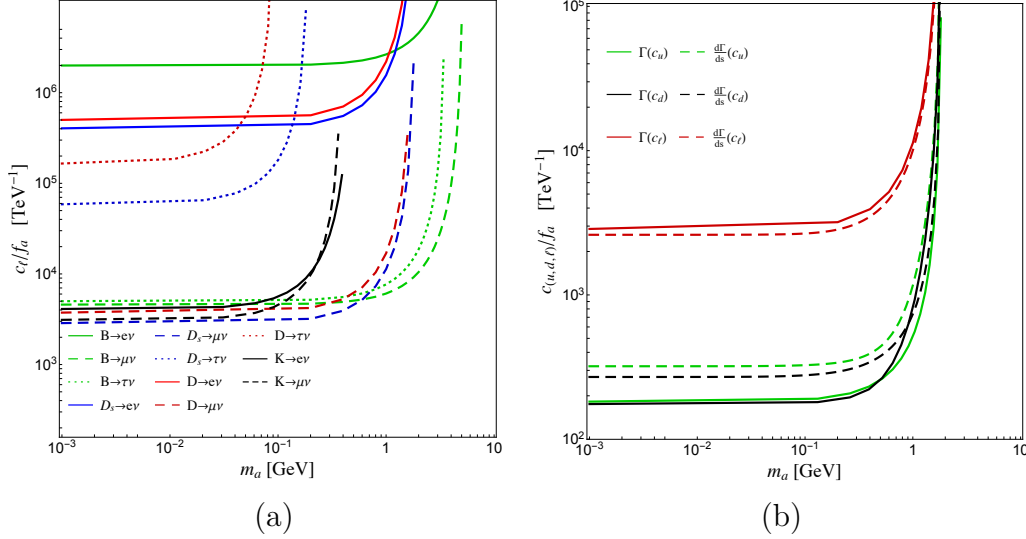
Figure 5.6: Limits on the coupling c_ℓ/f_a (a) derived from the leptonic meson decays indicated in the legend, as function of the ALP mass m_a. Figure (b) shows the limits obtained on all the couplings from the analysis of the $D_s \to \mu\nu_\mu a$ decay using the experimental BR (full lined) and the missing mass distribution (dashed line).

decay observed by BESIII [151] (dashed lines) and the bounds from the branching ratio (solid lines) are shown. The two methods give comparable bounds, with limits obtained from the differential decay rate analysis being somehow less stringent, showing that no clear improvement is obtained, with present data, by adding the available spectral information.

The reason can be easily understood by looking at Fig. 5.7. The red continuous line represents the experimentally smeared SM two body decays rate, $d\Gamma_{SM}/ds$, here shown only for $s > 0$, as shown in Fig. 2 of [151]. The $d\Gamma_{SM+NP}/ds$ distributions obtained including the three body decay $D_s \to \mu\nu_\mu a$ for $c_i/f_a = 200 \text{ TeV}^{-1}$ and different values of the ALP mass, m_a are shown as blue curves. BESSIII collaboration provides data (dots with error bands) on the missing mass distribution only for $s < 0.2 \text{ GeV}^2/c^4$, while most of the NP signal lies above $s > 0.5 \text{ GeV}^2/c^4$. Consequently, less stringent limits on c_i/f_a can be obtained by using available spectral information. Same conclusions can be extrapolated from the other few analysis with pub-
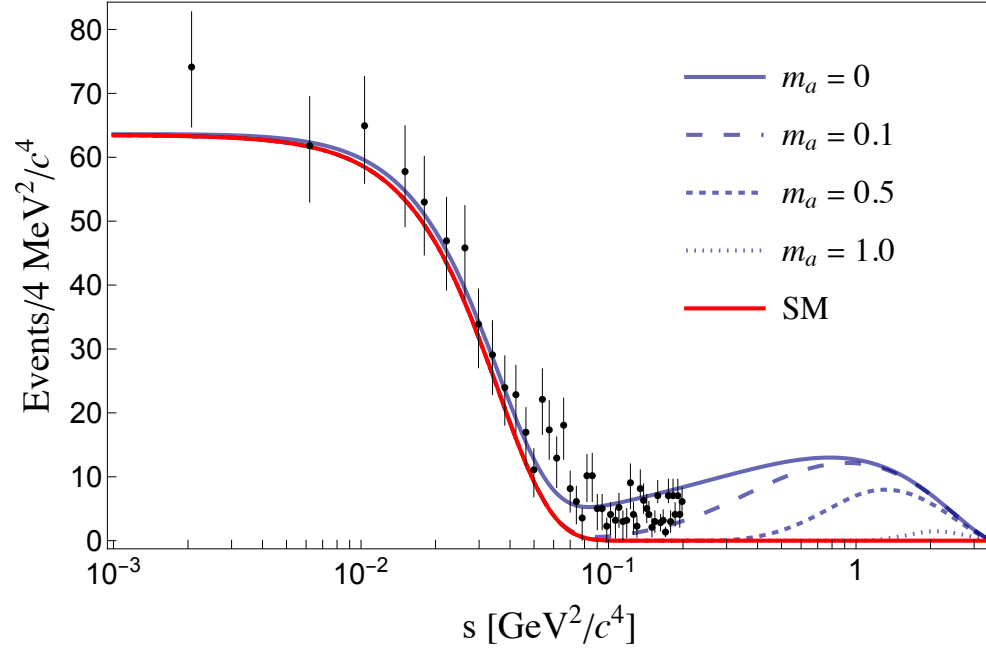
Figure 5.7: Missing mass squared distribution for the $D_s \rightarrow \mu\nu_\mu$ decay from BESSIII collaboration [151]. The red solid line corresponds to the SM smeared two–body differential decay rate $d\Gamma/ds$. Blue curves represent the predicted distributions once the three–body $D_s \rightarrow \mu\nu_\mu a$ decay is included, plotted for different values of the ALP mass, m_a.

lic missing mass squared distributions. An improvement to the bounds on the ALP-fermion couplings obtained from the total decay rate would require to have access to the complete experimental data of signal and background distributions, and is beyond the reach of this letter. Nevertheless one can clearly see from Fig.5.7 that, at least for small values of m_a, the difference in the signals between 2–body and 3–body justifies a dedicated analysis on a bigger M^2_{miss} range, as the signal is well separated from the background and from the smeared SM 2–body.

From Fig.5.7 one sees that as m_a increases the distribution for the 3–body signal gets increasingly smaller in fashion that is far from the usual kinematical suppression "1− Ratio of masses". Looking at the results one might think
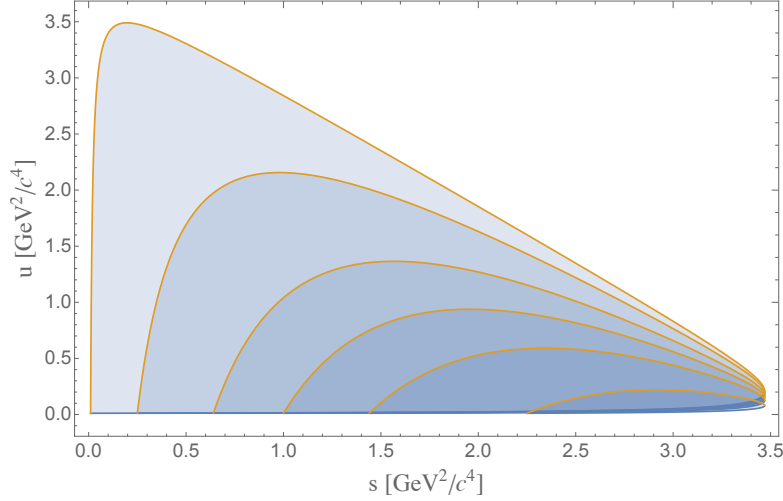
Figure 5.8: Decrease in the available integration region as $m_a \in [0.1, 1]$ in the case of a $D_s \to \mu a$.

that the culprit for such an unnatural suppression is in the model presented by the authors, perhaps the integrals cut–off in Eq.(5.11) is too harsh and as a result part of the contribution is getting excluded resulting in an unphysical suppression of the amplitude. This interpretation might be appealing but in reality this suppression effect comes directly from the Dalitz plot shrinking very rapidly under changes of m_a, as shown in Fig.5.8.

5.4 Monogamma Final States

Recently some interesting low background channels have been studied by the BELLE collaboration [161], namely the processes are $B^0 \to \text{INV}$ and $B^0 \to \text{INV} + \gamma$, with a reported Branching Ratio of 7.8 and 1.6 $\times 10^{-5}$ respectively. The study of the background can be found in [162, 163], showing plenty of room for NP measurements. The techniques developed in the present manuscript are well suited to study a process of the type $M \to \gamma a$, or in general any mesonic process with the vacuum as a final state. Processes like the one studied by the BELLE collaboration in [161] have been proven to be useful in bounding the ALP couplings, see [99], and represent a promising

opportunity to look into the ALPs parameter space.

5.4.1   Weak Effective Theory and ALP induced Flavor Violation

In the Standard Model Flavor Violation can only be mediated by the W's. Below the EW phase transition FV is induced in low–energy weak processes via higher order corrections to the effective interactions involving only light fermions. These effective interactions we are interested in were discussed by Inami and Lim in a seminal paper [164]. In BSM with ALPs one can induce change in flavor by having the ALP mediate the interaction, either via direct FV or, in a similar way to what happens with weak interactions, via higher order processes. In the Minimal Flavor Violation Ansatz the former is excluded while the aforementioned higher order corrections are exactly the top–enhanced penguin loop discussed in Sec.4.4.

Consider the process $B^0 \to \gamma a$, where the energies are the ones typical of B–factories. To describe the process one has to consider the Weak Effective Theory (WET). WET induces flavor change with the emission of a photon, at lowest order an on–shell one. From [164, 165] one recovers the form of the effective vertex associated to the gamma mediating a change in flavor:

$$\bar{d}_i \Gamma_\mu d_j = \frac{e G_F}{4\sqrt{2}\pi^2} V_{ki}^* V_{kj} \bar{d}_i \Big(F_1 (p_\gamma^2 \gamma_\mu - \slashed{p}_\gamma p_{\gamma\mu}) P_L + i F_2 \sigma_{\mu\nu} p_\gamma^\nu (m_{d_i} P_L + m_{d_j} P_R) \Big),$$
(5.22)

where F_1 and F_2 are mass dependent loop functions and p_γ is the photon momentum. Given that the contribution will be mediated by an on–shell photon the part proportional to F_1 will always be zero, so the effective vertex one has to consider is the one in Eq.(5.22) with F_1 put to zero. As mentioned above the other way of inducing FV is via the top–enhanced 1-loop penguin diagram. The effective Lagrangian associated with this term is, in the "Yukawa" basis

$$\bar{d}_i \Gamma' d_j = \frac{G_F m_t^2}{4\sqrt{2}\pi^2} c_{ij}^{(t)} \frac{a}{f_a} \left(m_j \bar{d}_i P_R d_j - m_i \bar{d}_i P_L d_j \right). \tag{5.23}$$

The prescription to hadronize the contribution are the ones discussed in Sec.4

and thanks to the nature of the process and the fact that we are considering only fermionic ALP couplings the amplitudes will always reduce to the first of Eq. (4.13). There are two effective vertices, Eqs.(5.22) and (5.23), contributing to this process that one needs to consider. If the photon is mediating the flavor violating interaction then the amplitude will be proportional to light quarks ALP–fermion couplings while if the ALP is mediating the flavor violation then the amplitude will be proportional to c_t. If both are present one will have interference in the final signal. Consider the effective vertex in Eq.(5.22) mediating a process $M^0 \to \gamma + \mathrm{INV}$ where M's partons are Q and $\bar{q}$, both down type quarks. The two possible amplitudes, from either Q or $\bar{q}$ emission, are given by

$$
\mathcal{A}_{\mathrm{WET}} = e \frac{G_F F_2}{4\sqrt{2}\pi^2 f_a} V_{ki}^* V_{kj} p_\gamma^\nu \epsilon^{\mu*}(p_\gamma) \bar{q} \Big[c_q m_q \frac{\gamma^5 \slashed{k} \sigma_{\mu\nu}(m_Q P_R + m_q P_L)}{m_a^2 - 2p_q \cdot k}
$$
$$
- c_Q m_Q \frac{\sigma_{\mu\nu}(m_Q P_R + m_q P_L)\slashed{k}\gamma^5}{m_a^2 - 2p_Q \cdot k} \Big] Q.
$$
$$(5.24)$$

As discussed before to hadronize correctly the contribution one takes the first of Eq.(4.13). One can easily show that applying Eq.(4.13) to Eq.(5.24) will give exactly zero as a consequence of the Ward–Identity and momentum conservation. Therefore any $M^0 \to \gamma + \mathrm{INV}$ amplitude under the MFV and invisble ALP assumptions is generated only by the vertex in Eq.(5.23). Therefore one has to compute the hard scattering process mediated by a Flavor Violating ALP with the effective vertex of Eq.(5.23). The sum of the two contributions, due to the possible exchange of the outgoing particles is

$$
\mathcal{A}_{\mathrm{FV}} = -ie \frac{G_F m_t^2}{4\sqrt{2}\pi^2} \frac{c_{ij}^{(t)}}{f_a} \epsilon_\mu^*(p_\gamma) \bar{q} \Big[Q_Q \frac{m_Q P_R - m_q P_L}{2p_Q \cdot k}(\slashed{p}_Q - \slashed{k} + m_Q)\gamma^\mu
$$
$$
+ Q_q \gamma^\mu (\slashed{p}_q - \slashed{k} + m_q)\frac{m_Q P_R - m_q P_L}{2p_q \cdot k} \Big] Q.
$$
$$(5.25)$$

Once again the relevant technique to hadronize the $M^0 \to \gamma a$ amplitude is to project the operator regulating the process applied to initial state onto the

vacuum in the final state. The result for the operator found in Eq.(5.25) is:

$$
\langle 0| \, \mathcal{A}_{\text{FV}} \, |M^0(P_M)\rangle = i \frac{G_F m_t^2}{4\sqrt{2}\pi^2} \frac{c_{ij}^a f_M}{2f_a} \frac{Q_q e(m_q + m_Q)}{M_M^2 - m_a^2}
$$
$$
\times \left(g_M(x) M_M k^\rho - (m_Q - m_q) P_M^\rho \right) \int dx \phi_M(x) \left(\frac{x - (1 - x)}{x(1 - x)} \right) \epsilon_\rho(P_\gamma).
$$

$$(5.26)$$

It is important to stress once again that in the case of an Invisible ALP with Minimal Flavor Violation, the only non zero contribution to these decays comes from the Pseudo–scalar annihilation of a neutral meson mediated by the term in Eq.(5.23), i.e. the FC penguin induced vertex of the ALP with an internal emission of a γ, and as such depends only on the c_t contribution. This setup produces a theoretically clean signal dependent only on the coupling between the top and the ALP through the Flavor Violating effective vertex.

5.4.2   Bounds From Monogamma final states

A single variable fit onto the BELLE data [161] for the monogamma final state allows one to extract a limit of $c_t < 2$. Therefore at the moment the measurement does not saturate the perturbativity bound. Nevertheless the rare decays $M^0 \to \gamma \text{INV}$ and $M^0 \to \text{INV}$ provide low background alternatives to measure c_t outside the K sector. In the present analysis the purely missing energy final state has been neglected since the limit it would produce is smaller than the one derived in Fig.5.9 from the monogamma data, mainly due to worse experimental resolution. In the future increasing attention should be given to these as typical Standard Model $M^0 \to \text{INV}$ are of order 10^{-14}, i.e. realistically any potentially observed signal would indicated NP. In Fig.5.9 the limits identified as "BELLE" and "Expected BELLE" are extracted by BELLE data and by BR$< 10^-6$ respectively. Moreover in Fig.5.9 the bound from BaBar's own monogamma is shown. The observed process is $\Upsilon(ns) \to \gamma + \text{INV}$, that in our MFV invisible ALP scenario bounds c_b rather then c_t. This is due to the $b\bar{b}$ composition of the Upsilon, allowing an annihilation to the vacuum without requiring loops or FV ALP couplings, for a complete and in depth study the authors refer to [99]. Finally the limits
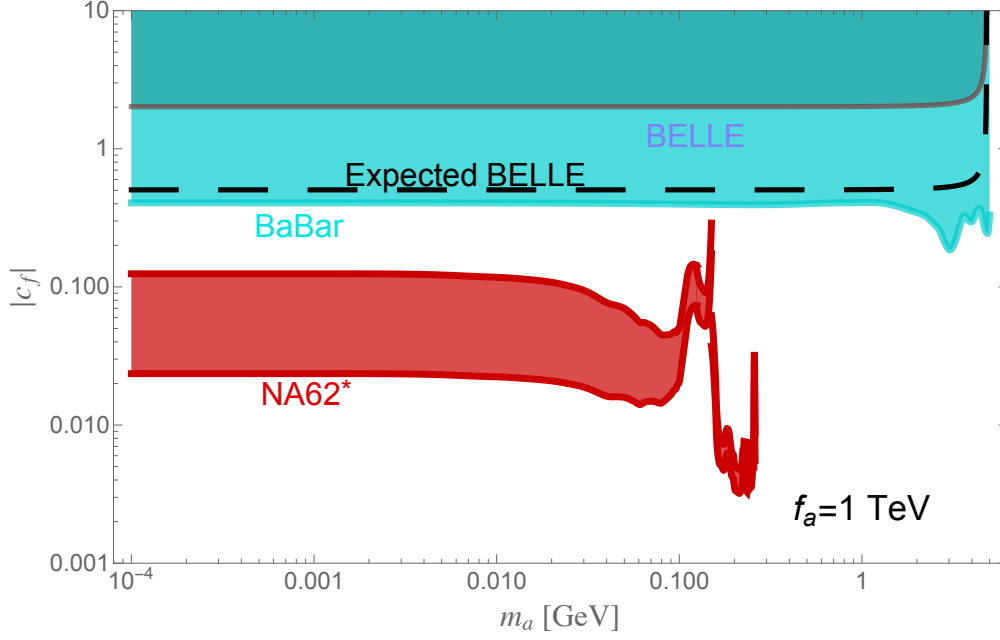
Figure 5.9: BELLE and BaBar limits extracted from monogamma signals. BELLE measures $B^0 \to \gamma\text{INV}$ while BaBar looks at $\Upsilon(ns) \to \gamma + \text{INV}$. The two experiments bound different couplings. The NA62* limit is obtained by fitting only the tree level contribution on the experimental data.

obtained on c_s via the $K \to \pi a$ channel, if the loop is turned off are shown in the plot. These provide the strongest bounds on the parameter in the considered mass region.

Chapter 6

Conclusions

The present manuscript is a brief, self–contained study of the phenomenology of ALPs in the fermionic sector, under the "Invisible Axion" assumption. The Standard Model is embedded with an ALP via an Effective Field Theory truncated at the lowest non–renormalizable order in the Laurent expansion. The field content and the symmetry group are minimally extended adding a single pseudo–scalar light resonance to the Standard Model, that is the Goldstone boson of an anomalous global $U(1)_{\mathrm{PQ}}$ symmetry spontaneously broken at some high energy scale f_a. The Effective Field Theory is then evolved along its Renormalization Group flow from this Ultra–Violet scale down to the perturbative limit of QCD. Some attention is dedicated to the non–perturbative regime of Strong Interactions with the QCD–Chiral Lagrangian.

A brief discussion on the cosmological and astrophysical implications of this light resonance is presented along with the possible signatures on the relative observables. Direct and indirect limits on the ALP parameter space from terrestrial experiments and non– are reviewed with some future prospects in the observation and search for light resonances. Particular attention is devoted to fixed target experiments such as NA62, KOTO, BELLE and BaBar. The phenomenology is then studied with the aid of the Brodsky–Lepage factorisation and Lattice QCD results. Short–range perturbative physics and long–range hadronic physics are supposed to be incoherent with each other in some limit and a model of meson ALP–interaction is recovered. A discussion on the issues and the successes of the approximation is given throughout the

manuscript in a number of different decay scenarios. An encouraging feature is given by the QCD Chiral Lagrangian results giving the same amplitudes and parametric dependences of the ones recovered in this manuscript within 10^{-3} accuracy.

Weak annihilation-induced ALP emissions generated by flavor conserving couplings and weak mesonic decays induced by flavor violating ALP couplings are studied in the framework of a single experimental signature. This allows to extract important bounds and correlation information on the low–energy ALP–fermion couplings from flavor factories data. ALP–leptonic final state decays are also studied, a correction on the massless ALP limit and the full mass dependence of the decay width is recovered. This opens up the study for a plethora of signals able to project limits onto ALP–leptons and ALP–quarks parameters. A discussion on the importance of 2–body vs 3–body kinematics is presented along with the analysis on leptonic final states. Finally an analysis of ALP–mono-photon final states is presented in light of the strong results obtained from BaBar data in the context of quarkonia resonances. A similar final state signature can be obtained from neutral meson decays and some encouraging results are discussed.

An important part of the research work summarized in this thesis is the systematic computation and study of meson-to-meson with ALP emission form factors presented here for the first time. Most of the discussed phenomenology is obtained via these formulas either at with tree–level contributions or effective 1–loop ones.

Future prospects in the line of research are numerous and not always tied to experimental results. One pressing matter is the projection onto the UV theory of the limits obtained and discussed in the manuscript, with an implementation of the UV flavor structure. A second possibility might be to include visible ALP signatures, opening up searches where final states do not contain missing energy. Finally an interesting possibility is to include Flavor Violating coupling at tree level and study their one–loop contributions to the ALP parameters.

The lesson one can learn from the phenomenology discussed in this thesis, beyond the pure exploration of the ALP theory space, has to do with the potential correlation and subsequent modification on the limits projected

onto the ALP–fermion parameters. Indeed in the manuscript it is studied how some particular flavor structure in the coefficients can radically modify the phenomenological bounds projected onto the parameters of the model. Ignoring these effects, induced by a combination of the coefficients flavor structure and the specific nature of the form factors, potentially leads to results that are off by orders of magnitude. Moreover the technology developed to compute and study meson-to-meson ALP decay can be recasted to any current with a similar Lorentz structure and has shown a promising way to connect measurements to theory via the hadronization routes explored here.

To conclude the results derived in this work show a correlated ALP–parameter space that is increasingly bounded and explored. In this picture the role of flavor physics and precision observables is critical and perpendicular to astrophysics and cosmological studies. As such form factors calculation are valuable and unavoidable if one wants to hunt for light physics in terrestrial facilities. These give process independent results and are useful beyond ALP exploration opening up the possibility to recast them to study different kinds of new physics in processes involving bound states.

Acknowledgements

Appendix A

Matter Fields and Higgs quantum numbers

				$SU(3)_c$	$SU(2)_L$	$U(1)_Y$
$Q_L^i =$	$\begin{pmatrix} u_L \\ d_L \end{pmatrix}$	$\begin{pmatrix} c_L \\ s_L \end{pmatrix}$	$\begin{pmatrix} u_L \\ d_L \end{pmatrix}$	3	2	$\frac{1}{6}$
$(u^c)_L^i =$	$(u^c)_L$	$(c^c)_L$	$(t^c)_L$	$\bar{3}$	1	$-\frac{2}{3}$
$(d^c)_L^i =$	$(d^c)_L$	$(s^c)_L$	$(b^c)_L$	$\bar{3}$	1	$\frac{1}{3}$
$L_L^i =$	$\begin{pmatrix} \nu_{eL} \\ e_L \end{pmatrix}$	$\begin{pmatrix} \nu_{\mu L} \\ \mu_L \end{pmatrix}$	$\begin{pmatrix} \nu_{\tau L} \\ \tau_L \end{pmatrix}$	1	2	$-\frac{1}{2}$
$(d^c)_L^i =$	$(d^c)_L$	$(s^c)_L$	$(b^c)_L$	1	1	1
$H =$		$\begin{pmatrix} H^+ \\ H^0 \end{pmatrix}$		1	2	$\frac{1}{2}$

Table A.1: The Standard Model Higgs and fermion fields and their associated gauge quantum numbers.

Appendix B

Low–Energy Feynman Rules

In this appendix we present a resource for the low–energy Feynman rules used in this work[1]. We start by discussing the propagators for fermions

$$\underset{f_i}{\bullet\!\!\longrightarrow\!\!\bullet} = i\frac{\slashed{p} + m_i}{p^2 - m_i + i\varepsilon}, \tag{B.1}$$

ALPs

$$\underset{a}{\bullet\!\!-\!-\!-\!-\!\bullet} = \frac{i}{p^2 - m_a + i\varepsilon}, \tag{B.2}$$

photons

$$\underset{\gamma}{\bullet\!\!\sim\!\!\!\sim\!\!\bullet} = -\frac{ig_{\mu\nu}}{q^2 + i\varepsilon}, \tag{B.3}$$

and W's

$$\underset{W}{\bullet\!\!\sim\!\!\!\sim\!\!\bullet} = \frac{-i\left(g_{\mu\nu} - \frac{q^\mu q^\nu}{m_W^2}\right)}{q^2 - m_W^2 + i\varepsilon}. \tag{B.4}$$
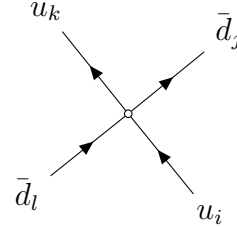
At the energies the measurements are taken it is customary to consider the vertex of the Weak Effective Theory (WET)

$$\delta\mathcal{L}_{\mathrm{WET}} = 4\frac{G_F}{\sqrt{2}}V_{ij}^* V_{kl}\left(J_{L\mu}\right)_{ij}\left(J_L^\mu\right)_{kl}^\dagger, \tag{B.5}$$
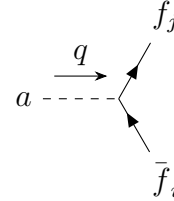
---

[1] All the results are discussed in the Unitary gauge. The R_ξ gauge case is discussed in [166]

where $(J_{L\mu})_{ij} = \bar{d}_j \gamma_\mu P_L u_i$. The 4–fermions contact interaction between L–handed chiral fermions is then described by:
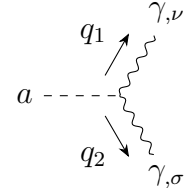
$$
\begin{array}{c}
u_k \qquad\qquad \bar{d}_j \\[2em]
\bar{d}_l \qquad\qquad u_i
\end{array}
\qquad = i \frac{4 G_F}{\sqrt{2}} V_{ij}^* V_{kl}. \tag{B.6}
$$

The ALP–fermion interaction is given by

$$
\begin{array}{c}
f_j \\
a \quad \overset{q}{\longrightarrow} \\
\bar{f}_i
\end{array}
\qquad = -\frac{1}{2 f_a} q_\mu \gamma^\mu (\mathbf{C}_V^{ij} + \mathbf{C}_A^{ij} \gamma^5) \tag{B.7}
$$

where the parameters discussed in Sec.2.3 and 2.5. For completeness, the anomalous ALP–photon vertex is

$$
\begin{array}{c}
q_1 \qquad \gamma,\nu \\
a \quad \text{-----} \\
q_2 \qquad \gamma,\sigma
\end{array}
\qquad = \frac{\alpha}{4\pi} \frac{c_\gamma}{f_a} \epsilon_{\mu\nu\rho\sigma} q_1^\mu q_2^\rho, \tag{B.8}
$$

a similar result can be obtained for the W's when they are considered dynamical.

Appendix C

ALP Couplings to Nucleons

The most reliable way to derive the axion and ALP coupling to nucleons is via an effective theory at energies $\ll \Lambda_{\rm QCD}$, relevant for light ALP masses, where the nucleons are non–relativistic. One uses the chiral effective Lagrangian discussed in [27] with a non–relativistic ALP–nucleons effective Lagrangian. This approach turns out to yield a more reliable approximation than current algebra techniques [167] or the chiral EFT for nucleons [28, 168]. The idea is to use iso–spin as an active flavor symmetry and the ALP as an external current:

$$
\begin{aligned}
\mathcal{L}_N = \bar{N} v_\mu \partial^\mu N + 2g_A \frac{c_{uu} - c_{dd}}{2} \frac{\partial_\mu a}{2f_a} \bar{N} S^\mu \sigma^3 N \\
+ 2g_0^{ud} \frac{c_{uu} + c_{dd}}{2} \frac{\partial_\mu a}{2f_a} \bar{N} S^\mu N + \cdots = \\
\bar{N} v_\mu \partial^\mu N + 2g_A \frac{c_{uu} - c_{dd}}{2} \frac{\partial_\mu a}{2f_a} (\bar{p} S^\mu p - \bar{n} S^\mu n) + \\
2g_0^{ud} \frac{c_{uu} + c_{dd}}{2} \frac{\partial_\mu a}{2f_a} (\bar{p} S^\mu p + \bar{n} S^\mu n) + \cdots
\end{aligned}
\tag{C.1}
$$

where $N = (p, n)^T$ is the is–spin doublet field, v^μ is the four–velocity of the non–relativsitc nucleon and S^μ is the spin operator. The g_A, and g_0^{ud} couplings are the axial iso–vector and axial iso–scalar combinations. To match the two effective Lagrangians, one takes a single nucleon–matrix element, e.g.

$\langle p| \mathcal{L}_a |p\rangle = \langle p| \mathcal{L}_N |p\rangle$, taking the lowest order in isospin breaking effects:

$$c_{uu} \langle p| \bar{u}\gamma_\mu\gamma^5 u |p\rangle + c_{dd} \langle p| \bar{d}\gamma_\mu\gamma^5 d |p\rangle =$$
$$g_A \frac{c_{uu} - c_{dd}}{2} \langle p| \bar{p}S^\mu p |p\rangle + 2g_0^{ud} \frac{c_{uu} + c_{dd}}{2} \langle p| \bar{p}S^\mu p |p\rangle \tag{C.2}$$

where one defines

$$2\bar{p}S^\mu p = \bar{p}\gamma^\mu\gamma^5 p,$$
$$\langle p| \bar{u}\gamma_\mu\gamma^5 u |p\rangle = s_\mu, \tag{C.3}$$
$$\langle p| \bar{u}(\bar{d})\gamma_\mu\gamma^5 u(d) |p\rangle = s_\mu \Delta u(d).$$

With these substitution one gets

$$g_A = \Delta u - \Delta d,$$
$$g_0^{u,d} = \Delta u + \Delta d. \tag{C.4}$$

This way one can substitute back in Eq.(C.1) and recover the nucleon–ALP interaction:

$$\frac{\partial_\mu a}{2f_a} \left\{ \frac{c_{uu} - c_{dd}}{2}(\Delta u - \Delta d)(\bar{p}\gamma_\mu\gamma^5 p - \bar{n}\gamma_\mu\gamma^5 n) \right.$$
$$\left. + \frac{c_{uu} + c_{dd}}{2}(\Delta u + \Delta d)(\bar{p}\gamma_\mu\gamma^5 p + \bar{n}\gamma_\mu\gamma^5 n) \right\}, \tag{C.5}$$

or in a more compact way

$$\frac{\partial_\mu a}{2f_a} \bar{N}\gamma^\mu\gamma^5 \mathbf{c}_{aN} N \tag{C.6}$$

where $\mathbf{c}_{aN}$ is a diagonal 2×2 matrix defined by Eq.(C.5).

Bibliography

[1] Lyndon Evans. The Large Hadron Collider. *Phil. Trans. Roy. Soc. Lond. A*, 370:831–858, 2012.

[2] Peter W. Graham, David E. Kaplan, and Surjeet Rajendran. Cosmological Relaxation of the Electroweak Scale. *Phys. Rev. Lett.*, 115(22):221801, 2015, arXiv: 1504.07551 [hep-ph].

[3] Yohei Ema, Koichi Hamaguchi, Takeo Moroi, and Kazunori Nakayama. Flaxion: a minimal extension to solve puzzles in the standard model. *JHEP*, 01:096, 2017, arXiv: 1612.05492 [hep-ph].

[4] J. S. Bell and R. Jackiw. A PCAC puzzle: $\pi^0 \to \gamma\gamma$ in the σ model. *Nuovo Cim. A*, 60:47–61, 1969.

[5] Stephen L. Adler. Axial vector vertex in spinor electrodynamics. *Phys. Rev.*, 177:2426–2438, 1969.

[6] Kazuo Fujikawa. Evaluation of the chiral anomaly in gauge theories with γ_5 couplings. *Phys. Rev. D*, 29:285–292, Jan 1984.

[7] Murray Gell-Mann. The Eightfold Way: A Theory of strong interaction symmetry. 3 1961.

[8] Murray Gell-Mann. Symmetries of baryons and mesons. *Phys. Rev.*, 125:1067–1084, 1962.

[9] J. C. Ward. An identity in quantum electrodynamics. *Phys. Rev.*, 78:182–182, Apr 1950.

[10] John F. Donoghue, Eugene Golowich, and Barry R. Holstein. *Dynamics of the Standard Model*. Cambridge Monographs on Particle Physics, Nuclear Physics and Cosmology. Cambridge University Press, 2 edition, 2014.

[11] R Jackiw and Claudio Rebbi. Vacuum periodicity in a yang-mills quantum theory. *Physical Review Letters*, 37(3):172, 1976.

[12] Cecilia Jarlskog. *CP violation*, volume 3. World Scientific, 1989.

[13] Sidney Coleman. *Aspects of symmetry: selected Erice lectures*. Cambridge University Press, 1988.

[14] Edward Witten. Current Algebra Theorems for the U(1) Goldstone Boson. *Nucl. Phys. B*, 156:269–283, 1979.

[15] Gabriele Veneziano. U (1) without instantons. *Nuclear Physics B*, 159(1-2):213–224, 1979.

[16] J. M. Pendlebury et al. Revised experimental upper limit on the electric dipole moment of the neutron. *Phys. Rev. D*, 92(9):092003, 2015, arXiv: 1509.04411 [hep-ex].

[17] Ann Nelson. Calculation of θ barr. *Physics Letters B*, 143(1-3):165–170, 1984.

[18] Stephen M Barr. Solving the strong cp problem without the peccei-quinn symmetry. *Physical Review Letters*, 53(4):329, 1984.

[19] Stephen M. Barr. A Natural Class of Nonpeccei-quinn Models. *Phys. Rev. D*, 30:1805, 1984.

[20] Kiwoon Choi, David B. Kaplan, and Ann E. Nelson. Is cp a gauge symmetry? *Nuclear Physics B*, 391(3):515–530, 1993.

[21] Michael Dine, Robert G. Leigh, and Douglas A. MacIntire. Of CP and other gauge symmetries in string theory. *Phys. Rev. Lett.*, 69:2030–2032, 1992, arXiv: hep-th/9205011.

[22] Steven Weinberg. A new light boson? *Phys. Rev. Lett.*, 40:223–226, Jan 1978.

[23] F. Wilczek. Problem of strong p and t invariance in the presence of instantons. *Phys. Rev. Lett.*, 40:279–282, Jan 1978.

[24] R.D. Peccei and Helen R. Quinn. CP Conservation in the Presence of Instantons. *Phys. Rev. Lett.*, 38:1440–1443, 1977.

[25] R. D. Peccei and Helen R. Quinn. Constraints imposed by CP conservation in the presence of pseudoparticles. *Phys. Rev. D*, 16:1791–1797, Sep 1977.

[26] Cumrun Vafa and Edward Witten. Parity Conservation in QCD. *Phys. Rev. Lett.*, 53:535, 1984.

[27] Giovanni Grilli di Cortona, Edward Hardy, Javier Pardo Vega, and Giovanni Villadoro. The QCD axion, precisely. *JHEP*, 01:034, 2016, arXiv: 1511.02867 [hep-ph].

[28] Howard Georgi, David B. Kaplan, and Lisa Randall. Manifesting the Invisible Axion at Low-energies. *Phys. Lett. B*, 169:73–78, 1986.

[29] P. Di Vecchia and G. Veneziano. Chiral Dynamics in the Large n Limit. *Nucl. Phys. B*, 171:253–272, 1980.

[30] T. W. Donnelly, S. J. Freedman, R. S. Lytel, R. D. Peccei, and M. Schwartz. Do Axions Exist? *Phys. Rev. D*, 18:1607, 1978.

[31] Lawrence J. Hall and Mark B. Wise. FLAVOR CHANGING HIGGS - BOSON COUPLINGS. *Nucl. Phys. B*, 187:397–408, 1981.

[32] Jihn E. Kim. Weak-interaction singlet and strong CP invariance. *Phys. Rev. Lett.*, 43:103–107, Jul 1979.

[33] M.A. Shifman, A.I. Vainshtein, and V.I. Zakharov. Can confinement ensure natural cp invariance of strong interactions? *Nuclear Physics B*, 166(3):493 – 506, 1980.

[34] A.R. Zhitnitsky. On Possible Suppression of the Axion Hadron Inter-actions. (In Russian). *Sov. J. Nucl. Phys.*, 31:260, 1980.

[35] Michael Dine, Willy Fischler, and Mark Srednicki. A simple solution to the strong cp problem with a harmless axion. *Physics Letters B*, 104(3):199 – 202, 1981.

[36] Marc Kamionkowski and John March-Russell. Planck scale physics and the Peccei-Quinn mechanism. *Phys. Lett. B*, 282:137–141, 1992, arXiv: hep-th/9202003.

[37] S. M. Barr and D. Seckel. Planck-scale corrections to axion models. *Phys. Rev. D*, 46:539–549, Jul 1992.

[38] S. Ghigna, M. Lusignoli, and M. Roncadelli. Instability of the invisible axion. *Physics Letters B*, 283(3):278 – 281, 1992.

[39] Richard Holman, Stephen D.H. Hsu, Thomas W. Kephart, Edward W. Kolb, Richard Watkins, and Lawrence M. Widrow. Solutions to the strong CP problem in a world with gravity. *Phys. Lett. B*, 282:132–136, 1992, arXiv: hep-ph/9203206.

[40] Anson Hook, Soubhik Kumar, Zhen Liu, and Raman Sundrum. High Quality QCD Axion and the LHC. *Phys. Rev. Lett.*, 124(22):221801, 2020, arXiv: 1911.12364 [hep-ph].

[41] Stephen W Hawking. Particle creation by black holes. In *Euclidean quantum gravity*, pages 167–188. World Scientific, 1975.

[42] Matthew A Bershady, M Ted Ressell, and Michael S Turner. Telescope search for a 3-ev to 8-ev axion. *Physical review letters*, 66(11):1398, 1991.

[43] Georg G Raffelt. Astrophysical methods to constrain axions and other novel particle phenomena. *Physics reports*, 198(1-2):1–113, 1990.

[44] Hajime Fukuda, Masahiro Ibe, Motoo Suzuki, and Tsutomu T. Yanagida. A "gauged" $U(1)$ Peccei–Quinn symmetry. *Phys. Lett. B*, 771:327–331, 2017, arXiv: 1703.01112 [hep-ph].

[45] Michael Duerr, Kai Schmidt-Hoberg, and James Unwin. Protecting the Axion with Local Baryon Number. *Phys. Lett. B*, 780:553–556, 2018, arXiv: 1712.01841 [hep-ph].

[46] Luca Di Luzio, Enrico Nardi, and Lorenzo Ubaldi. Accidental Peccei-Quinn symmetry protected to arbitrary order. *Phys. Rev. Lett.*, 119(1):011801, 2017, arXiv: 1704.01122 [hep-ph].

[47] Hye-Sung Lee and Wen Yin. Peccei-Quinn symmetry from a hidden gauge group structure. *Phys. Rev. D*, 99(1):015041, 2019, arXiv: 1811.04039 [hep-ph].

[48] Alex G. Dias, V. Pleitez, and M. D. Tonasse. Naturally light invisible axion in models with large local discrete symmetries. *Phys. Rev. D*, 67:095008, 2003, arXiv: hep-ph/0211107.

[49] Linda M. Carpenter, Michael Dine, and Guido Festuccia. Dynamics of the Peccei Quinn Scale. *Phys. Rev. D*, 80:125017, 2009, arXiv: 0906.1273 [hep-th].

[50] Howard Georgi and A. Pais. Calculability and naturalness in gauge theories. *Phys. Rev. D*, 10:539–558, Jul 1974.

[51] Rouven Essig et al. Working Group Report: New Light Weakly Coupled Particles. In *Community Summer Study 2013: Snowmass on the Mississippi*, 10 2013, arXiv: 1311.0029 [hep-ph].

[52] Ken Mimasu and Verónica Sanz. ALPs at Colliders. *JHEP*, 06:173, 2015, arXiv: 1409.4792 [hep-ph].

[53] Joerg Jaeckel and Michael Spannowsky. Probing MeV to 90 GeV axion-like particles with LEP and LHC. *Phys. Lett. B*, 753:482–487, 2016, arXiv: 1509.00476 [hep-ph].

[54] Marius Millea, Lloyd Knox, and Brian Fields. New Bounds for Axions and Axion-Like Particles with keV-GeV Masses. *Phys. Rev. D*, 92(2):023010, 2015, arXiv: 1501.04097 [astro-ph.CO].

[55] I. Brivio, M.B. Gavela, L. Merlo, K. Mimasu, J.M. No, R. del Rey, and V. Sanz. ALPs Effective Field Theory and Collider Signatures. *Eur. Phys. J. C*, 77(8):572, 2017, arXiv: 1701.05379 [hep-ph].

[56] G. Alonso-Álvarez, M.B. Gavela, and P. Quilez. Axion couplings to electroweak gauge bosons. *Eur. Phys. J. C*, 79(3):223, 2019, arXiv: 1811.05466 [hep-ph].

[57] Lucian Harland-Lang, Joerg Jaeckel, and Michael Spannowsky. A fresh look at ALP searches in fixed target experiments. *Phys. Lett. B*, 793:281–289, 2019, arXiv: 1902.04878 [hep-ph].

[58] Cristian Baldenegro, Sylvain Fichet, Gero von Gersdorff, and Christophe Royon. Searching for axion-like particles with proton tagging at the LHC. *JHEP*, 06:131, 2018, arXiv: 1803.10835 [hep-ph].

[59] J. Bonilla, I. Brivio, M. B. Gavela, and V. Sanz. One-loop corrections to ALP couplings. *JHEP*, 11:168, 2021, arXiv: 2107.11392 [hep-ph].

[60] Martin Bauer, Matthias Neubert, Sophie Renner, Marvin Schnubel, and Andrea Thamm. The Low-Energy Effective Theory of Axions and ALPs. *JHEP*, 04:063, 2021, arXiv: 2012.12272 [hep-ph].

[61] Martin Bauer, Matthias Neubert, Sophie Renner, Marvin Schnubel, and Andrea Thamm. Consistent treatment of axions in the weak chiral Lagrangian. arXiv 2102.13112, arXiv: 2102.13112 [hep-ph].

[62] R. E. Kallosh and I. V. Tyutin. The Equivalence theorem and gauge invariance in renormalizable theories. *Yad. Fiz.*, 17:190–209, 1973.

[63] Gerard 't Hooft and M. J. G. Veltman. DIAGRAMMAR. *NATO Sci. Ser. B*, 4:177–322, 1974.

[64] G. D'Ambrosio, G. F. Giudice, G. Isidori, and A. Strumia. Minimal flavor violation: An Effective field theory approach. *Nucl. Phys. B*, 645:155–187, 2002, arXiv: hep-ph/0207036.

[65] Mikael Chala, Guilherme Guedes, Maria Ramos, and Jose Santiago. Running in the ALPs. *Eur. Phys. J. C*, 81(2):181, 2021, arXiv: 2012.09017 [hep-ph].

[66] Gerard 't Hooft. Naturalness, chiral symmetry, and spontaneous chiral symmetry breaking. *NATO Sci. Ser. B*, 59:135–157, 1980.

[67] Martin Bauer, Matthias Neubert, and Andrea Thamm. Collider Probes of Axion-Like Particles. *JHEP*, 12:044, 2017, arXiv: 1708.00443 [hep-ph].

[68] Jorge Martin Camalich, Maxim Pospelov, Pham Ngoc Hoa Vuong, Robert Ziegler, and Jure Zupan. Quark Flavor Phenomenology of the QCD Axion. *Phys. Rev. D*, 102(1):015023, 2020, arXiv: 2002.04623 [hep-ph].

[69] M.B. Gavela, R. Houtz, P. Quilez, R. Del Rey, and O. Sumensari. Flavor constraints on electroweak ALP couplings. *Eur. Phys. J. C*, 79(5):369, 2019, arXiv: 1901.02031 [hep-ph].

[70] Vincenzo Cirigliano, Gerhard Ecker, Helmut Neufeld, Antonio Pich, and Jorge Portoles. Kaon Decays in the Standard Model. *Rev. Mod. Phys.*, 84:399, 2012, arXiv: 1107.6001 [hep-ph].

[71] J. E. Moody and Frank Wilczek. NEW MACROSCOPIC FORCES? *Phys. Rev. D*, 30:130, 1984.

[72] A. A. Geraci et al. Progress on the ARIADNE axion experiment. *Springer Proc. Phys.*, 211:151–161, 2018, arXiv: 1710.05413 [astro-ph.IM].

[73] Nicolò Crescini, Caterina Braggio, Giovanni Carugno, Paolo Falferi, Antonello Ortolan, and Giuseppe Ruoso. The QUAX-g_p g_s experiment to search for monopole-dipole Axion interaction. *Nucl. Instrum. Meth. A*, 842:109–113, 2017, arXiv: 1606.04751 [physics.ins-det].

[74] Luca Di Luzio. CP-violating axions. *PoS*, EPS-HEP2021:513, 2022, arXiv: 2108.09071 [hep-ph].

[75] Luca Di Luzio, Ramona Gröber, and Paride Paradisi. Hunting for the CP violating ALP. 10 2020, arXiv: 2010.13760 [hep-ph].

[76] Igor G. Irastorza and Javier Redondo. New experimental approaches in the search for axion-like particles. *Prog. Part. Nucl. Phys.*, 102:89–159, 2018, arXiv: 1801.08127 [hep-ph].

[77] David J. E. Marsh. Axion Cosmology. *Phys. Rept.*, 643:1–79, 2016, arXiv: 1510.07633 [astro-ph.CO].

[78] Davide Cadamuro, Steen Hannestad, Georg Raffelt, and Javier Redondo. Cosmological bounds on sub-MeV mass axions. *JCAP*, 02:003, 2011, arXiv: 1011.3694 [hep-ph].

[79] Luca Di Luzio, Maurizio Giannotti, Enrico Nardi, and Luca Visinelli. The landscape of qcd axion models. *Phys.Rept.*, 870:1–117, 2020, arXiv: 2003.01100 [hep-ph].

[80] T. W. B. Kibble. Topology of Cosmic Domains and Strings. *J. Phys. A*, 9:1387–1398, 1976.

[81] Adrian Ayala, Inma Domínguez, Maurizio Giannotti, Alessandro Mirizzi, and Oscar Straniero. Revisiting the bound on axion-photon coupling from Globular Clusters. *Phys. Rev. Lett.*, 113(19):191302, 2014, arXiv: 1406.6053 [astro-ph.SR].

[82] Oscar Straniero, Adrian Ayala, Maurizio Giannotti, Alessandro Mirizzi, and Inma Dominguez. Axion-Photon Coupling: Astrophysical Constraints. In *11th Patras Workshop on Axions, WIMPs and WISPs*, pages 77–81, 2015.

[83] Núria Vinyoles, Aldo Serenelli, Francesco L. Villante, Sarbani Basu, Javier Redondo, and Jordi Isern. New axion and hidden photon constraints from a solar data global fit. *JCAP*, 10:015, 2015, arXiv: 1501.01639 [astro-ph.SR].

[84] Martin Bauer, Matthias Neubert, Sophie Renner, Marvin Schnubel, and Andrea Thamm. Flavor probes of axion-like particles. 10 2021, arXiv: 2110.10698 [hep-ph].

[85] Evgueni Goudzovski et al. New Physics Searches at Kaon and Hyperon Factories. 1 2022, arXiv: 2201.07805 [hep-ph].

[86] Eduardo Cortina Gil et al. Measurement of the very rare $K^+ \to \pi^+ \nu \bar{\nu}$ decay. arXiv 2103.15389, arXiv: 2103.15389 [hep-ex].

[87] Eduardo Cortina Gil et al. Search for a feebly interacting particle X in the decay $K^+ \to \pi^+ X$. *JHEP*, 03:058, 2021, arXiv: 2011.11329 [hep-ex].

[88] Eduardo Cortina Gil et al. Search for π^0 decays to invisible particles. *JHEP*, 02:201, 2021, arXiv: 2010.07644 [hep-ex].

[89] J.K. Ahn et al. Search for the $K_L \to \pi^0 \nu \bar{\nu}$ and $K_L \to \pi^0 X^0$ decays at the J-PARC KOTO experiment. *Phys. Rev. Lett.*, 122(2):021802, 2019, arXiv: 1810.09655 [hep-ex].

[90] Roel Aaij et al. Search for hidden-sector bosons in $B^0 \to K^{*0} \mu^+ \mu^-$ decays. *Phys. Rev. Lett.*, 115(16):161802, 2015, arXiv: 1508.04094 [hep-ex].

[91] R. Aaij et al. Search for long-lived scalar particles in $B^+ \to K^+ \chi(\mu^+ \mu^-)$ decays. *Phys. Rev. D*, 95(7):071101, 2017, arXiv: 1612.07818 [hep-ex].

[92] Eduard Masso and Ramon Toldra. On a light spinless particle coupled to photons. *Phys. Rev. D*, 52:1755–1763, 1995, arXiv: hep-ph/9503293.

[93] A.J. Bevan et al. The Physics of the B Factories. *Eur. Phys. J. C*, 74:3026, 2014, arXiv: 1406.6311 [hep-ex].

[94] Eder Izaguirre, Tongyan Lin, and Brian Shuve. Searching for Axionlike Particles in Flavor-Changing Neutral Current Processes. *Phys. Rev. Lett.*, 118(11):111802, 2017, arXiv: 1611.09355 [hep-ph].

[95] Matthew J. Dolan, Torben Ferber, Christopher Hearty, Felix Kahlhoefer, and Kai Schmidt-Hoberg. Revised constraints and Belle II sensitivity for visible and invisible axion-like particles. *JHEP*, 12:094, 2017, arXiv: 1709.00009 [hep-ph].

[96] W. Altmannshofer et al. The Belle II Physics Book. *PTEP*, 2019(12):123C01, 2019, arXiv: 1808.10567 [hep-ex]. [Erratum: PTEP 2020, 029201 (2020)].

[97] Xabier Cid Vidal, Alberto Mariotti, Diego Redigolo, Filippo Sala, and Kohsaku Tobioka. New Axion Searches at Flavor Factories. *JHEP*, 01:113, 2019, arXiv: 1810.09452 [hep-ph]. [Erratum: JHEP 06, 141 (2020)].

[98] Patrick deNiverville, Hye-Sung Lee, and Min-Seok Seo. Implications of the dark axion portal for the muon g-2, B-factories, fixed target neutrino experiments and beam dumps. *Phys. Rev. D*, 98(11):115011, 2018, arXiv: 1806.00757 [hep-ph].

[99] L. Merlo, F. Pobbe, S. Rigolin, and O. Sumensari. Revisiting the production of ALPs at B-factories. *JHEP*, 06:091, 2019, arXiv: 1905.03259 [hep-ph].

[100] Bernard Aubert et al. A Search for Invisible Decays of the Upsilon(1S). *Phys. Rev. Lett.*, 103:251801, 2009, arXiv: 0908.2840 [hep-ex].

[101] P. del Amo Sanchez et al. Search for Production of Invisible Final States in Single-Photon Decays of $\Upsilon(1S)$. *Phys. Rev. Lett.*, 107:021804, 2011, arXiv: 1007.4646 [hep-ex].

[102] I. S. Seong et al. Search for a light CP-odd Higgs boson and low-mass dark matter at the Belle experiment. *Phys. Rev. Lett.*, 122(1):011801, 2019, arXiv: 1809.05222 [hep-ex].

[103] G.Peter Lepage and Stanley J. Brodsky. Exclusive Processes in Perturbative Quantum Chromodynamics. *Phys. Rev. D*, 22:2157, 1980.

[104] A.V. Efremov and A.V. Radyushkin. Factorization and asymptotic behaviour of pion form factor in qcd. *Physics Letters B*, 94(2):245–250, 1980.

[105] George F. Sterman and Paul Stoler. Hadronic form-factors and perturbative QCD. *Ann. Rev. Nucl. Part. Sci.*, 47:193–233, 1997, arXiv: hep-ph/9708370.

[106] E. D. Bloom, D. H. Coward, H. DeStaebler, J. Drees, G. Miller, L. W. Mo, R. E. Taylor, M. Breidenbach, J. I. Friedman, G. C. Hartmann, and H. W. Kendall. High-energy inelastic $e - p$ scattering at 6° and 10°. *Phys. Rev. Lett.*, 23:930–934, Oct 1969.

[107] J. D. Bjorken. Asymptotic sum rules at infinite momentum. *Phys. Rev.*, 179:1547–1553, Mar 1969.

[108] Y.G. Aditya, Kristopher J. Healey, and Alexey A. Petrov. Searching for super-WIMPs in leptonic heavy meson decays. *Phys. Lett. B*, 710:118–124, 2012, arXiv: 1201.1007 [hep-ph].

[109] Xing-Gang Wu and Tao Huang. Heavy and light meson wavefunctions. *Chin. Sci. Bull.*, 59:3801, 2014, arXiv: 1312.1455 [hep-ph].

[110] Stanley J. Brodsky and G. Peter Lepage. Large Angle Two Photon Exclusive Channels in Quantum Chromodynamics. *Phys. Rev. D*, 24:1808, 1981.

[111] V. L. Chernyak and A. R. Zhitnitsky. Exclusive Decays of Heavy Mesons. *Nucl. Phys. B*, 201:492, 1982. [Erratum: Nucl.Phys.B 214, 547 (1983)].

[112] A.H. Mueller. Perturbative qcd at high energies. *Physics Reports*, 73(4):237–368, 1981.

[113] James Botts and George Sterman. Hard elastic scattering in qcd: leading behavior. *Nuclear Physics B*, 325(1):62–100, 1989.

[114] Hsiang-nan Li and George Sterman. The perturbative pion form factor with sudakov suppression. *Nuclear Physics B*, 381(1-2):129–140, 1992.

[115] Alfredo Walter Mario Guerrera and Stefano Rigolin. Revisiting $K \to \pi a$ decays. *Eur. Phys. J. C*, 82(3):192, 2022, arXiv: 2106.05910 [hep-ph].

[116] Adam Szczepaniak, Ernest M. Henley, and Stanley J. Brodsky. Perturbative {QCD} Effects in Heavy Meson Decays. *Phys. Lett. B*, 243:287–292, 1990.

[117] Derek E. Hazard and Alexey A. Petrov. Lepton flavor violating quarkonium decays. *Phys. Rev. D*, 94(7):074023, 2016, arXiv: 1607.00815 [hep-ph].

[118] Sidney D. Drell and Tung-Mow Yan. Connection of elastic electromagnetic nucleon form factors at large Q^2 and deep inelastic structure functions near threshold. *Phys. Rev. Lett.*, 24:181–186, Jan 1970.

[119] A. Duncan and Alfred H. Mueller. Asymptotic Behavior of Exclusive and Almost Exclusive Processes. *Phys. Lett. B*, 90:159–163, 1980.

[120] Eduardo Cortina Gil et al. Search for K^+ decays to a muon and invisible particles. *Phys. Lett. B*, 816:136259, 2021, arXiv: 2101.12304 [hep-ex].

[121] J. Grygier et al. Search for $\boldsymbol{B \to h\nu\bar{\nu}}$ decays with semileptonic tagging at Belle. *Phys. Rev. D*, 96(9):091101, 2017, arXiv: 1702.03224 [hep-ex]. [Addendum: Phys.Rev.D 97, 099902 (2018)].

[122] N. Carrasco, P. Lami, V. Lubicz, L. Riggio, S. Simula, and C. Tarantino. $K \to \pi$ semileptonic form factors with $N_f = 2 + 1 + 1$ twisted mass fermions. *Phys. Rev. D*, 93(11):114512, 2016, arXiv: 1602.04113 [hep-lat].

[123] Aoife Bharucha, David M. Straub, and Roman Zwicky. $B \to V\ell^+\ell^-$ in the Standard Model from light-cone sum rules. *JHEP*, 08:098, 2016, arXiv: 1503.05534 [hep-ph].

[124] Nico Gubernari, Ahmet Kokulu, and Danny van Dyk. $B \to P$ and $B \to V$ Form Factors from B-Meson Light-Cone Sum Rules beyond Leading Twist. *JHEP*, 01:150, 2019, arXiv: 1811.00983 [hep-ph].

[125] A. V. Artamonov et al. Study of the decay $K^+ \to \pi^+\nu\bar{\nu}$ in the momentum region $140 < P_\pi < 199$ MeV/c. *Phys. Rev. D*, 79:092004, 2009, arXiv: 0903.0030 [hep-ex].

[126] A.V. Artamonov et al. New measurement of the $K^+ \to \pi^+\nu\bar{\nu}$ branching ratio. *Phys. Rev. Lett.*, 101:191802, 2008, arXiv: 0808.2459 [hep-ex].

[127] S. Adler et al. Measurement of the K+ –> pi+ nu nu branching ratio. *Phys. Rev. D*, 77:052003, 2008, arXiv: 0709.1000 [hep-ex].

[128] Eduardo Cortina Gil et al. The Beam and detector of the NA62 experiment at CERN. *JINST*, 12(05):P05025, 2017, arXiv: 1703.08501 [physics.ins-det].

[129] Matthew J. Dolan, Felix Kahlhoefer, Christopher McCabe, and Kai Schmidt-Hoberg. A taste of dark matter: Flavour constraints on pseudoscalar mediators. *JHEP*, 03:171, 2015, arXiv: 1412.5174 [hep-ph]. [Erratum: JHEP 07, 103 (2015)].

[130] Patricia Ball and Roman Zwicky. $B_{d,s} \to \rho, \omega, K^*, \phi$ decay form-factors from light-cone sum rules revisited. *Phys. Rev. D*, 71:014029, 2005, arXiv: hep-ph/0412079.

[131] Patricia Ball and Roman Zwicky. New results on $B \to \pi, K, \eta$ decay formfactors from light-cone sum rules. *Phys. Rev. D*, 71:014015, 2005, arXiv: hep-ph/0406232.

[132] Wei Wang, Yue-Long Shen, and Cai-Dian Lu. Covariant Light-Front Approach for B(c) transition form factors. *Phys. Rev. D*, 79:054012, 2009, arXiv: 0811.3748 [hep-ph].

[133] Wei Wang and Yue-Long Shen. Ds –> K, K*, phi form factors in the Covariant Light-Front Approach and Exclusive Ds Decays. *Phys. Rev. D*, 78:054002, 2008.

[134] Laurence J. Cooper, Christine T.H. Davies, Judd Harrison, Javad Komijani, and Matthew Wingate. $B_c \to B_{s(d)}$ form factors from lattice QCD. *Phys. Rev. D*, 102(1):014513, 2020, arXiv: 2003.00914 [hep-lat].

[135] Aidos Issadykov, Mikhail A. Ivanov, and Sayabek K. Sakhiyev. Form factors of the B-S-transitions in the covariant quark model. *Phys. Rev. D*, 91(7):074007, 2015, arXiv: 1502.05280 [hep-ph].

[136] V. Lubicz, L. Riggio, G. Salerno, S. Simula, and C. Tarantino. Scalar and vector form factors of $D \to \pi(K)\ell\nu$ decays

with N_f = 2 + 1 + 1 twisted fermions. *Phys. Rev.*, D96(5):054514, 2017, arXiv: 1706.03017 [hep-lat]. [erratum: Phys. Rev.D99,no.9,099902(2019); Erratum: Phys. Rev.D100,no.7,079901(2019)].

[137] E. McLean, C. T. H. Davies, A. T. Lytle, and J. Koponen. Lattice QCD form factor for $B_s \to D_s^* l\nu$ at zero recoil with non-perturbative current renormalisation. *Phys. Rev. D*, 99(11):114512, 2019, arXiv: 1904.02046 [hep-lat].

[138] E. McLean, C. T. H. Davies, A. T. Lytle, and J. Koponen. $B_s \to D_s^{(*)} l\nu$ form factors using heavy HISQ quarks. *PoS*, LATTICE2018:281, 2019, arXiv: 1901.04979 [hep-lat].

[139] Yuzhi Liu et al. $B_s \to K\ell\nu$ Form Factors with 2+1 Flavors. *EPJ Web Conf.*, 175:13008, 2018, arXiv: 1711.08085 [hep-lat].

[140] J. Grygier et al. Search for $\boldsymbol{B \to h\nu\bar{\nu}}$ decays with semileptonic tagging at Belle. *Phys. Rev. D*, 96(9):091101, 2017, arXiv: 1702.03224 [hep-ex]. [Addendum: Phys.Rev.D 97, 099902 (2018)].

[141] Bhubanjyoti Bhattacharya, Cody M. Grant, and Alexey A. Petrov. Invisible widths of heavy mesons. *Phys. Rev. D*, 99(9):093010, 2019, arXiv: 1809.04606 [hep-ph].

[142] Kevin J. Kelly, Soubhik Kumar, and Zhen Liu. Heavy axion opportunities at the DUNE near detector. *Phys. Rev. D*, 103(9):095002, 2021, arXiv: 2011.05995 [hep-ph].

[143] F. Arias-Aragon and L. Merlo. The Minimal Flavour Violating Axion. *JHEP*, 10:168, 2017, arXiv: 1709.07039 [hep-ph]. [Erratum: JHEP 11, 152 (2019)].

[144] L. Merlo, F. Pobbe, and S. Rigolin. The Minimal Axion Minimal Linear σ Model. *Eur. Phys. J. C*, 78(5):415, 2018, arXiv: 1710.10500 [hep-ph]. [Erratum: Eur.Phys.J.C 79, 963 (2019)].

[145] Javier Alonso-González, Luca Merlo, Federico Pobbe, Stefano Rigolin, and Olcyr Sumensari. Testable axion-like particles in the minimal linear σ model. *Nucl. Phys. B*, 950:114839, 2020, arXiv: 1807.08643 [hep-ph].

[146] N. Satoyama et al. A Search for the rare leptonic decays B+ —> mu+ nu(mu) and B+ —> e+ nu(nu). *Phys. Lett. B*, 647:67–73, 2007, arXiv: hep-ex/0611045.

[147] M. T. Prim et al. Search for $B^+ \to \mu^+\nu_\mu$ and $B^+ \to \mu^+ N$ with inclusive tagging. *Phys. Rev. D*, 101(3):032007, 2020, arXiv: 1911.03186 [hep-ex].

[148] I. Adachi et al. Evidence for $B^- \to \tau^-\bar{\nu}_\tau$ with a Hadronic Tagging Method Using the Full Data Sample of Belle. *Phys. Rev. Lett.*, 110(13):131801, 2013, arXiv: 1208.4678 [hep-ex].

[149] B.I. Eisenstein et al. Precision Measurement of $B(D^+ \to \mu^+\nu)$ and the Pseudoscalar Decay Constant $f(D^+)$. *Phys. Rev. D*, 78:052003, 2008, arXiv: 0806.2112 [hep-ex].

[150] M. Ablikim et al. Precision measurements of $B(D^+ \to \mu^+\nu_\mu)$, the pseudoscalar decay constant f_{D^+}, and the quark mixing matrix element $|V_{cd}|$. *Phys. Rev. D*, 89(5):051104, 2014, arXiv: 1312.0374 [hep-ex].

[151] Medina Ablikim et al. Determination of the pseudoscalar decay constant $f_{D_s^+}$ via $D_s^+ \to \mu^+\nu_\mu$. *Phys. Rev. Lett.*, 122(7):071802, 2019, arXiv: 1811.10890 [hep-ex].

[152] Medina Ablikim et al. Measurement of the $D_s^+ \to \ell^+\nu_\ell$ branching fractions and the decay constant $f_{D_s^+}$. *Phys. Rev. D*, 94(7):072004, 2016, arXiv: 1608.06732 [hep-ex].

[153] Medina Ablikim et al. Observation of the leptonic decay $D^+ \to \tau^+\nu_\tau$. *Phys. Rev. Lett.*, 123(21):211802, 2019, arXiv: 1908.08877 [hep-ex].

[154] A. Zupanc et al. Measurements of branching fractions of leptonic and hadronic D_s^+ meson decays and extraction of the D_s^+ meson decay constant. *JHEP*, 09:139, 2013, arXiv: 1307.6240 [hep-ex].

[155] C. Lazzeroni et al. Precision Measurement of the Ratio of the Charged Kaon Leptonic Decay Rates. *Phys. Lett. B*, 719:326–336, 2013, arXiv: 1212.4012 [hep-ex].

[156] F. Ambrosino et al. Measurement of the charged kaon lifetime with the KLOE detector. *JHEP*, 01:073, 2008, arXiv: 0712.1112 [hep-ex].

[157] P. A. Zyla et al. Review of Particle Physics. *PTEP*, 2020(8):083C01, 2020.

[158] E. Armengaud et al. Searches for electron interactions induced by new physics in the EDELWEISS-III Germanium bolometers. *Phys. Rev. D*, 98(8):082004, 2018, arXiv: 1808.02340 [hep-ex].

[159] Asher Berlin, Nikita Blinov, Gordan Krnjaic, Philip Schuster, and Natalia Toro. Dark Matter, Millicharges, Axion and Scalar Particles, Gauge Bosons, and Other New Physics with LDMX. *Phys. Rev. D*, 99(7):075001, 2019, arXiv: 1807.01730 [hep-ph].

[160] James B. Dent, Bhaskar Dutta, Doojin Kim, Shu Liao, Rupak Mahapatra, Kuver Sinha, and Adrian Thompson. New Directions for Axion Searches via Scattering at Reactor Neutrino Experiments. *Phys. Rev. Lett.*, 124(21):211804, 2020, arXiv: 1912.05733 [hep-ph].

[161] Y. Ku et al. Search for B^0 decays to invisible final states $(+\gamma)$ at Belle. *Phys. Rev. D*, 102(1):012003, 2020, arXiv: 2004.03826 [hep-ex].

[162] Andriy Badin and Alexey A Petrov. Searching for light Dark Matter in heavy meson decays. *Phys. Rev. D*, 82:034005, 2010, arXiv: 1005.1277 [hep-ph].

[163] T. M. Aliev, A. Ozpineci, and M. Savci. Rare B —> neutrino antineutrino gamma decay in light cone QCD sum rule. *Phys. Lett. B*, 393:143–148, 1997, arXiv: hep-ph/9610255.

[164] T. Inami and C. S. Lim. Effects of Superheavy Quarks and Leptons in Low-Energy Weak Processes k(L) —> mu anti-mu, K+ —> pi+

Neutrino anti-neutrino and K0 <—> anti-K0. *Prog. Theor. Phys.*, 65:297, 1981. [Erratum: Prog.Theor.Phys. 65, 1772 (1981)].

[165] Andrzej J. Buras. Weak Hamiltonian, CP violation and rare decays. hep-ph/9806471, arXiv: hep-ph/9806471.

[166] Jorge C. Romao and Joao P. Silva. A resource for signs and Feynman diagrams of the Standard Model. *Int. J. Mod. Phys. A*, 27:1230025, 2012, arXiv: 1209.6213 [hep-ph].

[167] Mark Srednicki. Axion Couplings to Matter. 1. CP Conserving Parts. *Nucl. Phys. B*, 260:689–700, 1985.

[168] David B. Kaplan. Opening the Axion Window. *Nucl. Phys. B*, 260:215–226, 1985.